A model-based assessment of observational methods to estimate anthropogenic CO_2

Dissertation
zur Erlangung des Doktorgrades
der Mathematisch-Naturwissenschaftlichen Fakultät
der Christian-Albrechts-Universität
zu Kiel

vorgelegt von
Inger Rohr

Kiel
2008

Referent:	Prof. Dr. Andreas Oschlies
Korreferent:	Prof. Dr. Arne Körtzinger
Tag der mündlichen Prüfung:	04.11.2008
Zum Druck genehmigt:	04.11.2008

Der Dekan

Zusammenfassung

Drei häufig in Beobachtungen angewendete Methoden zur Abschätzung von anthropogenem CO_2 im Ozean (ΔC^*-Methode, TTD-Methode (transit time distribution) und die Berechnung der Differenz von zwei Gleichgewichtskonzentrationen des gelösten anorganischen Kohlenstoffs) werden an ein $4/3^\circ$-Modell des Nordatlantischen Ozeans angepasst, um diese zu testen und mit direkt modelliertem anthropogenen CO_2 zu vergleichen.

Zusätzlich werden zwei Methoden zur Modellierung von anthropogenem CO_2 in einem klimatologischen Modelllauf verglichen. Wird anthropogenes CO_2 als passiver Tracer (dessen Oberflächenfluss die Information des anthropogenen CO_2-Anstiegs in der Atmosphäre enthält) modelliert, so sind die Konzentrationen von anthropogenem CO_2 um 15% bis 20% niedriger als das „wahre“ modellierte anthropogene CO_2. Dieses wird als Differenz des gelösten anorganischen Kohlenstoffs (DIC) aus einem Modelllauf mit realistisch ansteigendem atmosphärischen pCO_2 und dem DIC aus einem präindustriellen Modelllauf, mit konstantem atmosphärischen pCO_2, mithilfe eines an das physikalische Modell gekoppelten NPZD (Nährstoffe, Phytoplankton, Zooplankton, Detritus) Modells berechnet. Zur Korrektur dieser Unterschätzung des anthropogenen CO_2 durch den passiven Tracer wird eine Verbesserung für die Modellierung eines solchen Tracers durchgeführt.

Wird zur Abschätzung des anthropogenen CO_2 eine Methode verwendet, welche ein Altersspektrum (TTD-Methode) oder ein modelliertes Alter (Differenz zweier DIC-Gleichgewichtskonzentrationen) des betrachteten Wasserpakets verwendet, so ergeben sich Konzentrationen von anthropogenem CO_2, die kaum vom „wahren“ anthropogenen CO_2 des Modells abweichen. Im Gegensatz dazu wird bei der Methode, die ein spezifisches Alter aus Fluor-Chlor-Kohlenwasserstoffen (CFC) benutzt (ΔC^*-Methode), vor allem im tiefen Ozean, das „wahre“ anthropogene CO_2 des Modells deutlich überschätzt.

In einem Sensitivitätslauf, in dem die isopyknische Vermischung komplett abgeschaltet wird, wird der Einfluss auf die Ergebnisse der verschiedenen Abschätzungen von anthropogenem CO_2 untersucht. Es zeigt sich, dass diese nicht wesentlich von denen des Modelllaufs mit isopyknischer Vermischung abweichen. Für die Anwendung der ΔC^*-Methode ist dies verwunderlich, da eine Grundannahme dieser Methode die Vermischung hauptsächlich entlang von Isopyknen voraussetzt.

Ein anderer Sensitivitätslauf mit zwischenjährlich variablen Oberflächenflüssen wurde durchgeführt, um den Einfluss von zwischenjährlicher Variabilität auf die verschiedenen Methoden zur Abschätzung von anthropogenem CO_2 zu untersuchen. Dabei stellt sich heraus, dass die zwischenjährliche Variabilität des anthropogenen CO_2, welches nach der ΔC^*-Methode berechnet wurde, etwa genau so groß ist wie die Abweichung zum „wahren“ anthropogenen CO_2 des Modells. Das gesamt integrierte anthropogene CO_2 weicht mit etwa 1% kaum vom gesamten anthropogenen CO_2 des klimatologischen Referenzlaufs ab. Lokal treten allerdings Abweichungen von bis zu 10% zum klimatologischen Referenzlauf auf.

Abstract

Three methods to estimate anthropogenic CO_2 in the ocean ($\Delta C^\star$ method, TTD (transit time distribution) method and taking the difference of two DIC equilibrium concentrations), which are widely used in observations, were adapted to a coarse resolution ($4/3^\circ$) ocean general circulation model of the North Atlantic. This is done for testing the methods and comparing them to anthropogenic CO_2 modelled directly in this model.

Furthermore two methods for modelling anthropogenic CO_2 are compared in a climatological forced model run. Modelling anthropogenic CO_2 as a passive tracer with a surface flux containing the information of anthropogenic pCO_2 perturbation leads to 15% to 20% lower concentrations than the "true" anthropogenic CO_2 of the model. This is computed as the difference of DIC concentrations from a model run with realistically prescribed atmospheric pCO_2 concentrations minus a model run with a constant preindustrial atmospheric pCO_2 concentration, where in both cases a NPZD (nutrient, phytoplankton, zooplankton, detritus) model is coupled to the physical model. For correcting this underestimation by the passive anthropogenic CO_2 tracer an improvement to model this tracer is suggested.

Adapting a method which uses an age-spectrum (TTD method) or directly modelled water age (difference of two DIC equilibrium concentrations) of a water patch for estimating anthropogenic CO_2, leads to concentrations, which are close to the "true" modelled anthropogenic CO_2 concentrations. In contrast to that, estimating anthropogenic CO_2 by using a method which needs a single chlorofluorocarbon (CFC) derived water age ($\Delta C^\star$ method), leads to high overestimation of the "true" anthropogenic CO_2 of the model, especially in the deep ocean.

One assumption of the $\Delta C^\star$ method is that anthropogenic CO_2 is transported predominantly along isopycnal surfaces. To test this, a sensitivity model run excluding isopycnal mixing was performed. Especially estimating anthropogenic CO_2 with the $\Delta C^\star$ method using the output of this model run should fail. However, the results in comparison to the modelled anthropogenic CO_2 are differing in nearly the same magnitude as for the model run including isopycnal mixing. The same is the case for the other two methods (TTD method and taking the difference of two DIC equilibrium concentrations) for estimating anthropogenic CO_2.

Another sensitivity run forced by inter-annual variable surface fluxes was performed in order to determine the influence of inter-annual variability on the estimates of anthropogenic CO_2 by using the different methods. In this case the inter-annual variability of anthropogenic CO_2 by using the $\Delta C^\star$ method is of the same magnitude as the difference to the "true" modelled anthropogenic CO_2 itself. The inter-annual variability of the total amount of anthropogenic CO_2 deviates by just about 1% from the climatological reference experiment. Locally variations of up to 10% compared to the climatological mean occur.

Contents

Chapter 1

Introduction

CO_2 as a trace gas, absorbing and emitting infrared radiation, plays an essential role in the earth's energy budget in terms of climate change. Greenhouse gases like CO_2 absorb the infrared radiation emitted by the earth and emit infrared radiation up- and downward. Therefore they tend to raise the temperature near the earth's surface. In the past the glacial-interglacial cycle of the atmospheric CO_2 concentration varied between minimum concentrations during glacial maxima and maxima in interglacial periods. During the glacial maximum the atmospheric CO_2 concentration was 180 ppm, which was about 100 ppm lower than in an interglacial period (approximately 280 ppm). The history of atmospheric CO_2 concentrations is known from ice-core data (Vostok, Taylor Dome), and since about 1960 additionally from direct measurements (Manua Loa, South Pole). Before the beginning of industrialisation (around 1750) the atmospheric CO_2 concentration was about 280 ppm for several thousand years (Houghton et al. [2001]). It has risen continuously since then, reaching 379 ppm in 2005 (Solomon et al. [2007]). The present atmospheric CO_2 concentration is the highest since the last 420,000 years and likely since 20 million years. This increase is caused by anthropogenic emissions of CO_2 (Houghton et al. [2001] and Solomon et al. [2007]). Most of these emissions are due to fossil fuel burning (about 75%). For the period between 1751 and 2004 Marland et al. [2007] estimated the annual global emissions of fossil fuel. They found that roughly 315 billion tons of carbon have been released into the atmosphere from the consumption of fossil fuels and cement production. The released CO_2 cannot be completely detected in the atmosphere; so there must be several sinks for these anthropogenic emissions. The land (plants and soil) and the ocean are the main sinks for this CO_2. About one third to one half of the anthropogenic CO_2 emitted into the atmosphere has been taken up by the oceans (Siegenthaler and Sarmiento [1993]). In this sense, the North Atlantic

is the most important CO_2 sink (Takahashi et al. [1997]), as deep water formation occurs there. This means that a major part of the CO_2 that is taken up is sequestered on centennial timescales, because of the large-scale meridional overturning circulation. The oceans contain a large amount of dissolved inorganic carbon (DIC), which makes it difficult to separate the small portion (less than 3 %) of anthropogenic CO_2 from the DIC background.

The first anthropogenic CO_2 estimates in the ocean from direct observations were presented several years ago by Brewer [1978] and Chen and Millero [1979]. They corrected the measured DIC due to biological and physical processes that have taken place since the last contact to the atmosphere. Afterwards they subtracted a preformed preindustrial DIC, which gives a first guess for anthropogenic CO_2. In variations this approach has been pursued by several investigators in many regions of the world ocean (e.g.: Chen [1982], Papaud and Poisson [1986], Poisson and Chen [1987], Goyet and Brewer [1993], Goyet et al. [1998]). Gruber et al. [1996] proposed to improve this approach, since the uncertainties were generally regarded as too large (e.g.: Shiller [1981], Broecker et al. [1985]). They introduced a nearly conservative tracer, $\Delta C^{\star}$, which can be estimated from observed DIC, alkalinity, temperature, salinity, oxygen and nutrients (denoted as $\Delta C^{\star}$ method in the following). Furthermore they had to make some essential assumptions for using this method to estimate anthropogenic CO_2. In this case they assume that the ocean is in steady state with regard to biology, that the effective CO_2 air-sea disequilibrium has stayed constant within the outcrop region of a particular isopycnal surface and that water transport is predominantly along isopycnal surfaces. How to estimate anthropogenic CO_2 with this $\Delta C^{\star}$ method is described in Chapter 3.2. Additionally an information about the water age (a tracer containing the water age) is needed for estimating anthropogenic CO_2 by using this method. The possibility to determine the water age from observed tracers, chlorofluorcarbons (CFCs) in this case, is described in Chapter 3.5.

Another method is described by Touratier and Goyet [2004a] and Touratier and Goyet [2004b], where an independent tracer combining oxygen, inorganic carbon and total alkalinity (denote as TrOCA in the following) is introduced. They are able to estimate anthropogenic CO_2 by defining this tracer without any anthropogenic contribution, and assuming that oxygen and total alkalinity are in both cases identical.

Comparing historical with recent data of the same region gives an information about the anthropogenic CO_2 signal. For example Friis et al. [2005] or Tanhua et al. [2007] used an extended version of the multivariate time-series method of Wallace [1995].

In this method a predictive equation for DIC is derived by stepwise multiple linear regression (MLR) based on several independent chemical and hydrographic parameters. The difference between a measured DIC value and a predicted one, using the MLR-equation, is considered to provide a measure of the anthropogenic CO_2 increase between two sample periods. The two fundamental assumptions are that a region's spatially varying hydrographic DIC distribution can be described by a linear multi-parameter model. And secondly that the underlying natural correlations of DIC with the selected independent parameters do not change over the time period of interest.

In some variations the $\Delta C^\star$ method is the most widely used approach. Improvements of this method were suggested by Pérez et al. [2002] in case of a better estimation of the preformed alkalinity than in Gruber et al. [1996], which they used on a section in the eastern North Atlantic. They further concluded that no significant CO_2 disequilibrium exists when water masses are formed, and that previous claims of such a disequilibrium are based on an artefact arising from inaccuracy in estimation of preformed alkalinity, preindustrial equilibrium CO_2 and the true age of a water mass.

Other variations of the $\Delta C^\star$ method are based on the water mass age. Hall et al. [2002] used the transit time distribution (TTD) or age spectrum to get the age of a water mass and estimated anthropogenic CO_2 as a difference of two equilibrium concentrations of DIC ($DIC_{eq}^{t-\tau}$ as the equilibrium concentration of DIC when the water was in contact with the atmosphere last minus DIC_{eq}^{pi} as the preindustrial equilibrium concentration). How anthropogenic CO_2 is estimated by the TTD method is described in Chapter 3.4. The method using the difference of two equilibrium concentrations was suggested as a shortcut version of the $\Delta C^\star$ method by Gruber et al. [1996]. In a linearised form this method was involved as new by Thomas and Ittekkot [2001] and Thomas et al. [2001], where it was used in observations and an off-line 3D model. It implies the assumption of time independent air-sea disequilibrium of CO_2 and is described in Chapter 3.3 in more detail.

As shown by Thomas et al. [2001] and Sabine et al. [2004] the highest concentrations of anthropogenic CO_2 can be found in the North Atlantic, where formation of deep water masses takes place. These findings as well as the need to do several different experiments with long integration time-scales (from 1765 until 2001), starting in preindustrial times, were the reason to use a coarse resolution ($4/3^\circ$) ocean general circulation model of the North Atlantic for this study. In Chapter 2.1 this physical model is described in detail. In this model anthropogenic CO_2 is modelled in two different ways, an abiotic one (as a passive tracer), and one needing a biological model coupled to the physical ocean

general circulation model (Chapters 3.1 and 2.2.2). The biological model, coupled to the physical ocean model, is a simple nitrogen-based NPZD model, containing the four components nutrients (in terms of nitrate), phytoplankton, zooplankton and detritus as tracers (for details see Chapter 2.2.1). In this study these two methods for modelling anthropogenic CO_2 are compared with regard to physical properties of anthropogenic CO_2 uptake for the first time (see Chapter 4.2). Biastoch et al. [2007] analysed the spreading and uptake of anthropogenic CO_2 in an eddy-permitting model of the North Atlantic with comparison to a coarser resolution model by estimating anthropogenic CO_2 as a passive tracer (abiotic version of computing anthropogenic CO_2 in a model). Based on that one aim of this study is to evaluate the two methods of computing anthropogenic CO_2 in a coarse resolution model (Chapter 4.2).

Additionally three different methods to estimate anthropogenic CO_2, which are widely used in observations, were adapted to the model output and compared to the directly modelled anthropogenic CO_2 (Chapters 4.3, 4.4 and 4.5). The three methods are the $\Delta C^\star$ method, the TTD method and the method taking the difference of two DIC equilibrium concentrations by using a single tracer derived water mass age. These methods were chosen, because the other methods described above (TrOCA method and MLR method) are using alkalinity as independent parameter, which is not the case in this study. In the model used for this study, alkalinity is no independent parameter, but computed as a function of salinity. Applying methods to estimate anthropogenic CO_2 to model output is not new. Matsumoto and Gruber [2005] applied the $\Delta C^\star$ method to a global ocean circulation model for an evaluation of this method. They suggested in general two improvements: one concerning the air-sea disequilibrium and the other concerning the use of water age determined by measurements of CFC concentrations. But in contrast to that, in this study not only the $\Delta C^\star$ method is adapted to the model outputs for estimating anthropogenic CO_2 (Chapter 4.3). Additionally the difference of equilibrium concentrations of DIC and the TTD method were used to estimate anthropogenic CO_2 and compared to anthropogenic CO_2 directly computed in the model (Chapters 4.4 and 4.5). This allows an evaluation of these different methods with each other and additionally with the anthropogenic CO_2 directly computed in the model used here, which was not done before in this complexity with different methods to estimate anthropogenic CO_2.

For the period from 1765 until 1947 only experiments with climatological mean surface forcing can be done. Reliable and regional acceptable measurements (in terms of horizontal resolution) for the surface forcing exist only since 1948. In order to determine

the influence of inter-annual variability on anthropogenic CO_2 uptake, and the estimates of anthropogenic CO_2 using different methods, in the period between 1948 and 2001, two model experiments have been performed: one with climatological mean surface forcing and another one with monthly mean surface flux anomalies taken from the NCEP/NCAR reanalysis (Kalnay et al. [1996]). The inter-annual variation of anthropogenic CO_2 estimated by three different methods, also used in observations, adapted to the model output, and computed directly in the model is shown in Chapter 6.
Using the $\Delta C^\star$ method after Gruber et al. [1996] it is necessary to assume that anthropogenic CO_2 is predominantly mixed along isopycnal surfaces. In an ocean model it is possible to completely switch off the isopycnal mixing. In this case a method assuming mixing predominantly along isopycnal surfaces should fail. To proof this, another sensitivity run is performed for this study, in which isopycnic mixing is completely switched off. As for the output of the model run including isopycnal mixing, the same three methods to estimate anthropogenic CO_2, which are also used in observations, are applied to the model output of the sensitivity run without isopycnal mixing. Additionally this results are compared to the directly modelled anthropogenic CO_2 of this model run (for more details see Chapter 5).

Chapter 2

Model description and setup

The model used in this study is part of FLAME which is described in detail in FLAME group [1999] with a setup similar to Friedrich et al. [2006], and coupled to a simple NPZD model (Oschlies and Garçon [1999]) including dissolved inorganic carbon (DIC) and oxygen. Additionally CFCs and ideal age are computed as passive tracers.

2.1 Physical model

The physical model is based on the GFDL-MOM 2.1 z-coordinate primitive equation model (Pacanowski [1995]) which has been parallelised. This offers the opportunity to perform model integrations on computers with vector architecture as well as on massive-parallel computers.

The horizontal resolution is $4/3^\circ$ in longitude and $4/3^\circ \cos\phi$ in latitude (ϕ denotes the latitude), providing an isotropic grid (independent of latitude the zonal extent equals the meridional extent of each grid box). So the spacial distance between two grid points decreases from 147 km at the equator to 50 km at the northern boundary. In the vertical dimension the model is divided into 45 levels. The box thickness varies from 10 m near the surface up to 250 m in the deep ocean near the bottom. The model domain spans the Atlantic Ocean from 100°W to 16°E and 20°S to 70°N. This model has a realistic topography taken from the ETOPO5 [1988] dataset. To ensure realistic mass transports it is necessary to apply some hand tuning to the topography after box-averaging the topography from the dataset to the model's grid in specific regions, for instance in the Florida Strait and the Denmark Strait.

The northern boundary is closed with a zone of restoring to monthly mean climatological/NCEP data for salt and temperature. It includes the whole Greenland-Iceland-

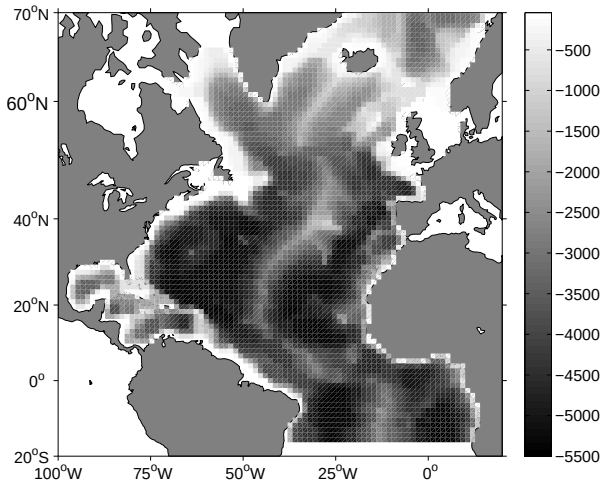

Figure 2.1: Topography of the model (negative depth in m).

Scotland-Sea up to 70°N and reaches down to 67°N at the east Coast of Greenland and to 60°N at the west coast of Norway. The timescales decrease from 3 days at the outer boundary linearly to 100 days at the inner margin of the restoring region. The Mediterranean impact is included by a circular restoring zone with a radius of 600 km around the Strait of Gibraltar and the Golf of Cadiz. It has a constant horizontal relaxation timescale for salinity and temperature with a vertical dependence in the shape of a Gauss-Curve centred at 1200 m with 10 days decaying with a depth scale of 400 m. The southern boundary is closed as well with a restoring zone of three grid boxes. CO_2 is restored to preindustrial GLODAP data and the anthropogenic CO_2 to zero.

Because mixing across isopycnals is seven orders of magnitude smaller than along isopycnals, the most natural coordinate system is the one aligned with local, instantaneous isopycnal surfaces. That is why tracers are approximately mixed along isopycnal surfaces. For reasons of numerical stability, there is a need for a small additional horizontal background diffusion to the isopycnal diffusion implemented by Cox [1987]. The isopycnic diffusion coefficient is $2.0 \cdot 10^7 f(z)g(s)$, where $f(z)$ and $g(s)$ are numerical exponential functions for the vertical dependency and the dependency of isopycnic slope s. The vertical function $f(z)$ has a maximum of 1 at 500 m decreasing to about 0.25 at depths greater than 4000 m. For depths shallower than 200 m the function is forced to zero. A similar vertical shape is used by Böning et al. [1995] and Döscher and Redler [1997]. Tapering the coefficient to the slope function $g(s)$ becomes necessary for numerical reasons in the case of large isopycnic slopes, when the projection

on the z-coordinate leads to too high vertical diffusive fluxes. The function $g(s)$ is a tanh-profile limiting the along-isopycnic diffusion coefficients for large slopes. To the usual tracer velocity a divergence-free eddy-induced advective velocity is added (Gent and J.McWilliams [1994]). This parametrisation is necessary because mesoscale eddies are not resolved in the resolution of this model. And in the presence of mesoscale eddies, the conversion of the available potential energy to eddy kinetic energy leads to a nearly adiabatic stirring mechanism that reduces isopycnal slopes (Gent and McWilliams [1990]). After Böning et al. [1995] this thickness diffusion is able to reduce the strong up-welling in mid-latitudes in coarse resolution models with the effect of a strengthening of the deep western boundary current. The parametrisation of eddy mixing has a large impact on anthropogenic carbon stored within the subtropical thermocline, which was shown by Völker et al. [2001]. According to this here the parametrisation nearly similar to GM/2 of Völker et al. [2001] was used for the model runs with isopycnal mixing, with thickness diffusivity ($1.0 \cdot 10^7 f(z)g(s)$) chosen as half of isopycnal diffusivity. In the GM/2 run of Völker et al. [2001] the isopycnal diffusivity is divided by two as well, so there the thickness diffusivity is chosen equal to the isopycnal diffusivity.
Instead of using a constant diffusivity, in the vertical the coefficient is parameterised proportional to the reciprocal of the Brunt-Väisälä frequency N, following Gargett [1984] and Cummins et al. [1990]:

$$K_v = \frac{K_0}{N}, k_{v,min} <= K_v <= K_{v,max}, N^2 > 0. \tag{2.1}$$

Using a stability depending vertical diffusivity is necessary in order to take the effect of turbulent mixing of internal waves into account. This is believed to be more intense in regions of wide spread isopycnals and reduced in regions of strong stratification. K_v is bounded between $K_{v,min}$ and $K_{v,max}$ for numerical reasons and holds for a stable stratification. In the case of vertical instabilities, the scheme of Rahmstorf (1993) is used, which realises the vertical exchange by a complete homogenisation of vertically adjoining boxes in case of an unstable stratification.
Similar to Oschlies and Garçon [1999], vertical diffusion and viscosity is given by the TKE scheme (Gaspar et al. [1990]). For advection of temperature, salt and all tracers (biological tracer of the NPZD model, dissolved inorganic carbon (DIC), oxygen and all other passive tracers like anthropogenic CO_2 and CFCs) a QUICKER advection scheme after Leonard [1979] is used. To avoid negative tracer concentrations (undershooting) the biological tracers are additionally flux limited with a MDPDC (multidimensional

positive definite central differences) scheme (Lafore et al. [1998]) as used by Oschlies and Garçon [1999].

2.2 Biological model and tracers

2.2.1 NPZD Model

The nitrogen-based NPZD model consists of the four compartments nitrate, phytoplankton, zooplankton and detritus. A detailed description of the interactions is described in Oschlies and Garçon [1999] (Figure 2.2). Here just a brief description of some principle aspects of the NPZD model is given.

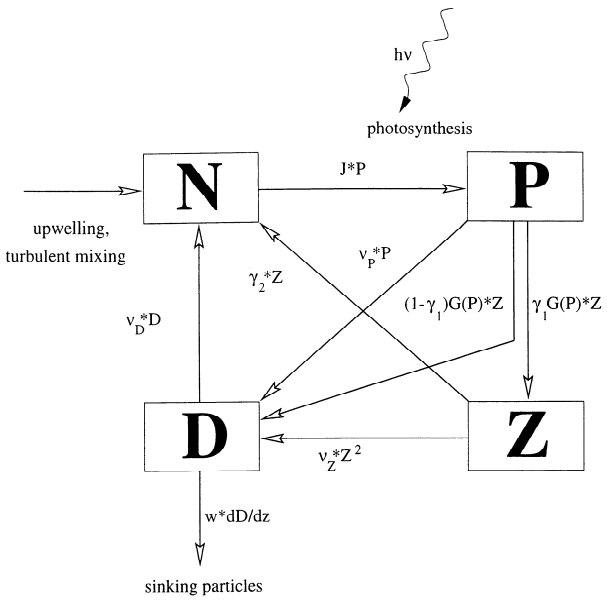

Figure 2.2: Compartments and interactions of the pelagic ecosystem.

Given the presence of nutrients, temperature dependent primary production of phytoplankton is driven by seasonally, latitudinally and vertically dependent solar irradiance. All four components of the NPZD model are measured in units of equivalent units of nitrate (i. e. mol m^{-3}). Newly produced phytoplankton (for example) is taken from the stock of nutrients. The four components of the NPZD model interact with each

other by special growth, grazing and mortality rates (Figure 2.2), which, combined with advection and diffusion, form the sources and sinks of the biological tracers. The total mass in terms of nitrogen of all four compartments together is conserved in this model. The tracers of dissolved inorganic carbon (DIC) and oxygen are coupled to the system in the case that sources and sinks are taken from the NPZD model, assuming a constant Redfield ratio of carbon versus nitrate ($r_{C:N} = 6.6$) and oxygen versus nitrate ($r_{O_2:N} = -10$). Similar to the four components of the NPZD model, DIC and oxygen are also subject to diffusion and advection by the physical model. With a constant sinking speed of 5 m d^{-1} gravitation additionally acts on detritus. The distribution of DIC and oxygen is also driven by surface fluxes with piston velocities estimated after Wanninkhof [1992], which is not the case for the four components of the NPZD model.

2.2.2 Additional passive tracers

In addition to this biological model there are four other passive tracers in the setup of the model, which are CFC11, CFC12, ideal age and anthropogenic CO_2.
CFC11 and CFC12 are introduced as in Beismann and Redler [2003] with a surface flux F_{CFC} prescribed as:

$$F_{CFC} = k_w * (CFC^{atm} - CFC^{oc}), \tag{2.2}$$

where k_w is the piston velocity, CFC^{atm} the CFC concentration in equilibrium with the atmosphere and CFC^{oc} the oceanic CFC concentration. Surface saturation is calculated using CFC concentrations for the northern and southern hemisphere in the period from 1931 until 1997 (by courtesy of Stephen Walker, 1998).
For the first time introduced to this model are ideal age and a tracer for anthropogenic CO_2. The ideal age has a surface flux of zero and the boundary condition of zero at ocean surface. During integration, the concentration is set up every time-step resulting in the ideal model age at every grid point.
Barnola et al. [1995] and Joos et al. [1999] found the pCO_2 variation in the last millennium before industrialisation to be very small, so the global carbon cycle seems to have been in an almost steady state in that time-period. With this basis it is possible to separate the oceanic carbon cycle into a steady state natural carbon cycle and an anthropogenic perturbation. This includes the assumption that the ocean circulation and the biological cycling of carbon from the surface to the deep ocean have not changed since preindustrial times. Under these approximations the anthropogenic CO_2 can

be treated as a passive tracer (like CFCs), and was, as by Sarmiento and Orr [1992], introduced to the model with a net surface flux (F_{dDIC}) of dDIC prescribed as:

$$F_{dDIC} = k_w \alpha \left(dpCO_2^{atm} - dpCO_2^{oc} \right) \quad \text{with} \quad dpCO_2^{oc} = \frac{z_0 dDIC}{1 - z_1 dDIC}, \tag{2.3}$$

where $dDIC$ is the anthropogenic CO_2, k_w is the piston velocity, α the solubility of CO_2 in seawater (calculated after Weiss [1974]) in the ocean (with $k_g = k_w \cdot \alpha$ as a gas exchange coefficient) and $dpCO_2^{oc/atm}$ are the increases of the CO_2 partial pressure above the preindustrial value in the surface ocean and the atmosphere, respectively (actual pCO_2 - preindustrial pCO_2). z_0 and z_1 are quadratic functions in T where

$$z_0 = 1.7561 - 0.031618 \cdot T + 0.0004444 \cdot T^2$$

and

$$z_1 = 0.004096 - 7.7086 \cdot 10^{-5} \cdot T + 6.10 \cdot 10^{-7} \cdot T^2.$$

Details are described in Sarmiento and Orr [1992]. The piston velocity k_w for this passive tracer is similar to that for DIC and O_2 and CFCs estimated after Wanninkhof [1992].

2.3 Integration strategy

The realisation of all integrations was done on a NEX-SX8 on 1 PE.

2.3.1 Initial conditions and spin-up

Before performing several experiments the model was started from an initial state given by the combined Levitus and Boyer [1994]/Boyer and Levitus [1997] climatology.
For nitrate and oxygen initial conditions are taken from Boyer and Levitus [1997]. Initial conditions for DIC are taken from the observational estimate of preindustrial DIC from GLODAP (Sabine et al. [2004]). In the initial state phytoplankton, zooplankton and detritus are set to zero.
The surface salinity is restored towards a climatology after Levitus and Boyer [1994] and Boyer and Levitus [1997], with a constant timescale of 15 days in the surface grid boxes.

The heat flux forcing is formulated as a combination of heat flux Q_0 and a flux correction restoring towards climatological sea surface temperatures (SST) (Haney [1971]):

$$Q = Q_0 + Q_2(SST_{model} - SST_{clim}) \quad \text{with} \quad Q_2 = \left.\frac{\partial Q}{\partial SST}\right|_{SST_{clim}} \tag{2.4}$$

Hereby Q_2 is a temporally and spatial varying timescale, determined directly from a linearisation of the bulk formula for the surface heat flux (Barnier et al. [1995]). If the model has a perfect SST in terms of climatology, the use of restoring boundary conditions alone would lead to the unrealistic situation of suppressed heat exchange. This combined procedure assures that in this case there is still a heat flux Q_0 between atmosphere and ocean. However, Equation 2.4 can be rewritten as a pure relaxation of the model SST to an apparent surface temperature T^*:

$$Q = Q_2(SST_{model} - T^*) \quad \text{with} \quad T^* = SST_{clim} - \frac{Q_0}{Q_2}. \tag{2.5}$$

In this formulation for the surface boundary condition it is assumed that there are no changes in the apparent atmospheric temperature resulting from changes in the modelled SST. This means that an atmosphere with an infinite heat capacity is assumed which absorbs the additional heat resulting from $\Delta Q = Q_2 \Delta SST_{model}$. For small-scale disturbances, where the atmosphere can transport and disperse the heat by wind this seems to be a valid assumption. In the case of large-scale (basin wide or global) SST anomalies the ability of the atmosphere to change its heat transport as a consequence of SST changes can be an important feedback mechanism of the coupled system (Marotzke [1996]). However condition 2.4 is widely used for simulations of the oceans mean state under climatological boundary conditions in order to examine small disturbances and internal variability within the ocean. But it is not quite well suited for studies of climate variability. In this case truly coupled models must be used, or ocean models coupled to a simplified but re-acting atmosphere, see e.g. Rahmstorf [1995]. For the experiments including a surface flux variability, the change in heat flux ΔQ_0 is added to Q_0, which alters also the apparent atmospheric temperature (SST_{clim} is not changed in 2.4). For a perfect model and a perfect model response to the change in the heat flux ΔQ_0 (and other forcing terms) this would mean that the flux correction term might damp the resulting SST anomaly. Hence the model response (in the SST) might be underestimated (also for the case of an imperfect model). Changing SST_{clim} also might result in the correct amplitude for the modelled SST in that hypothetical case of a perfect

model. But it would also result in an additional forcing for the modelled SST for the more realistic case of an imperfect model. Hence the modelled SST would seem to be better correlated to observations, but it would be hardly a prognostic variable anymore. Moreover, one would have to change also Q_2 in the presence of a changing SST_{clim}, to be consistent. Adding surface flux variability to the other surface flux components is straightforward. The surface flux anomalies were taken from NCEP/NCAR reanalysis (Kalnay et al. [1996]). These are monthly means of latent heat flux, sensible heat flux, net long-wave radiation and short-wave radiation fluxes, wind stress and precipitation.
In case of the effects of sea-ice just a simple parametrisation is included. If the SST is below or at the freezing point, surface cooling, surface freshwater fluxes and the surface fluxes of turbulent kinetic energy are set to zero, but surface heating and the surface wind stress are not altered. Since there would be no other mechanism as advection of warmer water for "melting" of the sea-ice in this simple parametrisation, surface heating is not altered. Wind stress is not altered to account for the drag of the sea-ice in the ocean.
All surface forcing data were linearly interpolated between the monthly means during the model run, which are slightly changed after Killworth [1996] beforehand, to preserve monthly means (except for the restoring time scales and restoring values for heat and freshwater fluxes).
The physical model is integrated for a 30 year spin-up integration to allow for a quasi steady dynamical equilibrium. In the spin-up integration the model is forced with monthly mean fields, originating from a 6-hourly analysis at the ECMWF of the years 1986-1989 (Barnier et al. [1995]). Afterwards the passive tracers (except CFCs, the anthropogenic CO_2 tracer and the ideal age tracer) are added and the coupled model is then integrated for further 30 years with climatological forcing.

2.3.2 Model experiments

Experiments with climatological forcing: For a first try with the new added tracers two experiments starting in the model year 1860, after the spin-up, were run for 141 years with climatological (ECMWF) forcing and a preindustrial atmospheric pCO_2 of 278 ppm and realistic atmospheric pCO_2 respectively. The realistic atmospheric partial pressure of CO_2 is prescribed using a spline fit (Enting et al. [1994]) to pCO_2 measurements from atmosphere and ice cores between 1765 and 1990, and the IPCC scenario S650 from 1990 onwards (Houghton et al. [2001]). These model runs were done especially for comparison of anthropogenic CO_2 computed as the DIC difference of a model run with

realistically prescribed atmospheric pCO_2 minus the DIC derived from a model run with constant preindustrial atmospheric pCO_2 (DDIC) and anthropogenic CO_2 computed as a passive tracer (ACO2TR) in this model (see Chapter 4.2). For the first model run ACO2TR was introduced exactly as described in Chapter 2.2.2. Afterwards a second run for ACO2TR was done with improved parametrisation adapted to the DDIC of the first run (see Chapter 4.2). In addition to this first try the following main model experiments were computed.
After spin-up, 236 years of a climatological (ECMWF) forced experiment was run with all tracers, starting in 1765 until 2001 (CFCs covering the years 1931-1997). For dissolved inorganic carbon (DIC) two experiments were done. One with constant preindustrial atmospheric pCO_2 of about 278 ppm (value of the starting year 1765) and another prescribing realistic pCO_2 in the atmosphere. The realistic atmospheric pCO_2 is prescribed as in the previously described experiment.
Another experiment was run for 141 years for the period from 1860 until 2001 to study the sensitivity of shorter integrated time series, which is useful for models with higher resolution. Here the constant atmospheric pCO_2 was set to 288, taking into account the "preindustrial" value of the year 1860. As before another experiment with realistic atmospheric pCO_2 was run.
To examine the accumulation and reconstruction of anthropogenic CO_2 according to isopycnal mixing, a sensitivity run without isopycnal mixing, where the horizontal diffusivity is completely switched off, was run for both periods both with constant preindustrial and realistic atmospheric pCO_2. This is in contrast to Völker et al. [2001], where only the GM (after Gent and J.McWilliams [1994]) parametrisation was switched off and the Laplacian isopycnal scheme was used instead.

Experiments with inter-annual forcing: For separating the effects of inter-annual variability, in addition to both climatological runs including isopycnal mixing, anomalies from the NCEP/NCAR climatology were added to the climatological forcing in the period from 1948-2001.

Chapter 3

Estimating anthropogenic CO_2

The ocean is one of the most important sinks of anthropogenic CO_2. As shown by Siegenthaler and Sarmiento [1993] one third to one half of the anthropogenic CO_2 emitted into the atmosphere has been taken up by the oceans. With less than 1% of the large amount of dissolved inorganic carbon (DIC) in the ocean (3% in surface waters), the anthropogenic CO_2 is very difficult to detect, and direct measurements of anthropogenic CO_2 in the oceans are not possible. But nevertheless, some methods have been developed to estimate anthropogenic CO_2 out of this large DIC background using observational parameters. Three of the methods that are used the most in observations are described in the following sections. The first method introduces a quasi conservative tracer $C^\star$, which can be constructed from measurements of DIC and other species using stoichiometric ratios (Redfield ratios). This tracer is assumed to be constant and uniform. Estimates of the pre-industrial $C^\star$ are then subtracted, leaving the anthropogenic component as a small residual. This method is described in more detail in Chapter 3.2. The second method estimates equilibrium concentrations of DIC for the time when the water had the last contact to the atmosphere minus that equilibrium concentration for pre-industrial times. Here one difficulty is to determine the time since the last surface contact. This can be done using tracers like CFCs, or as described in Chapter 3.4 by using transit time distributions. Estimating anthropogenic CO_2 by using transit time distributions is denoted as TTD method in the following, and representing the third observational method to estimate anthropogenic CO_2 presented in this study.

3.1 Anthropogenic CO_2 estimations directly in the model

For ocean models there are at least two ways of separating anthropogenic CO_2 from the total amount of carbon. One is taking the difference of the DIC from an experiment with realistically prescribed pCO_2 in the atmosphere minus the DIC from an experiment with constant pre-industrial atmospheric pCO_2, later referred to as DDIC (for delta DIC). Using this method the physical ocean model must be coupled to a biological model including DIC. This anthropogenic CO_2 is later also referred as "true" anthropogenic CO_2 of the model.
Another possibility to separate anthropogenic CO_2 from the total amount of carbon is to integrate it as passive tracer (ACO2TR) using the perturbation of anthropogenic pCO_2 in the atmosphere as surface flux (see Chapter 2.2.2 for more details). In this case no biological model is needed.
To test the different methods for estimating anthropogenic CO_2 and compare them to directly modelled anthropogenic CO_2 concentrations, the $\Delta C^\star$ method (after Gruber et al. [1996]), taking the difference of two DIC equilibrium concentrations, and the TTD method are simulated with the output of the model experiments in this thesis. A more detailed description of this methods to separate anthropogenic CO_2 out of the whole amount of DIC is given in the Chapters 3.2, 3.3 and 3.4. In this methods the time since a water patch had last contact with the surface is needed. CFCs and other tracers like He, ^{3}H, C^{14} , ... are used as age tracers in observations. For the TTD method transit time distributions are determined, whereas the other two methods, also used in observations, are using a single tracer derived water age.
All numerical experiments in this study have CFC11 and CFC12 integrated as passive tracers for the time period from 1931 until 1997 and in addition to this an idealised tracer is integrated as well, which gives the model age. So it is possible to use these for adapting the three observational methods to the model simulations.

3.2 Reconstruction of anthropogenic CO_2 using the $\triangle C^\star$ Method

There are several methods to estimate anthropogenic CO_2 out of observable parameters. Here one of the most widely used methods is described. The first to point out that anthropogenic CO_2 can be estimated out of measured DIC were Brewer [1978] and Chen

and Millero [1979]. They estimated anthropogenic CO_2 by correcting measured DIC of the effects due to remineralisation of organic matter and the dissolution of carbonates after the last contact to the atmosphere (ΔDIC_{bio}), and additionally subtracted a preformed pre-industrial DIC (DIC^0_{pi}).

$$C_{ant} = DIC^{obs} - \Delta DIC_{bio} - DIC^0_{pi}, \tag{3.1}$$

where DIC^{obs} is the measured DIC. ΔDIC_{bio} can be estimated out of the apparent oxygen utilisation (AOU) and the difference between in-situ alkalinity (ALK) and preformed alkalinity (ALK^0):

$$\Delta DIC_{bio} = \underbrace{-r_{C:O_2} AOU}_{\text{soft tissue pump}} \underbrace{+\frac{1}{2}(ALK - ALK^0 - r_{N_2:O_2} AOU)}_{CaCO_3 \text{ dissolution}}. \tag{3.2}$$

Here $r_{C:O_2}$ and $r_{N_2:O_2}$ are the stoichiometric C:O_2 and N:O_2 ratios during remineralisation of organic matter. The first term on the right represents the change in DIC due to remineralisation of organic matter and the second term represents changes due to dissolution of $CaCO_3$. The factor $\frac{1}{2}$ in this part results from the fact that the dissolution of $CaCO_3$ changes alkalinity and DIC in a 2:1 ratio. The expression $DIC^{obs} - \Delta DIC_{bio}$ is the concentration of DIC which a water parcel would have when it is taken adiabatically up to the surface where it was last in contact with the atmosphere, so it is equivalent to the computation of a preformed DIC concentration. In order to get the anthropogenic CO_2 concentration from this preformed DIC the preformed concentration which existed in pre-industrial times (DIC^0_{pi}) has to be subtracted from this.
However, there were very large uncertainties associated with the calculation of DIC^0_{pi}. Gruber et al. [1996] showed that this method can be improved by separating DIC^0_{pi} into two parts. One representing the DIC which is in equilibrium with the pre-industrial atmosphere (DIC^{pi}_{eq}) and a disequilibrium term ΔDIC_{diseq}:

$$DIC^0_{pi} = DIC^{pi}_{eq} + \Delta DIC_{diseq}. \tag{3.3}$$

Combining 3.1 and 3.3 gives

$$\begin{aligned} C_{ant} &= \underbrace{DIC^{obs} - \Delta DIC_{bio} - DIC^{pi}_{eq}}_{\Delta C^*} - \Delta DIC_{diseq} \\ &= \Delta C^* - \Delta DIC_{diseq}. \end{aligned} \tag{3.4}$$

Here the first three terms give the nearly conservative tracer ΔC^* which can be calculated on the basis of concurrent observations of DIC, ALK, temperature, salinity, oxygen and nutrients. So the last unknown in 3.4 is ΔDIC_{diseq}. The equilibrium time-scale for the air-sea exchange of CO_2 is nearly a year. Because the disequilibrium term corresponds directly with the ΔpCO_2 at the time a water parcel was last in contact with the atmosphere, this disequilibrium can be quite large.
For estimation of ΔDIC_{diseq} Gruber et al. [1996] made three important assumptions: The first one is that they assume ΔDIC_{diseq} to be constant in time, because the long-term changes of this disequilibrium driven by the anthropogenic CO_2 perturbation is expected to be on the order of a few μmol kg^{-1}. Which leads to an uncertainty of a few μmol kg^{-1} for the anthropogenic CO_2 concentration. Secondly Gruber et al. [1996] assume that mixing occurs predominantly along isopycnal surfaces. And the final assumption is that in the last 250 years the natural carbon cycle did not change significantly, which is equivalent to the assumption of remaining in a dynamic steady-state.
Taking these assumptions into account it is easy to estimate ΔDIC_{diseq} on isopycnal surfaces containing regions which are not affected by anthropogenic perturbation. These are regions with ventilation times larger than the time since industrialisation, so they cannot contain any anthropogenic CO_2. The disequilibrium on these isopycnal surfaces can be estimated by simply averaging ΔDIC_{diseq} in the regions of zero anthropogenic CO_2:

$$\Delta DIC^i_{diseq}(\sigma) = \overline{\Delta C^*}\big|_{\sigma=const}\,, \tag{3.5}$$

where i stands for a water mass. For the estimation of ΔDIC_{diseq} on isopycnal surfaces which are completely contaminated with anthropogenic CO_2 this approach fails. But with the availability of age tracers, which include information about the time (τ) since the water was last in contact with the atmosphere, Gruber et al. [1996] modified their ΔC^*. By estimating DIC_{eq} at the time the water parcel was last in contact with the atmosphere they developed a time dependent ΔC^*_t:

$$\Delta C^*_t = DIC^{obs} - \Delta DIC_{bio} - DIC_{eq}(S, T, Alk, pCO_2(t_{obs} - \tau)), \tag{3.6}$$

where t_{obs} is the time of the water sample and τ the time at which the water parcel was last in contact with the atmosphere.

This ΔC_t^* is also a measurement of the air-sea disequilibrium. So the air-sea disequilibrium on isopycnal surfaces contaminated everywhere with anthropogenic CO_2 can be estimated from ΔC_t^* of the dominant water mass:

$$\Delta DIC^i_{diseq}(\sigma) = \overline{\Delta C_t^*}\big|_{\sigma=const}\,, \tag{3.7}$$

where i stands for the dominant water mass.

3.3 Estimating anthropogenic CO_2 as the difference between two equilibrium concentrations

There is a possibility to make a shortcut in estimating anthropogenic CO_2, if there are enough samples. Then for every sample ΔDIC_{diseq} can be measured separately:

$$\begin{aligned} C_{ant} &= \underbrace{DIC^{obs} - \Delta DIC_{bio} - DIC^{pi}_{eq}}_{\Delta C^*} - \underbrace{\Delta DIC_{diseq}}_{=\Delta C_t^*} \\ &= \Delta C^* - \Delta C_t^* \\ &= DIC_{eq}(S,T,ALK,pCO_2(t_{obs}-\tau)) - DIC_{eq}(S,T,ALK,pCO_2(t_{pi})) \end{aligned} \tag{3.8}$$

In an ocean general circulation model it is possible to estimate the anthropogenic CO_2 for every grid point in this way. Nevertheless this implies the assumption of constant air-sea disequilibrium and the uncertainties with regard to the water age enter directly into the estimation of anthropogenic CO_2.
In the following, the equilibrium concentration of DIC was calculated by a cubic fit as a function of temperature, salinity and ΔpCO_2 (pCO_2 perturbation). For more details see Appendix A.

3.4 Estimating anthropogenic CO_2 using transit time distributions (TTD)

The basis of the TTD method is the assumption that anthropogenic CO_2 penetrates into the ocean as a passive tracer responding to an evolving history in surface waters. In addition to this, the following three other assumptions are made for using the TTD method in order to estimate anthropogenic CO_2. The first one is that the biological uptake

of carbon did not change since pre-industrial times. This is a reasonable assumption and also made in the $\Delta C^\star$ method, as CO_2 is not a limiting factor on the marine biosphere. The second assumption is that the circulation is in steady (time averaged) state, which is also assumed in the $\Delta C^\star$ method. And the final assumption is that a single surface source region dominates the water at each interior point. Using these assumptions the concentration $c(\mathbf{r}, t)$ at an interior point $\mathbf{r}$ is related to the concentration history $c_0(t)$, of surface waters as

$$c(\mathbf{r}, t) = \int_0^\infty c_0(t - t')G(\mathbf{r}, t')dt', \tag{3.9}$$

where $G(\mathbf{r}, t')$ is the TTD at location $\mathbf{r}$ (Hall and Plumb [1994]; Haine and Hall [2002]). To apply Equation 3.9 it is necessary to know the surface history of anthropogenic CO_2. This history is estimated by using equilibrium inorganic carbon chemistry, so that

$$C_{ant,0}(t) = DIC_{eq}(S, T, Alk^0, pCO_2(t)) - DIC_{eq}(S, T, Alk^0, pCO_2(t_{pi})),$$

where DIC_{eq} is the equilibrium concentration of DIC, T the temperature, S the salinity, Alk^0 the alkalinity and $pCO_2(t)$ the partial pressure of atmospheric CO_2 at time t (pi stands for pre-industrial). As for the $\Delta C^\star$ method and the difference in equilibrium concentrations described in Chapters 3.2 and 3.3, the equilibrium concentrations of DIC are computed using a fit as a function of T, S and pCO_2 as described in Appendix A. Also necessary for applying Equation 3.9 is the knowledge of the TTDs at each interior location. As in Waugh et al. [2004] for calculating the TTDs the assumption was made that they can be approximated by inverse Gaussian functions, that is

$$G(t) = \sqrt{\frac{\Gamma^3}{4\pi\Delta^2 t^3}} exp\left(\frac{-\Gamma(t - \Gamma^2)}{4\Delta^2 t}\right), \tag{3.10}$$

where $\Gamma = \int_0^\infty \xi G(\xi)d\xi$ is the mean transit time ('mean age'), and $\Delta^2 = \frac{1}{2}\int_0^\infty (\xi - \Gamma)^2 G(\xi)d\xi$ defines the width Δ of the TTD. Given Γ and Δ it is possible to determine anthropogenic CO_2 using Equations 3.9 and 3.10, with $C_{ant,0}$ calculated as difference of equilibrium concentrations as described above. For a specified Γ/Δ it is possible to determine the Γ and hence $G(t)$ for which an observed tracer (for example CFC11 or CFC12) is reproduced using Equations 3.9 and 3.10. Substituting now $c_0 = C_{ant,0}$ and $G(t)$ into convolution integral 3.9 to determine the anthropogenic CO_2 (C_{ant}). Waugh et al. [2004] found out that tracer distributions could be well described using TTDs

with the ratio $\Gamma/\Delta = 1$. That is why in this study this ratio was used to determine the TTDs.

3.5 How to determine the water age

The previous section described how to determine the transit time distribution out of observed CFC or other other transient tracers (e.g. Tr, He). The following paragraph will describe how a single water age can be determined from observations of transient tracers such as CFCs. This can be done in the same way in observations and in ocean models. As described in Khatiwala et al. [2001] the water ages using transient tracers are biased towards younger values with respect to ideal age or the mean age of a water parcel due to mixing.

CFC derived water age: As there is no possibility to measure the water age directly in observations, it is necessary to estimate it out of measurable species. By observing tracers with a known atmospheric history it is possible to estimate the water age. Two of these tracers, CFC11 and CFC12, are integrated in the ocean model used here. By comparing the partial pressure of CFC with former surface partial pressures of CFC, the water age can be estimated. With the modelled CFCs this was done as follows: First computing the partial pressure of CFC (for example CFC11):

$$pCFC11 = \frac{[CCl_3F]}{K_{CFC11}(T,S)}, \tag{3.11}$$

where $[CCl_3F]$ is the CFC11 concentration and $K_{CFC11}(T,S)$ is the solubility of CFC11 as a function of T and S according to Warner and Weiss [1985]. This partial pressure of CFC11 is then compared with the history of atmospheric partial pressure of CFC11 (by courtesy of Stephen Walker; Figure 3.1), getting the age τ of the water parcel, which can be directly used for estimation of anthropogenic CO_2 using Equation 3.8. Of course this way of computing the water ages is not very accurate because mixing does not occur in this estimation, leading to underestimation of water ages in regions with low CFC concentrations (which leads to a large overestimation of anthropogenic CO_2 using this age as water age). In addition to this, the time series for atmospheric pCFC used in the model reaches from 1931 to 1997 (Figure 3.1). That is why the oldest water that could be detected is that of 1931. To get no conflicts with the age out of CFC just the rising branches of CFC in the atmosphere were used. That is for CFC11 between 1942 and 1991 and for CFC12 between 1931 and 1997.

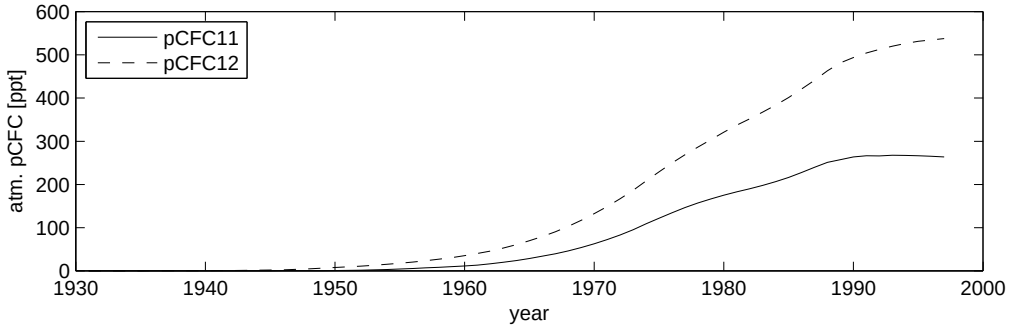

Figure 3.1: Time series of atmospheric pCFC [ppt] (partial pressure of CFC) for the Northern Hemisphere used as boundary condition for CFC modelling. Solid line: pCFC11; dashed line: pCFC12.

Ideal model age: In an ocean model it is possible to estimate the water age by computing an additional tracer representing the ideal age. This is done in the way that the model age is always zero at the surface and is then getting older while being transported into the interior by the physics of the model. This is not the true water age either (because the model is possibly not in steady state), however for a long integration time (in this model 141 or 236 years) it is a good choice. Additionally water older than the oldest model age does not contain any anthropogenic CO_2, because then it is from pre-industrial times.

Chapter 4

Comparison of anthropogenic CO_2 estimations

4.1 Distribution of anthropogenic CO_2 in the North Atlantic

For instance Thomas et al. [2001] and Sabine et al. [2004] showed that one of the most important areas of anthropogenic CO_2 accumulation is the North Atlantic. The distribution of the column inventory of anthropogenic CO_2 (Figure 4.1) shows the highest concentrations of anthropogenic CO_2 in the northern North Atlantic, where formation of deep water masses takes place, leading to high uptake rates. In addition to that, the transport of anthropogenic CO_2 is northward in the whole model domain (see also Völker et al. [2001] and Biastoch et al. [2007]). Especially northward transport within the warm surface waters of the subtropical Atlantic causes accumulation of anthropogenic CO_2 in the subpolar North Atlantic. In the western basin the southward propagation of North Atlantic Deep Water (NADW) can be seen as a tongue of high column inventories of anthropogenic CO_2. A smaller tongue of high values is found in the eastern basin. This may partly be caused by a too large fraction of the overflow flowing into the Rockhall Channel instead of into the Iceland Basin (Völker et al. [2001]). But the accumulation of anthropogenic CO_2 being significantly smaller in the eastern basin than in the western basin is consistent with data based estimates by Körtzinger et al. [1998]. These observations (Körtzinger et al. [1998]) are estimates along the WOCE A2 section (about 45°N). The absolute values on that section in this model simulation are about 10% to 15% smaller than the estimates by Körtzinger et al. [1998]. Further south in the sub-

tropical and tropical Atlantic anthropogenic CO_2 column inventories are generally low. Although in the upper water, near the surface, the anthropogenic CO_2 concentrations are even higher than in high latitudes. The higher column inventory of anthropogenic CO_2 is a result of the case that the ventilation of deeper water is much higher in the high latitudes than in the low latitudes of the North Atlantic. In observations the lowest values occur in the up-welling regions around the equator and along the African coast, where the strong horizontal flux divergence at the surface overcompensate the locally high air-sea flux rates. In these model simulations the lowest concentrations occur near the southern boundary of the model domain. This is the case, because all boundaries are closed with restoring to pre-industrial conditions. That is, of course, inconsistent with observations, and leads to underestimation of anthropogenic CO_2 by the model in regions where the influence of the southern boundary is high.

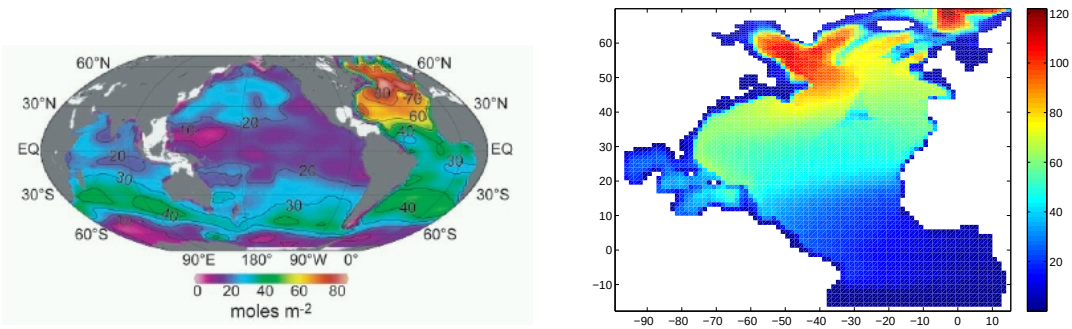

Figure 4.1: Column inventory of anthropogenic CO_2 [mol m^{-2}]. Left: of Sabine et al. [2004] and right: DDIC (difference of dissolved inorganic carbon (DIC) from a model run with realistically prescribed atmospheric pCO_2 minus the DIC of a model run with constant preindustrial atmospheric pCO_2) column inventory of the year 1994 of the climatological model run starting in 1765.

Estimates of the total inventory of anthropogenic CO_2 were done by Gruber [1998] within 10° latitude intervals throughout the North Atlantic. This total inventory was interpolated from sections (SAVE and TTO) to a basin wide integral and Gruber [1998] assumes the error to be of the order of 20%, although the error resulting from sections to a basin wide distribution is not easy to quantify. Nearly the same method to estimate anthropogenic CO_2 was used for the GLODAP data set (Key et al. [2004]). In Figure 4.2 Gruber [1998] and GLODAP data are compared to the model results. As a result of the closed southern boundary in the model, and the resulting difficulties described above, the total inventories south of about 10°N are in both observations (Gruber [1998] and

GLODAP) much higher than in the model simulation. Between 20°N and 50°N the modelled data is very close to the GLODAP estimations, but further north it overestimates these observations. This might also be an artefact of the closed northern boundary, because in the model anthropogenic CO_2 is accumulating at the northern boundary due to northward transport and high uptake rates. On the other hand the observations in GLODAP just reach up to about 65°N excluding the region north of Iceland, where also high anthropogenic CO_2 values occur in the model. Biastoch et al. [2007], who also

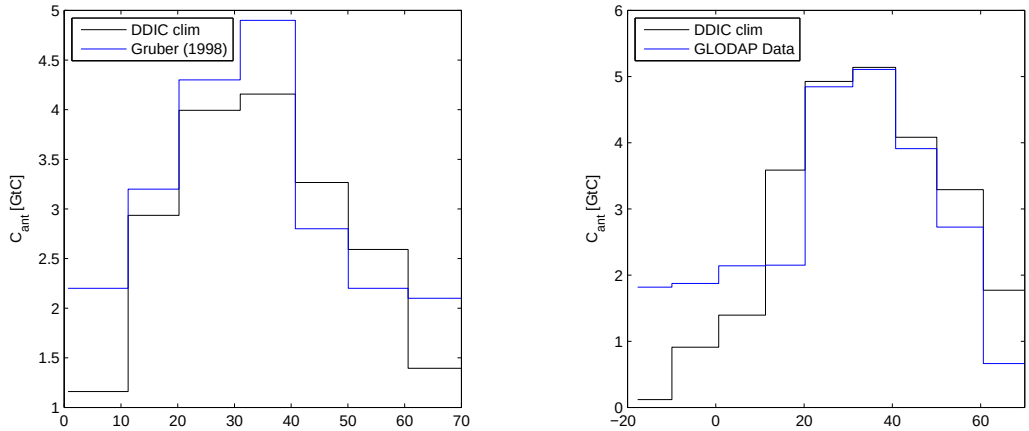

Figure 4.2: Vertical integrated anthropogenic CO_2 of the modelled DDIC (black line) and observations (blue line). Left: The observations are from the analysis of Gruber [1998] and inventories of the modelled data are from year 1982 of the climatological run starting in 1765. Right: Observations are from GLODAP (Key et al. [2004]) and inventories of the modelled data are from the year 1994 of the climatological run starting in 1765.

used models of the FLAME group (both 4/3 and 1/3 of a degree horizontal resolution) show that their anthropogenic CO_2 tracer underestimates the analysis of Gruber [1998] and GLODAP throughout the whole model domain (Figure 4.3). In contrast to the results presented here, Biastoch et al. [2007] used a passive tracer for the estimation of anthropogenic CO_2, whereas here the difference of DIC concentrations from two model runs, one with realistic atmospheric pCO_2 minus the one with constant pre-industrial pCO_2, is shown. Using the original version for the anthropogenic CO_2 tracer as used by Sarmiento and Orr [1992] (and as used by Biastoch et al. [2007]) leads to underestimation of anthropogenic CO_2 (see also Chapter 4.2). Additionally they started their model run in the year 1900, which also might lead to too low anthropogenic CO_2 values (see Chapter 4.2.2). But by using open boundaries they get results closer to observations in

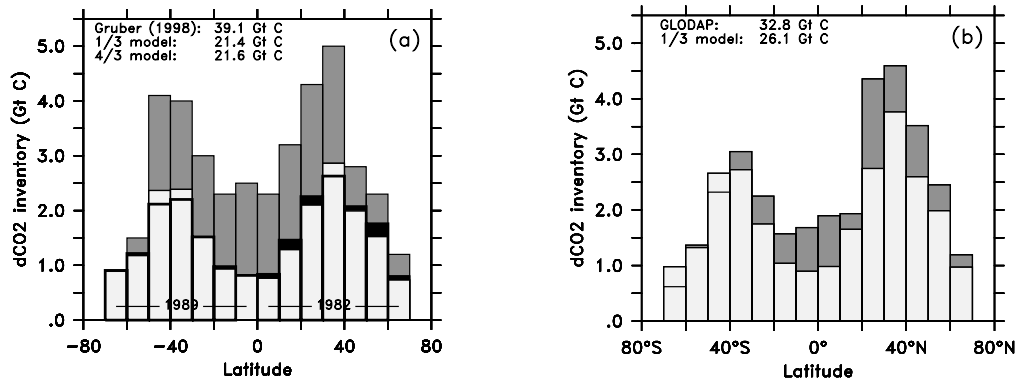

Figure 4.3: Figure 3 from Biastoch et al. [2007]: (a) Latitudinal dependence of vertically integrated anthropogenic CO_2 inventory of the two models (4/3°: black, 1/3°: light gray). Similar to the analysis of Gruber [1998] (dark gray) inventories for the North Atlantic were calculated from year 1982, for the South Atlantic from year 1989. (b) Similar for 1/3° model, year 1990, and GLODAP data [Sabine et al., 2004] (dark gray).

the northern North Atlantic and also in the southern North Atlantic. In the southern North Atlantic this is not only the case because of the choice of open boundaries but also because they used a model version reaching further south (down to 70°S).

The section of anthropogenic CO_2 along 35°W for modelled DDIC and anthropogenic CO_2 of the GLODAP data set is shown in Figure 4.4. It can be seen that the vertical structure of anthropogenic CO_2 in mid latitudes are in both cases very similar, leading to small differences in the specific inventory (Figure 4.2). In high latitudes the anthropogenic CO_2 is reaching much deeper than in the observations (GLODAP: Key et al. [2004]), but with lower anthropogenic CO_2 concentrations at the surface. This might be on the one hand the result of deep convection in the Labrador Sea, reaching down to about 1000 m in winter and slowly decreasing DDIC concentrations there up to about 2200 m. This indicates rapid vertical homogenisation within the Labrador Sea Water (LSW) in the model, probably by diffusion. The absolute values are lower in the model, probably because in the estimations of anthropogenic CO_2 for the GLODAP data set, CFC ages were used. But by assuming a saturation of 90% to 100% for CFCs, which is typical for the LSW (Smethie and Fine [2001]), this would indicate the same saturations for anthropogenic CO_2 which seem to be very high. This is because anthropogenic CO_2 has an about tenfold longer equilibration time than CFCs, due to the buffering of the carbonate system, that in the model is expressed by using a NPZD model.

Figure 4.5 shows the time-series of the prescribed atmospheric pCO_2 in the model (black

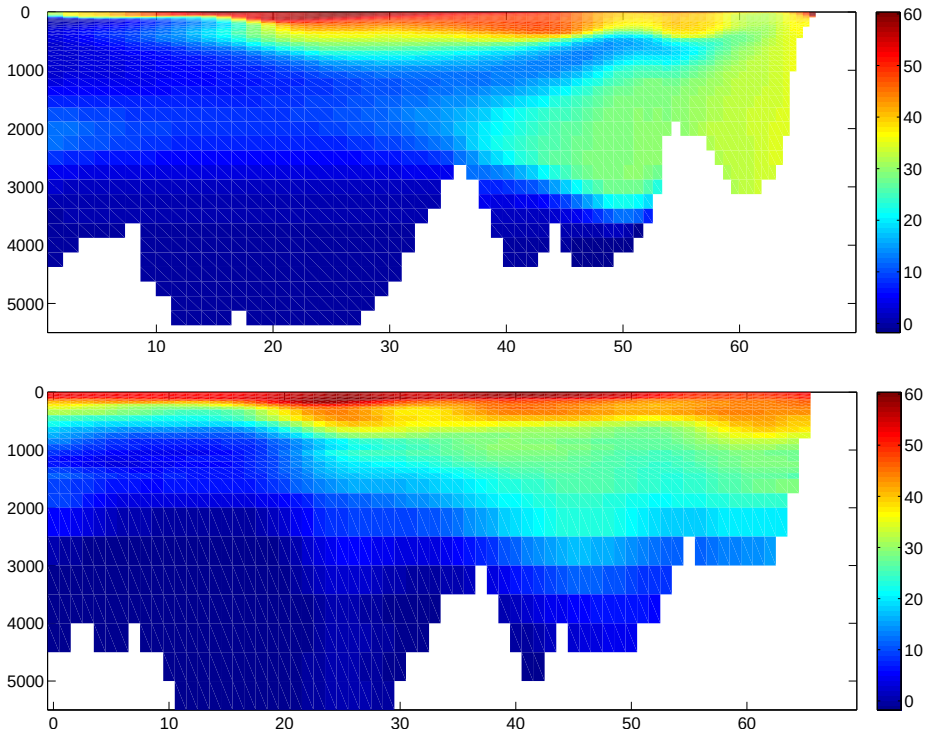

Figure 4.4: Section of anthropogenic CO_2 [mmol m^{-3}] along 35°W. Upper: DDIC of the model for the year 1994 from the climatological model runs starting in the year 1765; lower: anthropogenic CO_2 of the GLODAP data set (Key et al. [2004]).

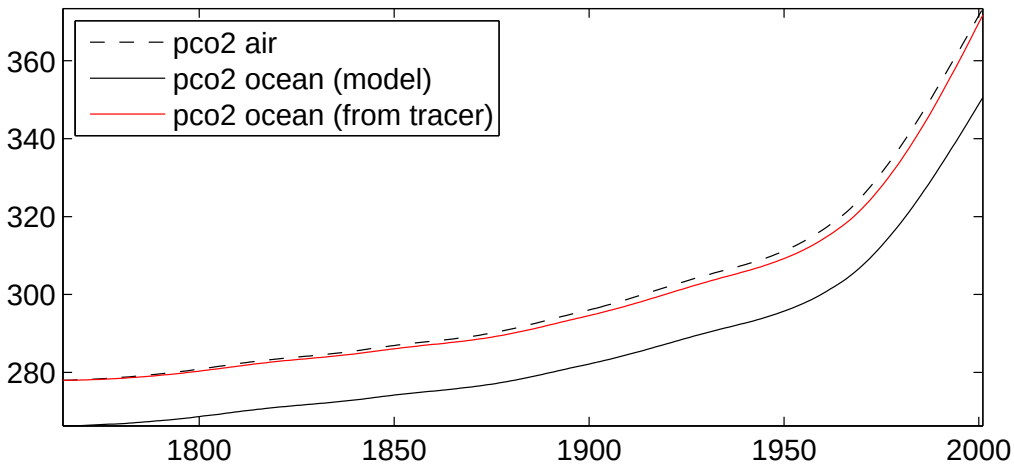

Figure 4.5: Prescribed atmospheric partial pressure of CO_2 (in ppm, dashed line and modelled surface values (solid line) at BATS station (64°W, 32°N).

dashed) in comparison to modelled surface pCO_2 values at BATS station (64°W and 32°N). The pCO_2 concentration modelled by the anthropogenic CO_2 tracer (red) is much closer to the prescribed atmospheric concentration than the modelled values by using DDIC concentrations (black). Compared to observations of Bates [2001], surface pCO_2 concentrations modelled as DDIC are comparable to observations, whereas the surface pCO_2 modelled by the anthropogenic CO_2 tracer are much closer to the atmospheric pCO_2 concentrations than observed. Biastoch et al. [2007] got ocean surface pCO_2 values between this two solutions by computing anthropogenic CO_2 as a passive tracer.

4.2 DDIC compared to ACO2TR

For the model experiments two independent methods of modelling anthropogenic CO_2 where introduced to the model of the North Atlantic used here, an abiotic passive tracer method (ACO2TR) on the one hand, and on the other a method using a simple biological (NPZD) model (DDIC). In the case of the tracer method the anthropogenic CO_2 is integrated as a passive tracer with a pCO_2 perturbation at the surface boundary (see Chapter 2.2.2 and Sarmiento and Orr [1992]), including the assumption that the ocean circulation and the biological carbon cycle are in steady state. This method is very useful to minimise the computational costs, because only one tracer has to be added to an ocean general circulation model and no biology is needed. In contrast to that is the other method in which anthropogenic CO_2 is computed as the difference of two model runs including a simple biological (NPZD) model. In this case four tracers (nutrients, phytoplankton, zooplankton and detritus) plus a tracer for dissolved inorganic carbon (DIC) are needed. Here the anthropogenic CO_2 is the difference between the total CO_2 of a model run with constant pre-industrial atmospheric pCO_2 subtracted from a run with realistically rising atmospheric pCO_2 (DDIC). The physics in both methods are the same, so the results of both methods can be compared directly. The remaining problem might be that in the case of ACO2TR a model trend is remaining and not easy to remove. It is not possible to remove a linear trend as in other experiments, because the boundary condition is the nonlinear rising pCO_2 in the atmosphere. In case of the DDIC a possible trend of the model is automatically removed by taking the difference of the two modelled DIC solutions. That is why this version of modelled anthropogenic CO_2 is called the "true" anthropogenic CO_2 of the model. The observational methods, adapted to the model output, as well as the tracer method (ACO2TR) directly modelled are in the further analyses compared to this "true" anthropogenic CO_2. Although this

is of course not the true anthropogenic CO_2 of the real ocean. But as all methods are used in the same model, this is the basis to which the best comparison can be done.
The relative deviation of the vertical integral of ACO2TR from DDIC (as shown in Figure 4.6 for the model year 1996 of a model run starting in 1860) makes clear that in nearly the whole model domain the ACO2TR underestimates the true anthropogenic CO_2 of the model. In the northern part of the model region (north of about 20°N) the true anthropogenic CO_2 is underestimated by the tracer by about 15% to 20%. This underestimation occurs nearly in the whole model domain except of the boundaries in the south and in deep waters near the bottom, where nearly no anthropogenic CO_2 accumulation is suspected. In the south, the underestimation is lower because on the one hand the absolute amount of anthropogenic CO_2 here is lower, and on the other hand the influence of the closed southern boundary with restoring to no anthropogenic CO_2, which is the case in both solutions, is more present in that region.

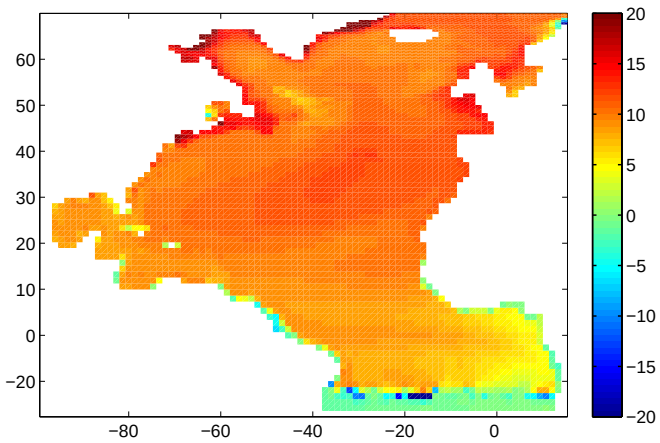

Figure 4.6: Relative difference (in %) of the vertical integral of anthropogenic CO_2 integrated as difference to that as a passive tracer ((DDIC - ACO2TR)/DDIC*100) for the model year 1996 of a climatological run with reference pCO_2 of 278 ppm in the pre-industrial atmosphere (after 136 years of integration).

For parametrisation of the surface flux of anthropogenic CO_2 Sarmiento and Orr [1992] first approximate the pre-industrial surface ocean being in equilibrium with the atmospheric $pCO_{2,0}$ of 280 ppm ($pCO^{oc}_{2,0}$), taking a modelled temperature of a global ocean model, imposing a uniform salinity of 35 and an alkalinity of 2300 μeq kg^{-1}. Out of that $pCO^{oc}_{2,0}$ they computed a corresponding pre-industrial ocean surface DIC (DIC_0),

yielding DIC_0 as a function of temperature. Then the surface DIC was increased incrementally and the pCO_2 was calculated. In this way they got a table relating DIC and pCO_2 to each other and to temperature. Using this relationship in conjunction with the pre-industrial values ($pCO^{oc}_{2,0}$ and $pCO_{2,0}$) they were able to obtain z_0 and z_1 from Equation 2.3. As a first try in a model run exactly these values were used, leading to an underestimation of anthropogenic CO_2 in comparison with the also modelled DDIC (see above). With this modelled DDIC it is possible to estimate the exact $dpCO^{oc}_2$ in the ocean model, and to recompute z_0 and z_1 by using the modelled DDIC and $dpCO^{oc}_2$, which takes also into account that the ocean is not everywhere in equilibrium with the atmosphere. The resulting functions of temperature for z_0 and z_1 are

$$z_0 = 1.289066 + 0.002111 \cdot T - 0.000187 \cdot T^2 \tag{4.1}$$

and

$$z_1 = 0.004919 - 1.70 \cdot 10^{-4} \cdot T + 2.00 \cdot 10^{-7} \cdot T^2. \tag{4.2}$$

Using this improved parameterisation for another model run leads to concentrations of ACO2TR much closer to the true anthropogenic CO_2 (DDIC) of the model. Figure 4.7 shows that the total inventory of the whole model domain of the anthropogenic CO_2 tracer derived by the corrected parametrisation (red dashed) is less then 2% lower than that of DDIC (black). In contrast to that in the uncorrected model run the total inventory was much lower (red) (10% underestimation of DDIC after 1940).
Regional differences can be seen in the vertical integrated anthropogenic CO_2 (Figure 4.8(b)). Before the correction there was an underestimation of DDIC by the tracer everywhere (Figure 4.6). In contrast to that, now there are some regions in which DDIC is slightly overestimated and others where it is underestimated by ACO2TR, but the relative difference in both cases is less than 5%. Larger deviations occur only in some grid points near the basin boundaries, where for some unknown reason anthropogenic CO_2 is accumulating. Overestimation takes place in the Labrador Sea, where a high amount of anthropogenic CO_2 enters the ocean, because of deep water formation. This overestimation is a result of an overestimation by about 20% of the prescribed surface flux of ACO2TR in this region (Figure 4.8(a)). Before correcting the parametrisation the surface flux in the deep water formation areas was the same as or slightly underestimating the true DDIC flux, which led to high underestimation of anthropogenic CO_2 in this region. On a section along 35°W for the model year 1996 (with integration

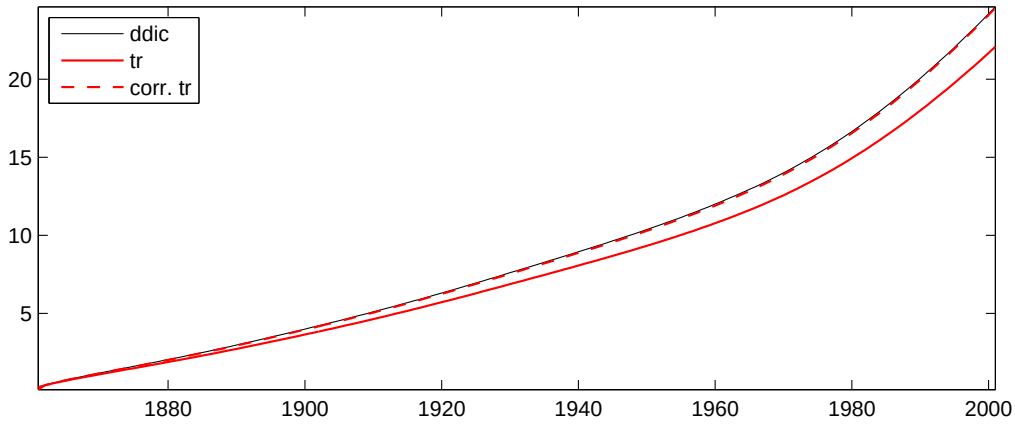

Figure 4.7: Time-series of total inventory of anthropogenic CO_2 in Gt C; black: DDIC, red: ACO2TR with original parameterisation of Sarmiento and Orr [1992], red dashed: ACO2TR with corrected parameterisation (using 4.1 and 4.2; can not be clearly seen); model run starting in 1860 with pre-industrial atmospheric reference pressure of 278 ppm.

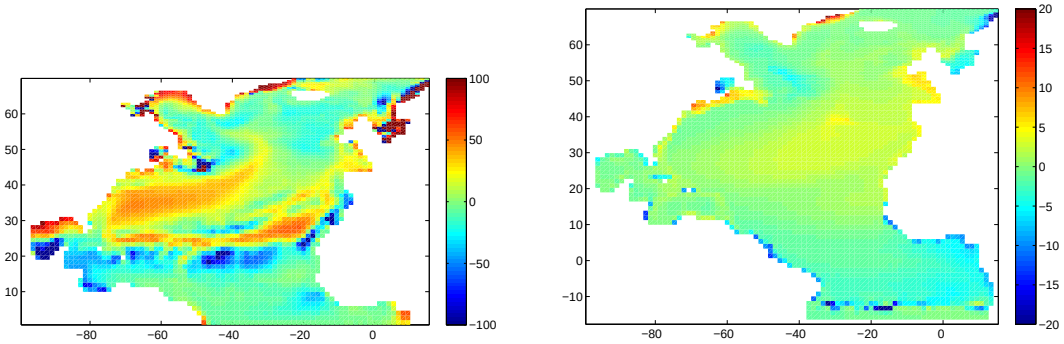

(a) Relative difference of CO_2 surface fluxes

(b) Relative difference of vertically integrated anthropogenic CO_2 concentration

Figure 4.8: Relative difference (in %) of (a) anthropogenic CO_2 surface fluxes and (b) vertically integrated anthropogenic CO_2 concentrations [$mol\,m^{-2}$] of DDIC to the same of the passive tracer with corrected parameterisation ((DDIC - ACO2TR^{corr})/DDIC*100). Shown is the model year 1996 of a climatological run with reference pCO_2 of 278 ppm in the pre-industrial atmosphere (after 136 years of integration).

since 1860) the underestimation of DDIC by the corrected ACO2TR takes place in the upper 1500 m of the mid latitudes (Figure 4.9). The black lines are the isopycnals $\sigma_\theta = 26.7$ and $\sigma_\theta = 27.3$, representing the density classes of Central and Intermediate

water masses lying above deep water masses. These water masses originate mainly from subducted water of the subtropical convergence and the mid latitudes, where the DDIC surface flux is underestimated by the prescribed ACO2TR-flux (by about 30%) even after recomputing the flux parametrisation. In the original version this underestimation was much larger (up to 60%). The influence of these water masses is also visible by positive values for the relative difference of the vertical integral of anthropogenic CO_2 (Figure 4.8(b)) in mid latitudes. North Atlantic Central water crops out at about 30°N to 40°N and it reaches down to about 1000 m. The Intermediate water is lying underneath, reaching down to about 1500 m and out-cropping at about 50°N in the eastern basin of the North Atlantic, and is getting thinner from east to west. The main pathway of North Atlantic Deep Water (NADW) is through the western basin of the North Atlantic. That is why the underestimation of anthropogenic CO_2 by ACO2TR decreases from east to west in mid latitudes, where the influence of the much thicker deep water layers is getting stronger by integrating over the whole water column.

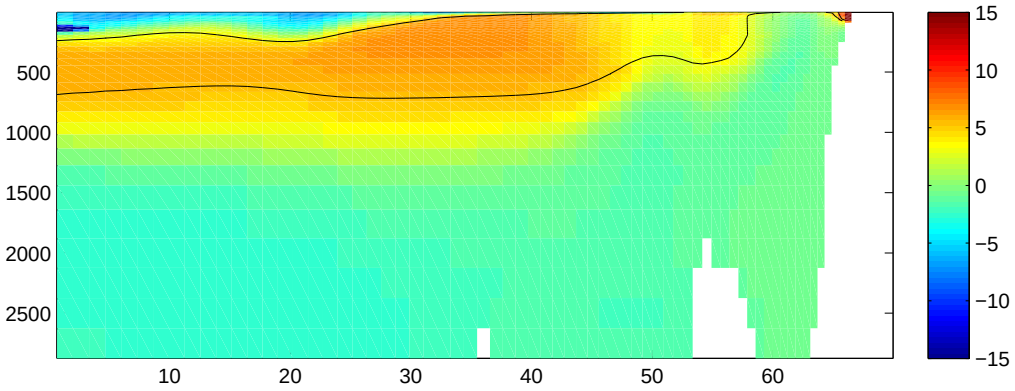

Figure 4.9: Section of DDIC relative to ACO2TR (with corrected parameterisation) in % along 35°W. The black lines are the isopycnals $\sigma_\theta = 26.7$ and $\sigma_\theta = 27.3$; model year 1996 (climatological run with reference pCO_2 of 278 ppm in the pre-industrial atmosphere; after 136 years of integration).

In all other experiments described in Chapter 2.3, and used for studies in the further chapters, ACO2TR was computed with the improved parameterisation after Sarmiento and Orr [1992].

4.2.1 Discrepancies with aspect to boundary conditions

As described in Chapter 2.1 all lateral boundaries of the model are closed with restoring to pre-industrial conditions. Especially near the southern boundary and the Mediter-

ranean inflow (into the North Atlantic) this leads to underestimation of anthropogenic CO_2 in the model compared to the suspected anthropogenic CO_2 concentrations of the real ocean. Transports near the southern boundary are not comparable with observations, because inflow of anthropogenic CO_2 entering the Atlantic Ocean by the Aghulas Current, or with deep water masses formed in the Southern Ocean, is not represented in the model region. In Völker et al. [2001] nearly the same model, reaching from 70°S to 70°N, was used with open boundaries and restoring to time dependent profiles of anthropogenic CO_2. Additionally a reference run with restoring to zero instead of time dependent profiles for anthropogenic CO_2 was done in that study. They found out that north of 24°N the influence of the southern boundary leads to about 4% difference of anthropogenic CO_2 inventory between the original experiment and the control run with restoring to zero. The effect of restoring near the Mediterranean inflow is centred around the isopycnals $27.4 < \sigma_\theta < 27.6$ resulting in a local increase of about 30% near the Gulf of Cadiz for the model run with restoring to time dependent anthropogenic CO_2 profiles compared to the model with restoring to zero. This means that in the model used here, the anthropogenic CO_2 might be highly underestimated in this region, but in other regions, especially in the most contaminated northern North Atlantic, and in deep water regions, the representations are comparable with other model simulations and observations.

4.2.2 Influence of integration starting time

The higher the resolution of a model the longer it takes to make long integrations and thereby the higher are computational costs. Using a regional model with relatively coarse resolution gives the opportunity to run an experiment comparing absolute values of anthropogenic CO_2 according to the starting point of integration. As described in Chapter 2.3 in addition to a long integration, starting in the year 1765, where no anthropogenic CO_2 was released to the atmosphere, another experiment starting in the year 1860 was done. To get comparable results of the absolute values of both model based anthropogenic CO_2 solutions (DDIC and ACO2TR) in both cases the pre-industrial pCO_2 value of the starting year was taken for the pre-industrial reference run. So for the long run the pre-industrial atmospheric pCO_2 is 278 ppm and for the shorter run 288 ppm, taken from the prescribed atmospheric pCO_2 of the model (see Chapter 2.3). In all cases anthropogenic CO_2 is zero at the beginning of the integration. But for the shorter run the difference of the actual atmospheric pCO_2 to the pre-industrial reference is always 10 ppm smaller than that of the longer run, because the difference for the

prescribed pre-industrial pCO_2 of the atmosphere differs by 10 ppm. This leads to lower anthropogenic CO_2 concentrations in the shorter model run. Figure 4.10 shows this for the time-series of the total DDIC inventory (in Gt C). In both cases the inventory is zero at the beginning of the integration and then continuously rising. Nevertheless, as supposed, the total amount of anthropogenic CO_2 in the longer model run is by about 4 Gt C to 6 Gt C higher than in the model run beginning in the year 1860. As a result of increasing anthropogenic CO_2 with time, the relative difference between the two experiments decreases down to 20% at the end of integration in the year 2001.

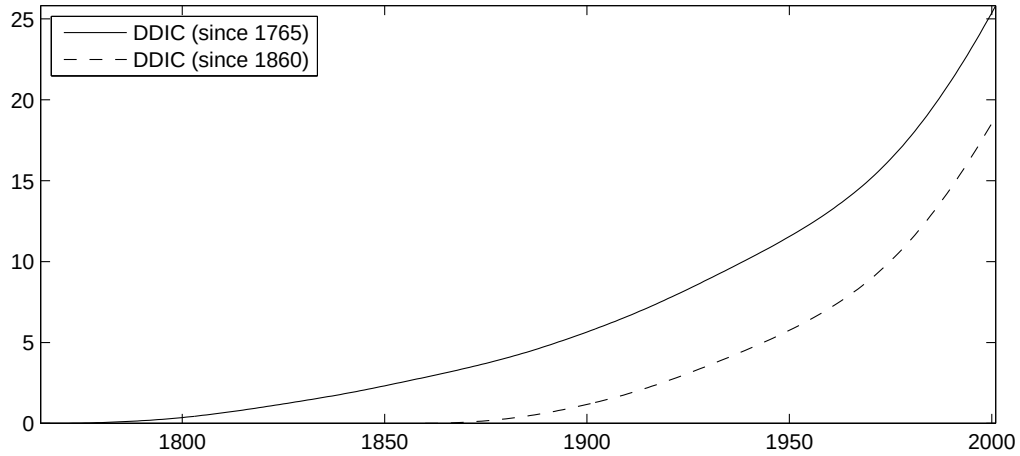

Figure 4.10: Total inventory of anthropogenic CO_2 (DDIC) in Gt C of the two different climatological model runs; solid line: run since 1765 (with pre-industrial atm. pCO_2 of 278 ppm); dashed line: run since 1860 (with pre-industrial atm. pCO_2 of 288 ppm).

Locally the results differ from each other in the same way. In regions with high anthropogenic CO_2 concentrations the relative difference between the two experiments is 15% to 20% at the end of integration time and in regions which are less contaminated with anthropogenic CO_2 it is much higher. In contrast to that, the absolute difference at each point is just slightly increasing with time (with a difference of about 1 $mmol\,m^{-3}$ between 1900 and 2001).

4.3 $\triangle C^{\star}$ Method

Another question, not only interesting for ocean modelling, but especially for field measurements, is that of estimating anthropogenic CO_2 out of measurable variables. A method widely used for this purpose is the so called $\Delta C^{\star}$ method after Gruber et al.

[1996], as described in Chapter 3.2. This method is used on isopycnals because mixing is assumed to occur predominantly on isopycnal surfaces, and as described in Gruber et al. [1996] there is a possibility to estimate a quasi conservative tracer ΔC^*:

$$\Delta C^* = DIC^{obs} - DIC_{eq}(S, T, Alk, pCO_2|_{pi}) \\ - r_{C:O_2}(O_2 - O_2^{sat}) - \frac{1}{2}(ALK - ALK^0 + r_{N_2:O_2}(O_2 - O_2^{sat})) \quad (4.3)$$

The other two important assumptions for this method are on the one hand that the ocean is in a dynamic steady-state, implying that the natural carbon cycle did not change significantly since pre-industrial times. And on the other hand it is assumed that the air-sea disequilibrium of the oceanic surface DIC concentrations remains constant in time. On isopycnals that are supposed to have regions with no anthropogenic CO_2 this disequilibrium can be estimated as an average of ΔC^* in this region, so that the anthropogenic CO_2 (C_{ant}) can be estimated as

$$C_{ant} = \Delta C^* - \overline{\Delta C^*}|_{\sigma=const},$$

where $\overline{\Delta C^*}|_{\sigma=const}$ represents the mean ΔC^* of the isopycnal surface interval in the region without anthropogenic influence.
On isopycnals that are everywhere contaminated with anthropogenic CO_2 the tracer ΔC^* was replaced by a time dependent tracer ΔC_t^*, where the equilibrium concentration with the pre-industrial atmosphere (DIC_{eq}) is replaced by the equilibrium concentration at the time the water parcel was last in contact with the atmosphere (DIC_{eq}(t)). As on the other isopycnals the disequilibrium can be estimated as an average of this time dependent tracer. In this case C_{ant} can then be estimated by

$$C_{ant} = \Delta C^* - \overline{\Delta C_t^*}|_{\sigma=const},$$

where $\overline{\Delta C_t^*}|_{\sigma=const}$ is the mean ΔC_t^* on the density surface under consideration.
By adapting this method to the model, the estimation of equilibrium DIC concentrations (DIC_{eq}) was not exactly done as in Gruber et al. [1996], where DIC_{eq} was estimated as a linearisation around ocean mean values of temperature, salinity and alkalinity. In this model, alkalinity is not computed directly, but as a function of salinity, and there is the possibility to compute true DIC_{eq} from a model run including biology. Out of this, a cubic fit for DIC_{eq} as a function of temperature, salinity and ΔpCO_2 was created

(see Appendix A). Estimating ΔC^* or ΔC_t^* with modelled data for the biological part of Equation 3.2 (DIC_{bio}), only the part of the soft tissue pump was computed. This was done, because alkalinity is not directly part of the model, but linked to salinity. Which means that there is no calcification in the model, so that the part of the $CaCO_3$ dissolution cannot be estimated out of the modelled data. The Redfield ratio that was used for this estimation is -0.66 for $r_{C:O_2}$, which is the same used in the NPZD model. The resulting formula for the estimation of anthropogenic CO_2 on an isopycnal containing anthropogenic CO_2 everywhere is:

$$\begin{aligned} C_{ant} &= DIC - DIC_{eq}^{pi} - r_{C:O_2}(O_2 - O_2^{sat}) - \\ &\quad - \underbrace{\left(\overline{DIC - DIC_{eq}(t) - r_{C:O_2}(O_2 - O_2^{sat})}\right)|_{\sigma=const}}_{\overline{\Delta C_t^*}|_{\sigma=const}} . \end{aligned} \tag{4.4}$$

The mean value of ΔC_t^* on an isopycnal was estimated for water younger than 30 years. In Gruber [1998] this was done because CFC- or tritium and helium-3 ages lead to an acceptable error for ΔC_t^* if the water age is not larger than 30 years. Here it is possible to compare the results by using both, the modelled ideal age, and CFC ages in the same way. A southern end member of a water mass, like in Gruber [1998] cannot be taken into account in this study, because the southern boundary of the model region is closed at 20°S. If the outcrop region is known, the disequilibrium at the time a water parcel was last in contact with the atmosphere can be estimated by averaging ΔC_t^* at that time in the outcrop region. Using this disequilibrium in Equation 4.4 should improve this method, because in that case the time dependency of the air-sea disequilibrium is taken into account (as in Hall et al. [2004]) and not assumed to be constant.

4.3.1 Comparing the $\Delta C^\star$ method with modelled DDIC on different isopycnals

As shown by Sabine et al. [2004] one of the most important areas of anthropogenic CO_2 accumulation are the formation areas of deep water in the North Atlantic (Labrador Sea and Greenland Sea). In the model used here, isopycnals with a mean value of $\sigma_\theta = 27.45$ (reaching from 27.3 to 27.6) outcrop in this regions (Figure 4.11). Estimating anthropogenic CO_2 by using the $\Delta C^\star$ method (with $\Delta C^\star{}_t$) there tends to underestimate the true anthropogenic CO_2 (DDIC) by about 20% directly in the formation regions. But further south on this isopycnal it overestimates DDIC by 20% and more (Figure 4.12).

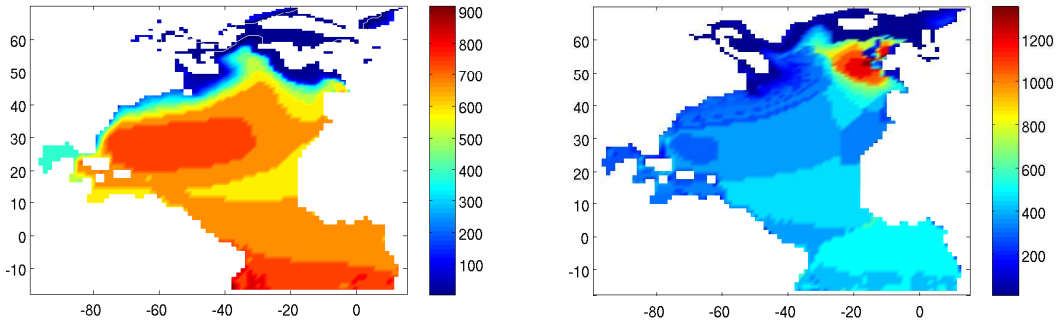

(a) Depth of σ_θ =27.3 (b) Thickness of σ_θ = 27.3 - 27.6

Figure 4.11: Depth [m] of the isopycnal σ_θ = 27.3 and thickness [m] of the core of North Atlantic Intermediate water (σ_θ = 27.3 - 27.6) for the model year 1996 of the climatological experiment starting in 1765 with pre-industrial atmospheric reference pCO_2 of 278 ppm.

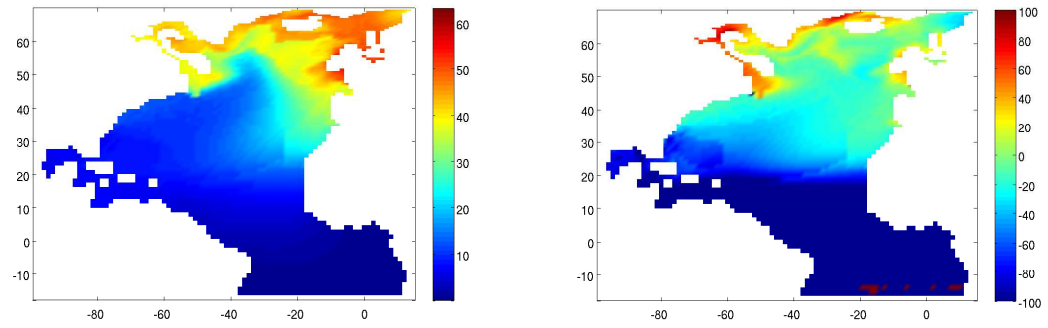

(a) DDIC (b) rel. diff DDIC $\Delta C^{\star}$ method

Figure 4.12: Anthropogenic CO_2 on the isopycnal σ_θ = 27.3 - 27.6 in the model year 1996 (run since 1765); a) DDIC [mmol m^{-3}]; b) relative difference of DDIC - $\Delta C\star$ method [%].

In fact this overestimation might be an artefact of numerical problems (dividing by small numbers), because of the low concentrations of anthropogenic CO_2 in the deeper regions further south on the isopycnal. On the other hand this overestimation may have its origin in the influence of Antarctic Intermediate Water entraining anthropogenic CO_2. This cannot be part of the modelled DDIC, because the southern boundary is closed. But by adapting the $\Delta C^{\star}$ method to the model, by using data from the model output, this influence can be seen. DIC is restored to pre-industrial data and oxygen, temperature and salinity (which are needed in the $\Delta C^{\star}$ method) are restored

to climatological mean values at the boundaries (which are the same for both model runs, the pre-industrial one and the one with realistically rising atmospheric pCO_2). But by restoring to climatological mean values for oxygen, temperature and salinity at the southern boundary the influence of the Southern Ocean is represented, leading to higher anthropogenic CO_2 concentrations using the $\Delta C^\star$ method there. Not shown is the ideal water age reaching from 0 in the outcrop region getting older further south up to about 170 years off the coast of Guinea. Using CFC12 ages of modelled CFC12 (as described in Chapter 3.5 and Equation 3.11) instead of ideal age on these isopycnals, leads to anthropogenic CO_2 concentrations which are slightly higher than the estimations using ideal age (less than 1%). Nevertheless the water age estimated from CFC12 differs substantially from the modelled ideal age. In the formation areas of deep water in the North Atlantic CFC12 is undersaturated by about 5% to 8% leading to slightly overestimated water ages in relation to ideal age (inducing water ages of a few years even at the surface). But especially in deeper regions CFC ages (both that of CFC11 and CFC12) tend to underestimate the ideal age the longer the water has lost contact to the atmosphere. This problem occurs because CFCs started penetrating into the ocean about 1930. And as soon as a water parcel is mixed with CFC-free water it is biased towards younger ages (see England and Holloway [1998]).

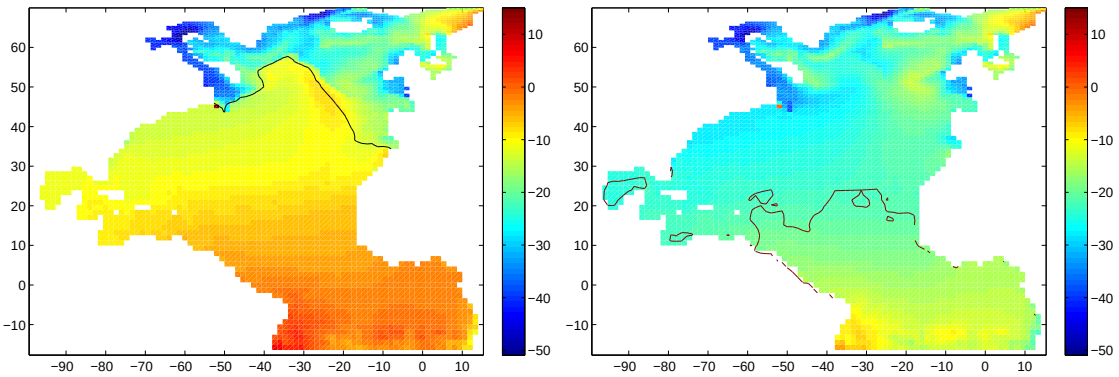

Figure 4.13: $\Delta C_t^\star$ [mmol m^{-3}] (time dependent quasi conservative tracer as used for the $\Delta C^\star$ method after Gruber et al. [1996]) on the isopycnal $\sigma_\theta = 27.3 - 27.6$. Left using ideal model age and right using CFC12 derived age. The black line is the 30 year contour line for the represented water age. Shown is the model year 1996 of the climatological model run starting in 1765.

Nevertheless it might surprise that the two different ages lead to nearly the same results. In both cases $\Delta C_t^\star$ is estimated in the same way and a constant value (ΔDIC_{diseq}), which is a mean value of $\Delta C^\star{}_t$ along an isopycnal, is added to this. Gruber et al. [1996] noted

that $\Delta C^\star{}_t$ is more or less constant within the scatter of their data. In the model this is not really the case, but for water younger than 30 years things look slightly better (Figure 4.13). Nevertheless at the boundary of the outcrop region of the isopycnal surface with a mean value of $\sigma_\theta = 27.45$, large negative values occur using either ideal age or CFC12 derived water age. These values occur in some regions near the surface, where the nutrient concentration is very low. Because of constant Redfield ratios this leads to high oxygen and low DIC concentrations. Here the problem is that the annually averaged concentrations are used. And in this regions low nutrient concentrations from algae blooms in summer are dominating the annual mean. This occurs in the region between Greenland and Iceland. On the other hand some regions of the Labrador Sea are covered with ice in wintertime. In the model all tracer fluxes are set to zero if the temperature falls below freezing point. This leads to under-saturation of DIC and oxygen, leading to high negative values of $\Delta C^\star{}_t$ in that region. In the remaining areas on this isopycnal $\Delta C^\star{}_t$ is more or less constant (about -17 mmol C m^{-3}) by using CFC12 derived water ages. But using ideal age gives higher values the older the water is. This implies that the disequilibrium is not constant with time (the variation of the air-sea disequilibrium with time is discussed in Chapter 4.4.1). Using the actual disequilibrium of the outcrop region when the water has lost contact with the atmosphere should improve the estimation of anthropogenic CO_2. This was done in case of the ideal age, and leads to small improvements on this isopycnal in the mid latitudes. Large underestimation due to supersaturation of DIC at the northern boundary of the outcrop regions remains.

As an example for the $\Delta C^\star$ method without time dependence the deep isopycnal $\sigma_4 = 45.838$ - 45.863, representing lower North Atlantic Deep Water (NADW), was chosen. This is comparable to observations by Gruber et al. [1996], but the depth range of this isopycnal in the model differs from that of observations. It reaches from about 2800 m to 3300 m in the model whereas Gruber et al. [1996] found depths of 3500 m to 3800 m for this isopycnal. Nevertheless it is representing the same water mass in both cases. For the region between 20°S and 20°N Gruber et al. [1996] assumed to have no anthropogenic CO_2 on this isopycnal. Therefore the method just using the time-independent quasi conservative tracer $\Delta C^\star$ can be used, where ΔDIC_{diseq} can be estimated as mean value in a region of no anthropogenic CO_2. By this Gruber et al. [1996] got -16 mmol m^{-3} for ΔDIC_{diseq}, in contrast to ΔDIC_{diseq} of about 4.4 mmol m^{-3} in this study. The result for anthropogenic CO_2 using this method is shown in Figure 4.14. It can be seen that on such an isopycnal this method leads to large errors in the whole region. Near the southern boundary up to about 10°N the $\Delta C^\star$

method overestimates the true anthropogenic CO_2 of the model, whereas everywhere else anthropogenic CO_2 is underestimated. One problem might be the fact that in the model the influence of alkalinity cannot be taken into account, because it is not part of the model. On the other hand in this model there is nearly no region which is not contaminated with anthropogenic CO_2 on that isopycnal (as can be seen in Figure 4.14a). Just close to the southern boundary of the model region there is no DDIC, which is determined by the restoring to pre-industrial conditions at the boundaries.

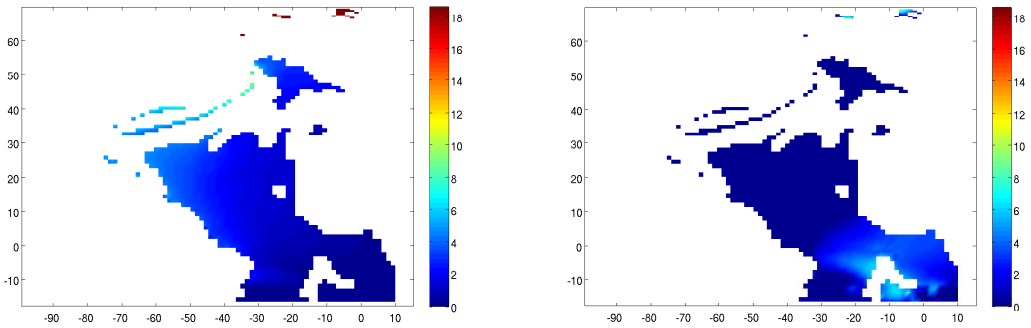

(a) DDIC (b) $\Delta C^{\star}$ method

Figure 4.14: Anthropogenic CO_2 [mmol m^{-3}] on the isopycnal σ_4 = 45.838 - 45.863 (lower NADW) in the model year 1996 of the climatological model run starting in 1765.

For comparison Table 4.1 shows the volume and anthropogenic CO_2 inventory for different isopycnic intervals throughout the whole model domain in the model year 1996 (of the climatological model run starting in 1765). It can be seen that in about 30% of the North Atlantic most of the anthropogenic CO_2 is accumulated. This is all water with densities of $\sigma_\theta < 27.7$. As described before the errors of using the $\Delta C^{\star}$ method are very large on deeper isopycnals. That is why in the region of $\sigma_\theta > 27.7$ it was not applied to the model. On shallow isopycnals ($\sigma_\theta < 26.3$) the amount of anthropogenic CO_2 estimated with the different methods are comparable. The modelled anthropogenic CO_2 tracer (ACO2TR) slightly overestimates DDIC in this regions (as described already in Chapter 4.2). In contrast to that all methods using a single water age (anthropogenic CO_2 estimated as the difference of two DIC equilibrium concentrations (ACO2EQDIFF) and both versions using the $\Delta C^{\star}$ method) are overestimating the DDIC concentrations by about 20%. On these shallow isopycnals this overestimation is smallest by using the $\Delta C^{\star}$ method with ideal age for determining the water age, followed by the difference of

two equilibrium concentrations (ACO2EQDIFF; with ideal age). The highest overestimation occurs by using the $\Delta C^\star$ method with CFC12 for information about the water age. In the region of central water masses and the upper part of deep water masses ($26.3 < \sigma_\theta < 27.7$) ACO2TR slightly underestimates DDIC whereas it is slightly overestimated by ACO2EQDIFF. The overestimation using the $\Delta C^\star$ method is, at about twice the amount of DDIC, much more drastical on these isopycnals.

To sum up it can be said that the $\Delta C^\star$ method leads to anthropogenic CO_2 concentrations in the range of modelled DDIC in well ventilated regions. Here the differences are just a few mmol m^{-3}. But in regions of older water high overestimation of up to 50% (as shown in Table 4.1) takes place. On deeper isopycnals, which are supposed to contain no anthropogenic CO_2, the adaption of the $\Delta C^\star$ method leads to unacceptable discrepancies in comparison to modelled DDIC. By taking the mean value of the quasi conservative tracer $\Delta C_t^\star$ along an isopycnal locally large differences in comparison to modelled DDIC arise, because in the model this tracer is not constant along an isopycnal surface (Figure 4.13).

Table 4.1: Anthropogenic CO_2 inventory of the model year 1996 on different isopycnals throughout the whole model domain.

σ_θ	<26.3	26.3-27.7	>27.7
volume [10^6 km^3]	5.56	51.22	136.12
total inv. of DDIC [Gt C]	2.40	9.49	11.73
total inv. of ACO2TR [Gt C]	2.46	9.11	11.86
total inv. of ACO2EQDIFF [Gt C]	3.02	9.87	13.04
total inv. of CANT (ideal age) [Gt C]	2.99	18.35	-
total inv. of CANT (CFC12 age) [Gt C]	3.36	19.15	-
quantum of total volume [%]	2.9	26.6	70.6
quantum of total inv. (DDIC) [%]	10.1	40.2	49.5
quantum of total inv. (ACO2TR) [%]	10.5	38.9	50.6
quantum of total (ACO2EQDIFF) [%]	11.7	38.1	50.3

4.4 Anthropogenic CO_2 as the difference between two equilibrium concentrations

Estimating anthropogenic CO_2 as the difference of the equilibrium concentration at the time of the last surface contact minus pre-industrial equilibrium (ACO2EQDIFF) is also possible with modelled data (with use of Equation 3.8). As for the $\Delta C^\star$ method in Chapter 4.3 the equilibrium concentrations are computed by using the formula developed for the model used here (see also Appendix A). Using this method, the assumption of a time-independent air-sea disequilibrium remains, but as a great advantage this is estimated for every grid-point individually, and not necessarily on isopycnal surfaces as in the $\Delta C^\star$ method. Especially local discrepancies in calculating $\Delta C^\star$ vanish by estimating two equilibrium concentrations as a function of temperature, salt and water age (one pre-industrial and one recent). In this case the influence of algae blooms in the annual mean does not have any influence on the anthropogenic CO_2 concentration, because for this estimation no biological parameters are needed.

By this method the influence of the lateral boundaries has to be taken into account. In the model all boundaries are closed and all physical parameters are restored to climatological mean values. The ideal water age is set to zero at the surface and, for the deeper grid points of the model, increased every time step. So it is penetrating into the ocean by mixing of the physical model. At the lateral boundaries it is then not equal to pre-industrial time (which would be the integration time). This should lead to overestimation of anthropogenic CO_2 in regions where the influence of a boundary is strong, because here the ideal water age may be smaller than integration time. Especially near the southern boundary this is an important point. Anthropogenic CO_2 is transported northwards in the whole model domain (Völker et al. [2001]), and concludingly pre-industrial conditions (with no anthropogenic CO_2) are penetrating northwards from the southern boundary. In contrast to that, estimating equilibrium concentrations do not see the southern boundary as pre-industrial (because of the younger water age), resulting in higher anthropogenic CO_2 values in the influence region of the southern boundary. Nevertheless the water masses of the southern ocean are not included in this calculation, because even though the climatological mean values at the southern boundary are containing information about the southern ocean, this is not the case for the ideal water age. Especially the age information of Antarctic Bottom Water (AABW) influencing the deep water masses in the North Atlantic and carrying anthropogenic CO_2 information is missing in this model simulation. And in conclusion the anthropogenic

CO_2 concentrations of ACO2EQDIFF could not represent the real concentration in the ocean, even if this estimation method was perfect.

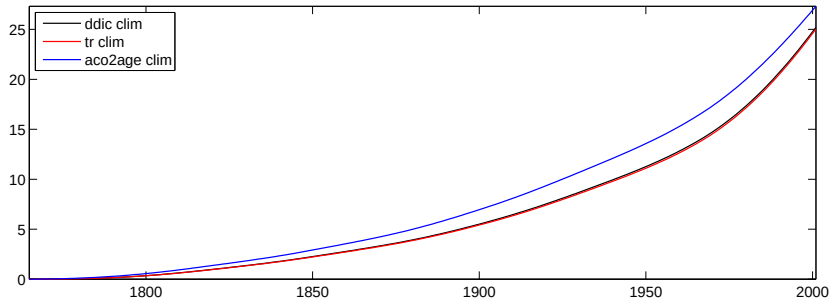

Figure 4.15: Time-series of total inventory of anthropogenic CO_2 [Gt C] of the whole model domain; black: DDIC; red: ACO2TR with corrected parameterisation; and blue: difference between two equilibrium concentrations (using ideal age); Shown is the Model run starting in 1765 with pre-industrial atmospheric reference pressure of 278 ppm.

The total inventory of anthropogenic CO_2 (Figure 4.15) of the climatological model run starting in the year 1765 shows that this method overestimates the "true" anthropogenic CO_2 (DDIC) of the model. This overestimation decreases with rising integration time, from about 30% between 1850 and 1900 to less than 10% in 2001. For the model run starting in the year 1860 with constant pCO_2 of 288 ppm things look quite similar. Relative overestimation is large at the beginning of integration time (more than 50% in 1900) and getting smaller with time up to less than 20% in 2001. Absolute values of anthropogenic CO_2 are lower in the model run starting in 1860, because of anthropogenic CO_2 accumulation starting about 100 years later and with 10 ppm less ΔpCO_2 in the atmosphere between the pre-industrial and actual pCO_2. The longer the integration and thereby the higher atmospheric pCO_2, the lower is the relative difference in total anthropogenic CO_2 between the two model runs (see also Chapter 4.2.2).
For the total amount of anthropogenic CO_2 north of 25°N, away from the influence of the southern boundary, DDIC is even underestimated by ACO2EQDIFF at the end of integration time (for the model run starting in 1765). So obviously anthropogenic CO_2 is not systematically overestimated by the method taking the difference of two equilibrium concentrations. Locally overestimation takes place in relatively young water, especially near the surface, in the formation region of NADW and its pathway to the south in the deep Atlantic Ocean. In the mid ocean the regions of underestimated anthropogenic

CO_2 are getting larger with integration time. Especially those are regions of older water within the boundary of a sharp gradient from young to old waters. For the model year 1996 of the longer model run this sharp gradient is for waters with ideal ages between 20 years and 80 years. Since about 1980 of the model run starting in 1765 most of the water older than 20 years and north of 24°N, where the influence of the southern boundary is very small (see also 4.2.1), underestimates anthropogenic CO_2 if estimating is by the difference of two equilibrium concentrations (Figure 4.16).

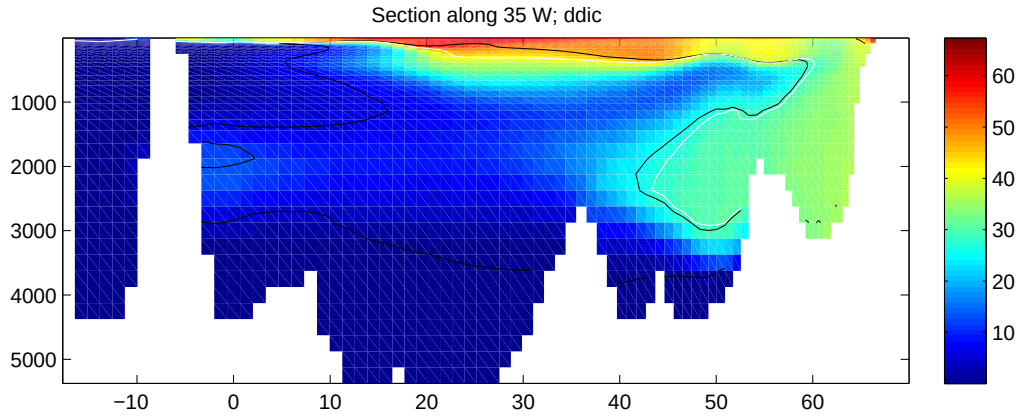

Figure 4.16: Section of DDIC [mmol m^{-3}] along 35°W of the model year 1996 after 231 years of integration. The white line is the 20 year ideal age isoline and the black line is the isoline separating regions which are overestimated by ACO2EQDIFF (difference of the DIC equilibrium concentration when the water was in contact with the atmosphere last minus the pre-industrial DIC equilibrium concentration) and those which are underestimated. At the surface and in the north ACO2EQDIFF is overestimating DDIC and in the interior it underestimates DDIC.

When estimating anthropogenic CO_2 by ACO2EQDIFF information about water mass age can be taken from the modelled ideal age (as done for the time series in Figure 4.15) or using tracer derived ages such as CFCs or He/Tr. In the model CFC11 and CFC12 are introduced as passive tracers from the model year 1931 until 1997. As described in Chapter 3.5 the water age can be determined by using CFC concentrations in the water column. This is done in the way that partial pressure of these CFC concentrations (pCFC) in the ocean are compared to the historical surface pCFC concentrations. Using this water age for estimating anthropogenic CO_2 by ACO2EQDIFF leads to high overestimation of anthropogenic CO_2 in comparison to estimating anthropogenic CO_2 using the same method but using the modelled ideal age instead, especially in deeper water. Near the surface and in regions where the water masses are relatively young (younger

than about 25 years) using either of the two water mass ages leads to nearly the same anthropogenic CO_2 concentrations. This can be seen in Figure 4.17, where a section of anthropogenic CO_2 along 35°W for the model year 1996 of the climatological model runs starting in 1765 is shown. Anthropogenic CO_2 was estimated by ACO2EQDIFF using modelled ideal age and CFC12 age. Near the surface (in the mixed layer) and in the northern part of this section, where the water is young, the concentrations of anthropogenic CO_2 using the different water ages are quite similar, with differences of a few $mmol\ m^{-3}$. In deeper regions the differences are with 10 $mmol\ m^{-3}$ or more than that much higher. The reason for this discrepancies is that in regions where CFCs are undersaturated (as for example in the Labrador Sea), the CFC derived water age overestimates the true water age, because a saturation of 100% is assumed. This leads to lower anthropogenic CO_2 concentrations in comparison to using ideal age (which is younger there). In Figure 4.17 this can be seen in the tongue of NADW north of about 45°N, where the anthropogenic CO_2 concentrations using CFC12 age are slightly lower than the results by using ideal age. In the surface layer south of 50°N the saturation of CFCs is nearly 100% leading to nearly the same water ages as the ideal age and consequently to nearly the same anthropogenic CO_2 concentrations. South of about 10°N in the surface region the absolute values using CFC12 ages are smaller than when using ideal age, because of the southern boundary condition. At the southern boundary all tracers (except ideal age) in the model are set to pre-industrial, which is zero in the case of CFCs. This leads to low CFC concentrations in the influence region of this boundary. Determining the water mass age using CFC concentrations in regions with very low concentrations leads to high underestimation of the water mass age. This can be explained by the young atmospheric history of CFCs starting in 1931, so that the oldest water that can be detected by this method is that of 1931. In addition to this no attention to mixing is made by determining the water mass age using CFCs in this way. That is one reason why Hall et al. [2002] used transit time distributions (TTD) for estimating anthropogenic CO_2. This method and the results concerning differences to ACO2EQDIFF are described in Chapter 4.5. But nevertheless, estimating anthropogenic CO_2 as the difference of two DIC equilibrium concentrations in well ventilated regions leads to higher anthropogenic CO_2 concentrations in comparison to DDIC of about 10% to 15%. This is nearly the same magnitude of overestimation than using the $\Delta C^\star$ method described in Chapter 4.3. In deeper regions, with older water masses ACO2EQDIFF using ideal age slightly underestimates the modelled DDIC, but using CFCs, as can be done in observations, leads to higher values than DDIC. This is the

case, because of the bias to too young water ages using tracers like CFCs for determining the water age.

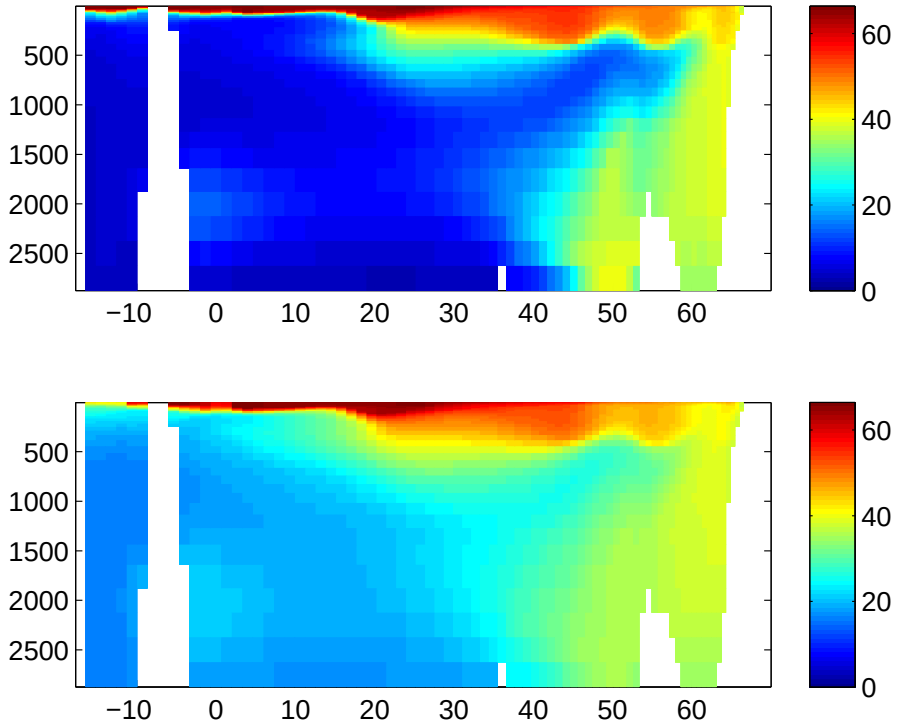

Figure 4.17: Section of anthropogenic CO_2 [mmol m^{-3}] along 35°W estimated using the difference of two equilibrium DIC concentrations (the one for the time when the water was last in contact with the atmosphere minus the pre-industrial DIC equilibrium concentration; ACO2EQDIFF) using ideal age (upper) and CFC12 age (lower). Model year 1996.

4.4.1 Air-sea disequilibrium of anthropogenic CO_2 in the model

Estimating anthropogenic CO_2 using the $\Delta C^\star$ method Gruber et al. [1996] assume that the air-sea disequilibrium of DIC (DIC_{diseq}) remains more or less constant within the outcrop region of a particular isopycnal surface. In Matsumoto and Gruber [2005] a correction for this assumption is proposed, by assuming that the air-sea disequilibrium becomes more negative with time. And thus the anthropogenic CO_2 would be overestimated by assuming a constant air-sea disequilibrium. By scaling this air-sea disequilibrium with the uncorrected estimation of anthropogenic CO_2 Matsumoto and

Gruber [2005] proposed to correct the estimation of anthropogenic CO_2 (for details see the auxiliary material of Matsumoto and Gruber [2005]).
In the model the air-sea disequilibrium of DIC can be estimated for every surface grid box. Especially the difference of DDIC minus ACO2EQDIFF gives the time-series of ΔDIC_{diseq} for the model:

$$\begin{aligned} DDIC - ACO2EQDIFF &= DIC - DIC^{pi} - (DIC_{eq} - DIC^{pi}_{eq}) \\ &= DIC - DIC_{eq} - (DIC^{pi} - DIC^{pi}_{eq}) \\ &= DIC_{diseq} - DIC^{pi}_{diseq} = \Delta DIC_{diseq} \end{aligned}$$

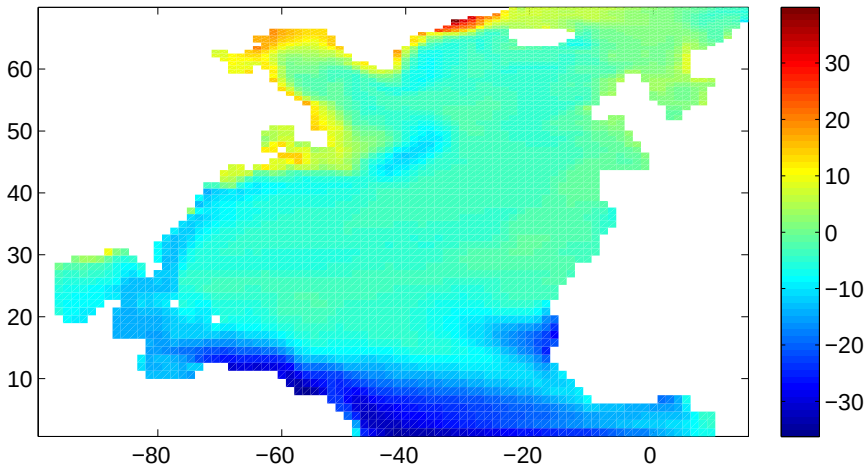

Figure 4.18: Change of DIC_{diseq} (air-sea disequilibrium of dissolved inorganic carbon) for the model year 1996 since 1765: ΔDIC_{diseq} [mmol m^{-3}] (DDIC - ACO2EQDIFF) of the model year 1996. Model run starting in 1765 with pre-industrial atmospheric reference pressure of 278 ppm.

As shown in Figure 4.18 for the model year 1996 of the model run starting in 1765 the air-sea disequilibrium of anthropogenic CO_2 is not constant in the whole model domain, as assumed by Gruber et al. [1996]. But in the water formations regions (as the central Labrador Sea and the Irminger Sea) changes in disequilibrium are just a few $mmol\,m^{-3}$. Larger variations occur along the shores north of 40°N and in the whole tropical Atlantic south of 15°N. The large variations along the shores of the northern North Atlantic may be an artefact of sea ice coverage in the model. As soon as the temperature falls below

the freezing point all fluxes are set to zero. Thus using the biological model no more DIC can be taken up. In contrast to that estimating the DIC equilibrium concentration as a function of temperature, salinity and atmospheric pCO_2 leads to high equilibrium concentrations, because the equilibrium concentration of DIC increases with decreasing temperature. In this case DIC is undersaturated in regions covered by ice. This undersaturation becomes larger with time, because the atmospheric pCO_2 is rising and the surface ocean cannot take up more CO_2 (because the DIC surface flux is set to zero in this regions). This leads to the conclusion that in general, adapting a method assuming constant air-sea pCO_2 disequilibrium is not a good solution in regions where ice covering is highly variable in different years.

4.5 TTD method

As described in Chapter 3.4, the assumptions made using the TTD method are in general the same as for the $\Delta C^\star$ method, despite the fact, that mixing of anthropogenic CO_2 occurring predominantly along isopycnal surfaces, is not needed to assume. For estimating anthropogenic CO_2 with the $\Delta C^\star$ method (in Chapter 4.3) a single water age is determined, using pCFC ages or the modelled ideal age. The same was done in Chapter 4.4 where the anthropogenic CO_2 is estimated by the difference of two equilibrium concentrations. Using the TTD method, anthropogenic CO_2 is also estimated by computing the difference of two equilibrium concentrations, but using an age spectrum instead of a single tracer derived water age (as done previously). This is done in the way that the anthropogenic CO_2 concentration is the integral of a history of surface anthropogenic CO_2 concentrations (see Chapter 3.4 and Waugh et al. [2006]). CFCs are assumed to be 100% saturated (as in the determination of a single CFC derived water age in the previous chapters). And the ratio $\Gamma/\Delta = 1$ was chosen due to the fact that Waugh et al. [2004] found the tracer distributions to be well described using TTDs with this ratio. Waugh et al. [2004] also determined an uncertainty of only 2 $mmol\ m^{-3}$ in anthropogenic CO_2 for a 10% uncertainty in CFC saturation (see also Tanhua et al. [2008]).

In Figure 4.19 can be seen that for the period from 1972 until 1997 the total anthropogenic CO_2 inventory using the TTD method and CFC data (red lines) is of the same magnitude as the "true" modelled anthropogenic CO_2 (DDIC; black line) and the difference of DIC equilibrium concentrations using the ideal age (black dashed line). With a difference of maximal about 2 Gt C to 3 Gt C this is in the same order of magnitude

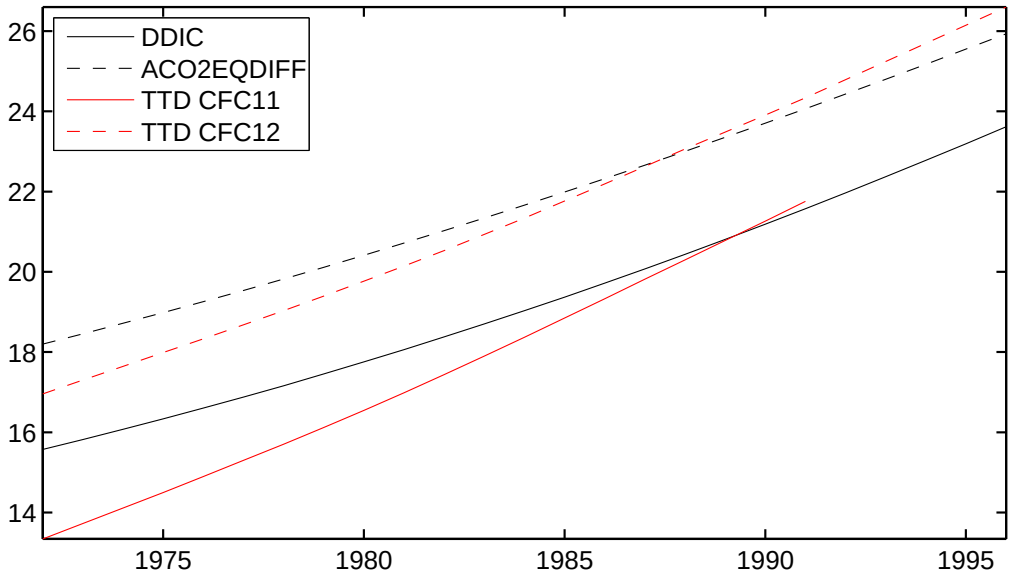

Figure 4.19: Time series of anthropogenic CO_2 [Gt C] using different estimation methods for anthropogenic CO_2: black solid line: modelled DDIC; black dashed line: difference of two equilibrium concentrations ("actual" minus pre-industrial) using modelled ideal water age; red solid line: using the TTD method (method using the transit time distribution) with CFC11; red dashed line: using the TTD method with CFC12. The estimation methods are adapted to the climatological model run starting in 1765.

as found in similar adaptions of this method to models by Waugh et al. [2006] and Waugh et al. [2004]. For the different tracers CFC11 and CFC12 the results are slightly different. Using CFC11 in the TTD method leads to a total amount of anthropogenic CO_2 which is about 2 Gt C to 4 Gt C smaller than when using CFC12. A reason for this difference are supposed to be the different surface histories of CFC11 and CFC12. On the one hand the usable part of rising atmospheric CFC11 concentrations is from the year 1942 to 1991 whereas for CFC12 this is for the time period from 1931 until 1997. So that time since when CFC11 could penetrate into the ocean is shorter than that for CFC12. On the other hand the gradient of the CFC12 history is steeper and the total concentrations, in terms of the partial pressure [ppt], are higher than those of CFC11. As described by Waugh et al. [2004] this leads to older CFC11 derived water mass ages in young water masses, whereas the reverse is true for ages older than 25 years for a sampling year in the 1990s. This can also be seen in the water age calculations of this study. Keeping the different ages in mind, this leads to higher anthropogenic CO_2 concentrations in water younger than 25 years by using CFC11 and the reverse for older

water mass ages. In fact the magnitudes of these differences are quite dissimilar. In the younger water masses the difference in anthropogenic CO_2 using CFC11 or CFC12 is less than 1 mmol m^{-3} (higher using CFC11) whereas it is 2 mmol m^{-3} to 4 mmol m^{-3} (lower using CFC11) in water masses older than 25 years. Integrating the anthropogenic CO_2 in the whole model region than leads to a higher amount of anthropogenic CO_2 using CFC12 than using CFC11 for the TTD method.

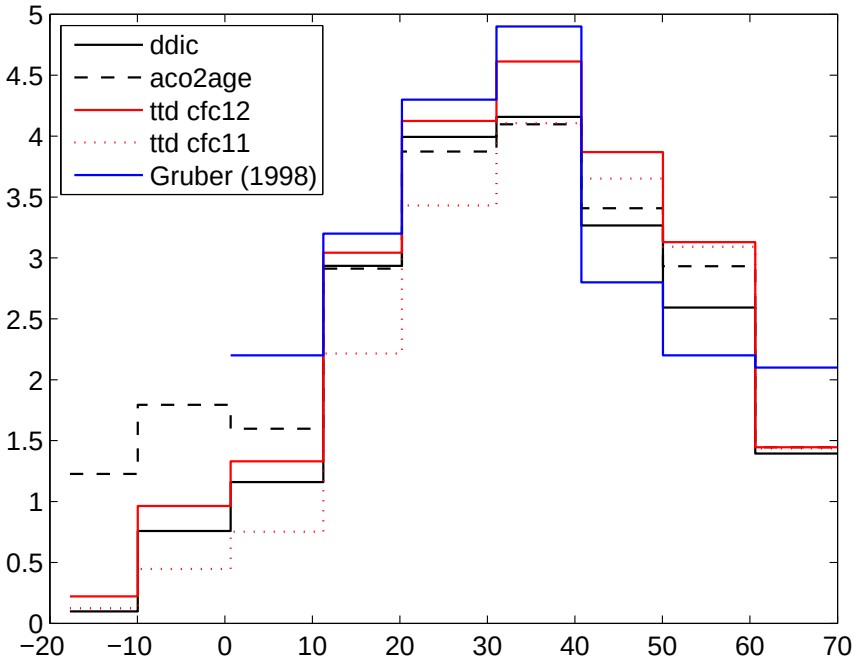

Figure 4.20: Vertical integrated anthropogenic CO_2 [Gt C] of the modelled DDIC (black solid line), observations from the analysis of Gruber [1998], estimation using the difference of two equilibrium concentrations ("actual" minus pre-industrial; black dashed line), and in red using the TTD method (with CFC12: red solid line; and CFC11: red dashed line).

This effect can also be detected by computing the latitudinal dependence of vertically integrated anthropogenic CO_2 inventory (Figure 4.20). North of 50°N the TTD method using CFC11 or CFC12 leads to nearly the same specific inventories for the 10° latitude bands. South of 50°N this method using CFC12 leads to higher specific inventories than using CFC11, because of higher anthropogenic CO_2 concentrations in water masses older than 25 years (as described above). The difference of the specific inventories to the "true" anthropogenic CO_2 of the model (DDIC) is relatively small. North of 40°N the TTD method in both cases (using CFC11 or CFC12) slightly overestimates the modelled

DDIC specific inventories. This is a result of the overestimation due to the high amount of young water masses in this region (influence of NADW). South of that the TTD using CFC12 slightly overestimates DDIC and using CFC11 slightly underestimates the DDIC specific inventories. This is probably also the effect of the influence of older water masses in which the TTD method using CFC11 leads to lower anthropogenic CO_2 concentrations than using CFC12. In shallower water (approximately the upper 1000 m) using CFC11 or CFC12 for the TTD method leads to higher concentrations of anthropogenic CO_2 compared to DDIC, due to water ages biased to younger water. As for the modelled DDIC, the lateral boundary conditions for CFCs are those of pre-industrial times, so they are restored to zero at the boundaries. In contrast to the method using ideal age for estimating anthropogenic CO_2 by computing the difference of two equilibrium DIC concentrations (ACO2EQDIFF), the TTD method (which also uses this difference of equilibrium concentrations) using CFC data for determining the TTD leads to lower anthropogenic CO_2 concentrations near the southern boundary of the model domain than ACO2EQDIFF. Therefore the concentrations using the TTD method are closer to the modelled DDIC.

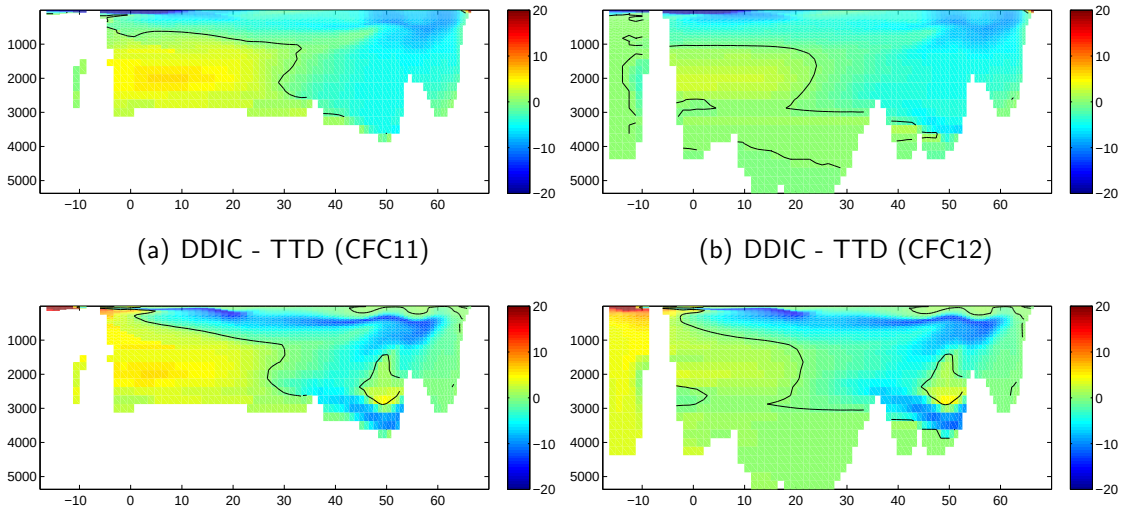

(a) DDIC - TTD (CFC11)

(b) DDIC - TTD (CFC12)

(c) ACO2EQDIFF - TTD (CFC11)

(d) ACO2EQDIFF - TTD (CFC12)

Figure 4.21: Differences in anthropogenic CO_2 concentrations [mmol m^{-3}] between DDIC and the TTD method (upper) and ACO2EQDIFF and TTD method (lower) along 35°W. The black line is the zero contour of the difference. Shown is the model year 1991 of the climatological model run starting in 1765. In (a) and (c) there are no values in deeper regions, because CFC11 has not penetrated deeper than approximately 3000 m south of 30°N.

In a section along 35°W (Figure 4.21) the differences in anthropogenic CO_2 concentrations using different methods for estimating anthropogenic CO_2 are shown for the model year 1991 (model run starting in 1765). As described previously it can be seen that, in regions of younger water masses, using the TTD method with both CFC11 or CFC12 leads to lower concentrations of anthropogenic CO_2 in comparison to modelled DDIC of a few mmol m^{-3}. On the shown section this occurs in the upper 1000 m and throughout the whole water column north of about 40°N. Overestimation by the TTD method takes place in the interior south of 40°N. The differences are with up to about 5 mmol m^{-3} relatively small. In Figure 4.21(a) and (c) there are no values in regions deeper than 3000m south of 30°N, because in this regions the CFC11 was not entrained such deep in the model. Comparing the method using the difference of two DIC equilibrium concentrations (ACO2EQDIFF) with model age to the TTD method is shown in Figures 4.21(c) and (d). It can be seen that the TTD method leads to higher concentrations of anthropogenic CO_2 compared to ACO2EQDIFF in nearly the same regions as it overestimates the "true" modelled anthropogenic CO_2 (DDIC). As a consequence of ACO2EQDIFF underestimating DDIC in some regions (see Chapter 4.4), these are the regions where the largest differences between the TTD method and ACO2EQDIFF occur. In the interior and in the deeper ocean the lower anthropogenic CO_2 concentrations using the TTD method in comparison to ACO2EQDIFF are nearly of the same magnitude than the underestimation of DDIC by the TTD method. In contrast to that, south of the equator the difference between ACO2EQDIFF and the anthropogenic CO_2 using the TTD method is much larger then the difference of DDIC and the anthropogenic CO_2 estimated by the TTD method. There, anthropogenic CO_2 concentrations estimated by the TTD method are lower than when using ACO2EQDIFF (using ideal age), because of the closed southern boundary, where CFCs are restored to zero. As a consequence the anthropogenic CO_2 is biased to pre-industrial (too low) values by using the TTD method.

As described in Chapter 4.3 the $\Delta C^\star$ method leads to much higher concentrations of anthropogenic CO_2 compared to modelled DDIC in nearly the whole North Atlantic. In Chapter 4.4 can be seen that the estimations using the $\Delta C^\star$ method are leading to anthropogenic CO_2 concentrations with nearly the same magnitude than using the method of two DIC equilibrium concentrations with CFC for determining a single water age. Consequently the $\Delta C^\star$ method leads to higher anthropogenic CO_2 concentrations than the TTD method (Figure 4.22). Only in the upper 800 m between 30°N and 50°N (about the North Atlantic Mode Water region) the TTD method leads to higher anthro-

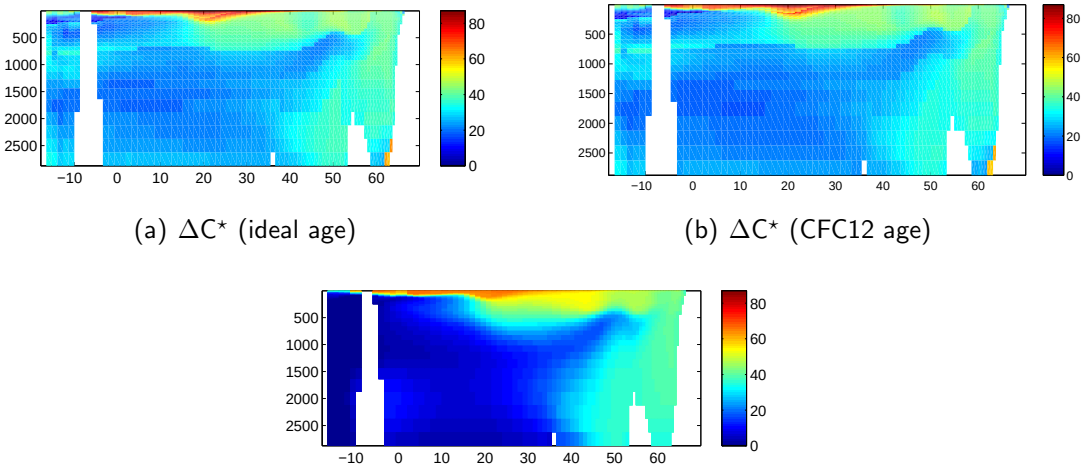

(a) $\Delta C^\star$ (ideal age)

(b) $\Delta C^\star$ (CFC12 age)

(c) TTD (CFC12)

Figure 4.22: Section of anthropogenic CO_2 [mmol m^{-3}] along 35°W estimated using the $\Delta C^\star$ method with ideal age and CFC12 age (upper) and the TTD method using CFC12 (lower) for the model year 1996 of the climatological model run starting in 1765. (The double maximum near the surface in the upper figures is a consequence of the composition of different isopycnal intervals for plotting this section.)

pogenic CO_2 concentrations than the $\Delta C^\star$ method. The sections of anthropogenic CO_2 estimated by the $\Delta C^\star$ method are a composite of the calculations on different isopycnals. That is why in some cases the boundaries of the sections can be seen (especially in the "double" maximum in the upper 200 m at about 20°N).

As a consequence of the previously described results from comparing the different methods to estimate anthropogenic CO_2 it seems that the TTD method is a better method for estimating anthropogenic CO_2 in observations than the $\Delta C^\star$ method. This is the case, because in the TTD method the role of mixing in the ocean has an influence on the estimation. In contrast to that mixing does not occur in the right way by using the $\Delta C^\star$ method. On the other hand in recently ventilated regions the TTD method and the $\Delta C^\star$ method lead to results in the same magnitude and are with a few mmol m^{-3} difference to the modelled DDIC in the same range as the "true" anthropogenic CO_2. These are especially those regions where the absolute anthropogenic CO_2 concentration is relatively high, so that a few mmol m^{-3} difference are a relatively small deviation.

4.6 Summary and conclusions

The North Atlantic is the ocean with the highest anthropogenic CO_2 concentrations (Figure 4.1 and Sabine et al. [2004]). As shown in Chapter 4.1, the distribution of anthropogenic CO_2 is well represented in the ocean circulation model used here. Computing anthropogenic CO_2 in the model either as the difference of DIC concentrations with realistically prescribed surface pCO_2 values minus the DIC concentration of a pre-industrial reference experiment (with constant pre-industrial atmospheric pCO_2) or as a passive tracer (after Sarmiento and Orr [1992]), shows that the passive tracer systematically underestimates the "true" anthropogenic CO_2 (DDIC) by 15% to 20%. A reason for this underestimation is that Sarmiento and Orr [1992] computed the surface forcing for their tracer out of a pre-industrial global ocean model experiment, by using the temperatures of this model run, a uniform salinity of 35 and a uniform alkalinity of 2300 μ eq kg^{-1}, and assuming that in the pre-industrial ocean the DIC is in equilibrium at the surface. In Chapter 4.2 is shown how the surface flux after Sarmiento and Orr [1992] can be improved by using surface pCO_2 concentrations of a model run including biology. Using these improvements leads to a total anthropogenic CO_2 inventory of the modelled tracer which differs less then 2% from that of the "true" anthropogenic CO_2 (DDIC). Locally the difference of the anthropogenic CO_2 concentration of the tracer to that of DDIC is less than 7%.

In Chapters 4.3 to 4.5 three different methods to estimate anthropogenic CO_2, which can also be used in observations, were adapted to the model. These are the $\Delta C^\star$ method after Gruber et al. [1996], taking the difference of two DIC equilibrium concentrations, and the TTD method (as in Waugh et al. [2006]), which also uses differences of DIC equilibrium concentrations for estimating anthropogenic CO_2. For the first two methods a single water age was determined for the time of last surface contact. For ages determined by observable tracers like CFCs no mixing occurs. In contrast to that in the TTD method mixing is taken into account. In this case not a single water age is determined by using CFC concentrations, but a time range instead. There are regionally large differences by using the three methods, which are in general due to the fact that the water age is represented differently. In well ventilated regions and younger water each of the three methods leads to anthropogenic CO_2 concentrations differing just a few mmol m^{-3} from the "true" modelled anthropogenic CO_2 (DDIC). But in the ocean interior, where the water masses are older, the $\Delta C^\star$ method leads to very large overestimation by 50% and more due to highly underestimated CFC ages in this regions. Using ideal model age makes things just slightly better, but another problem in this method is, that the

quasi conservative tracer $\Delta C_t^\star$ is not constant on an isopycnal surface as assumed. This leads to a large uncertainty in the air-sea DIC disequilibrium. The method taking the difference of two DIC equilibrium concentrations avoids this problem by computing the air-sea disequilibrium at every grid point, although it is assumed to be constant over time. Using a single CFC derived water age for the ACO2EQDIFF method leads to the same problems as using the $\Delta C^\star$ method due to the fact that in older waters CFC ages are determined as too young. Using ideal age or TTD instead leads to anthropogenic CO_2 concentrations which differ from modelled DDIC by maximal 10%. This leads to the conclusion that in water masses with supposed water ages older than about 25 years (for observations in the 1990s), the TTD method is the best choice to estimate anthropogenic CO_2 in observations.
As a comparison of this conclusions in Figure 4.23 a mean profile of the different water ages leading to different anthropogenic CO_2 concentrations using the TTD method or ACO2EQDIFF method is shown for the Labrador Sea and the subtropical North Atlantic. In the Labrador Sea all shown methods are overestimating DDIC in the whole water column. In contrast to that in the subtropical North Atlantic the methods using a single CFC derived water mass age lead to too high anthropogenic CO_2 concentrations. The other methods are leading to anthropogenic CO_2 concentrations which are very close to the "true" modelled anthropogenic CO_2 (DDIC).

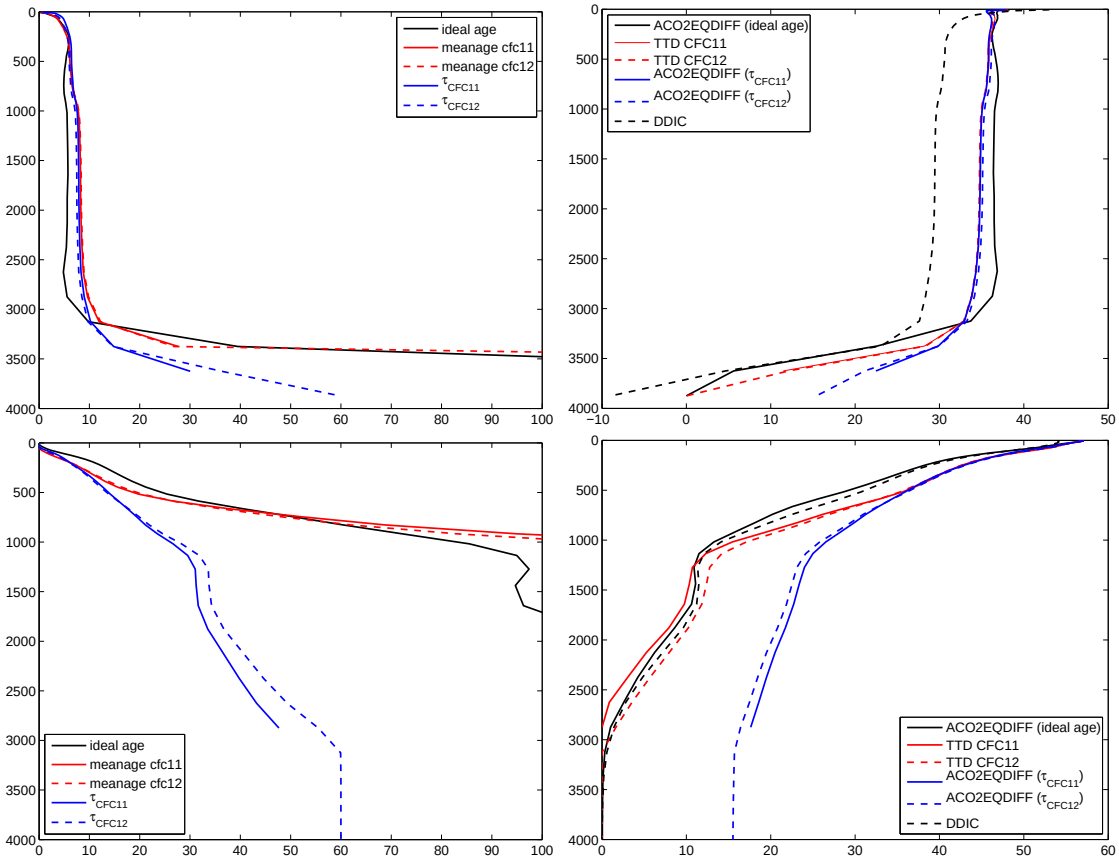

Figure 4.23: Mean profiles of water mass age (left) and anthropogenic CO_2 [mmol m^{-3}] (right) in the Labrador Sea (north of 52°N and west of 44°W; upper) and in the subtropical Atlantic (20°W to 30°W and 25°N to 35°N; lower) of the model year 1991 from the climatological model run starting in the year 1765. The different line colours for the profiles showing water mass age (left): ideal age (black); mean age of TTD using CFC11 (red); mean age of TTD using CFC12 (red dashed); CFC11 age (blue); CFC12 age (blue dashed). The different colours for the profiles of anthropogenic CO_2: ACO2EQDIFF with ideal age (black); TTD method with CFC11 (red); TTD method with CFC12 (red dashed); ACO2EQDIFF with CFC11 age (blue); ACO2EQDIFF with CFC12 age (blue dashed) and DDIC (black dashed).

Chapter 5

Sensitivity of the $\triangle C^{\star}$ Method to isopycnal mixing

As described in Chapter 2.1 the parametrisation of net isopycnal eddy advection of tracers due to Gent and McWilliams [1990], with thickness diffusivity chosen as half of the isopycnal diffusivity is included in the model. This was done not in the original version but with full isopycnal diffusivity (2×10^7 cm s^{-1}) and halved thickness diffusivity (1×10^7 cm s^{-1}), nearly similar to the model run GM/2 in Völker et al. [2001] (where both the isopycnal and the thickness diffusivity where halved). For pointing out the influence of isopycnal mixing on the different methods for estimating anthropogenic CO_2, a special experiment where the isopycnal mixing is completely switched off was done. In this model run, in contrast to the run noGM of Völker et al. [2001] (where the Laplacian isopycnal scheme is used instead), no isopycnal diffusion scheme is used (neither GM nor any other) for horizontal mixing. The vertical mixing for this model run was not touched, so vertical diffusivity and vertical friction are the same as in the model run including isopycnal mixing.

In the total inventory of anthropogenic CO_2 the influence of isopycnal mixing is with less than 7% reduction at the end of integration time not really detectable (Figure 5.1). For the total inventory only DDIC and ACO2EQDIFF are shown in the whole time period. The also integrated anthropogenic tracer leads to nearly the same results as DDIC (see also Chapter 4.2). The total inventory of estimating anthropogenic CO_2 using the TTD method for the time period from 1972 until 1996 (using CFC11 it is just shown until 1991, because just until that atmospheric CFC11 concentrations are rising) is shown in Figure 5.2 in comparison to the modelled DDIC. As for the climatological model run including isopycnal mixing the total anthropogenic CO_2 inventory using the TTD

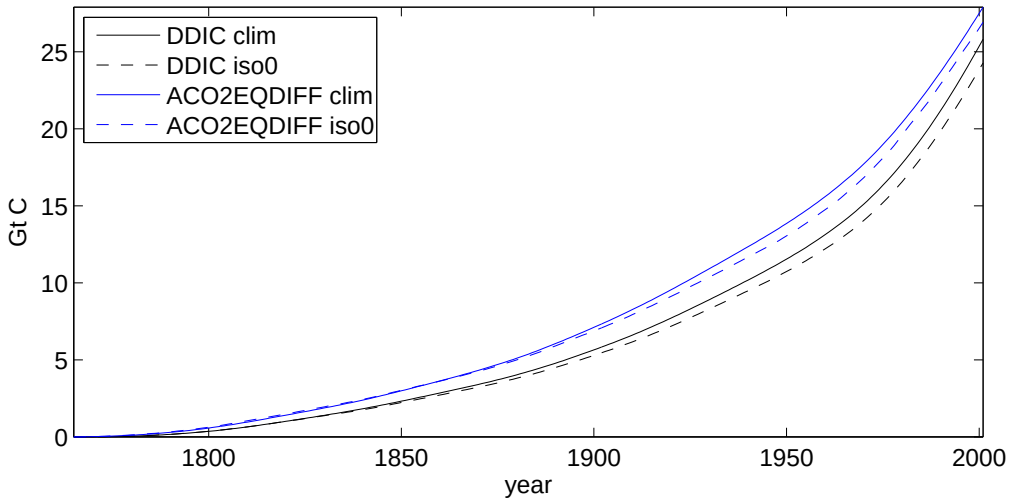

Figure 5.1: Time series of total anthropogenic CO_2 inventory in Gt C for the climatological model run including isopycnal mixing (solid lines) and the one without isopycnal mixing (dashed lines); black: DDIC; blue: AOC2EQDIFF; model run starting in 1765.

method in the model run without isopycnal mixing differs insignificantly from that of DDIC. Nevertheless the total amounts of anthropogenic accumulation using the TTD method with CFC12 are about 2 Gt C lower for the model run without isopycnal mixing compared to the model run including isopycnal mixing. For the TTD method using CFC11 and the modelled DDIC the difference is around 1 Gt C for the shown time period.

The ΔC^* method can only be used on individual isopycnals, and large uncertainties occur in regions of old water, for example in the deep ocean (as shown in Chapter 4.3). For this reason in Table 5.1 the total inventory of anthropogenic CO_2 and the volume on different isopycnals are shown. In addition the proportion of the total inventory and volume of these water masses are listed. Comparing these results with the model run including isopycnal mixing (Table 5.2) makes clear that, especially on shallower isopycnals above the permanent thermocline, in the tropics and subtropics and in mode water regions (isopycnals reaching from $\sigma_\theta = 26.0$ to 27.3), the ocean volume in the model run without isopycnal mixing is smaller (by about 1%) than in the run with isopycnal mixing. In contrast to that the total amount of anthropogenic CO_2 by using the ΔC^* method is around about 50% higher without isopycnal mixing in this regions. In contrast to this it is just about 10% higher when using the method of DIC equilibrium differences (ACO2EQDIFF). A reason for this is that the thickness in this range of isopycnals is increasing in regions where ACO2EQDIFF already overestimates DDIC

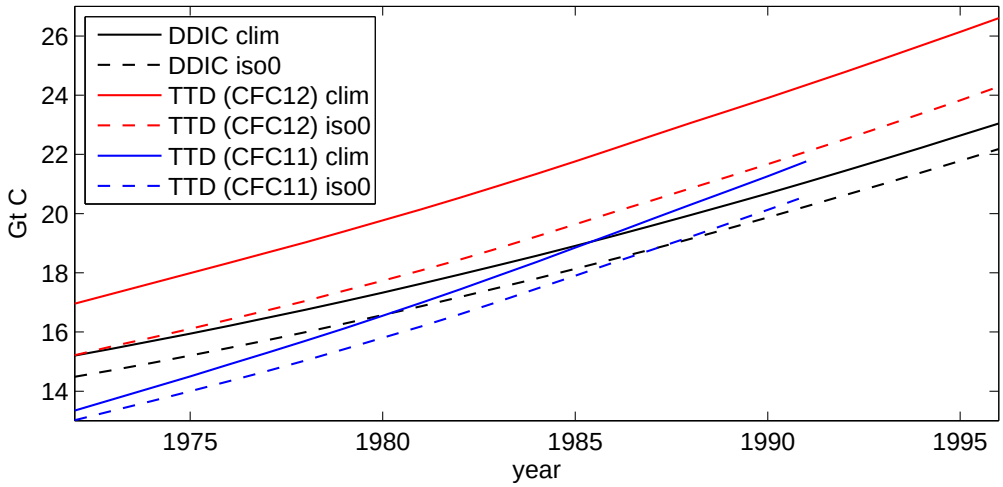

Figure 5.2: Time series of the years 1972 to 1996 of total anthropogenic CO_2 inventory in Gt C for the climatological model run including isopycnal mixing (solid lines) and the one without isopycnal mixing (dashed lines), both starting in the year 1765; black: DDIC; red: using the TTD method with CFC12; blue: using the TTD method with CFC11 (these end in the year 1991, because after that year the atmospheric CFC11 concentrations are not continuously rising any more).

(see also Chapter 4.4). These results differ from the results of Völker et al. [2001], who found that the anthropogenic CO_2 (computed as passive tracer) changes above the permanent thermocline (there defined by $\sigma_\theta < 27.5$) between 50°S and 50°N are nearly proportional to the changes in volume. In the experiment used here this is not the case either, because the total amount of anthropogenic CO_2 by DDIC, ACO2TR and the TTD method with CFC12 reduces by about 5% to 8% in comparison to the model run including isopycnal mixing which is more than the reduction of volume for these isopycnals.

The local distribution of anthropogenic CO_2 on the isopycnals reaching from $\sigma_\theta = 26.7$ to 27.3 (Figure 5.3) gives one explanation for this large discrepancies. Using the $\Delta C^\star$ method leads to very high anthropogenic CO_2 concentrations off the coast of Africa in the regions between 10°S and 10°N, where the depth range of this isopycnal reaches from about 200 m to 700 m. In contrast to that the modelled DDIC shows nearly no anthropogenic CO_2 in this region and the anthropogenic CO_2 concentrations using the TTD method with CFC12 differ from DDIC by just a few mmol m^{-3}. The region of extremely high anthropogenic CO_2 concentrations using the $\Delta C^\star$ method is where in the tropical Atlantic oxygen minimum zones (OMZ) or shadow zones are located. In

these regions the water is only slowly ventilated, leading to very low oxygen values. Figure 5.4 shows the negative apparent oxygen utilisation (AOU=O_2^{sat} - O_2) on the isopycnal $\sigma_\theta = 26.7$ to 27.3 of the model run without isopycnal mixing in comparison to the reference run including isopycnal mixing. It can be seen that in the model run with no isopycnal mixing the zones in the tropical Atlantic off the African coast, where oxygen is highly undersaturated, are much larger and higher undersaturated than in the model run including isopycnal mixing. It seems that in this regions, while switching off isopycnal mixing, denitrification could play an important role, which is not the case in the model run including isopycnal mixing. In the biological model no denitrification is included, which leads to very high nutrient concentrations when nearly no oxygen is present. This is the case, because no production is taking place without oxygen. The sources and sinks of DIC are coupled to those of nutrients by Redfield ratio. Consequently in such regions the DIC concentrations are extremely high. Estimating anthropogenic CO_2 by using the ΔC^* method, these high DIC concentrations in addition to highly undersaturated oxygen concentrations in these regions lead to extremely high anthropogenic CO_2 concentrations. That is the result of the extremely high DIC concentrations in this region (especially DIC concentrations are much higher than the preindustrial DIC equilibrium concentrations), which cannot compensate the under-saturation of oxygen. Using the method of estimating two DIC equilibrium concentrations this effect vanishes, because then both (preindustrial and actual) equilibrium concentrations are not affected by this high amount of DIC occurring in the region of very low oxygen concentrations. This is the case, because the DIC equilibrium concentrations are computed as a function of temperature, salinity and atmospheric pCO_2 concentrations (see Appendix A).

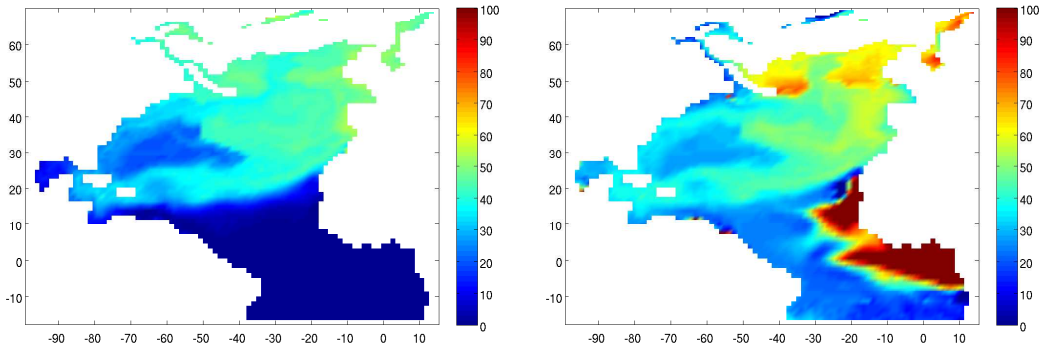

Figure 5.3: Anthropogenic CO_2 concentration [mmol kg^{-3}] on $\sigma_\theta = 26.7$ - 27.3; left: DDIC; right: ΔC^* method with ideal age; year 1996 of the model run excluding isopycnal mixing and starting in 1765.

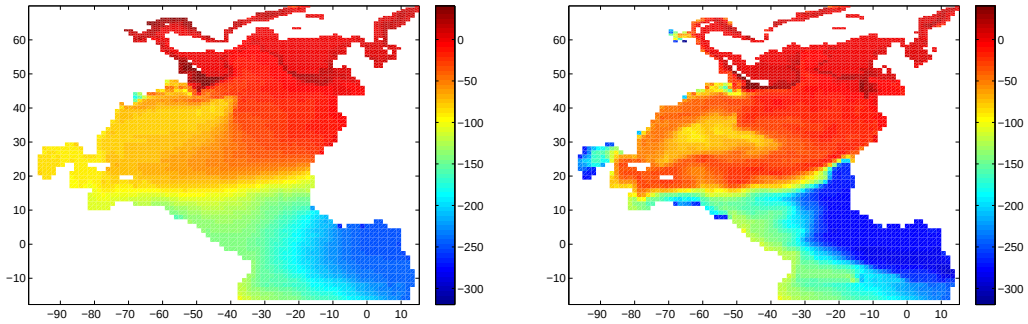

Figure 5.4: O_2-O_2^{sat} [mmol m^{-3}] on σ_θ = 26.7 - 27.3; left: including isopycnal mixing; right: without isopycnal mixing; year 1996 of model runs starting in 1765.

In the auxiliary material of Matsumoto and Gruber [2005] is described how denitrification is taken into account. In regions with low oxygen concentrations Equation 3.2 has been extended by a term involving $N^\star = NO_3^-$ - 16 PO_4^{3-} + const. (Gruber and Sarmiento [1997]). Sabine et al. [1999] explained that this accounts for the fact that denitrification remineralises organic matter and thus increases DIC without consuming oxygen. During denitrification nitrate is consumed instead of oxygen by producing phosphate, which has a strong impact on $N^\star$. So this can be used to diagnose how much DIC has been added to the water column by denitrification. In Matsumoto and Gruber [2005] they have no nitrogen in the model data and therefore used preformed PO_4, which also requires an estimate of preformed alkalinity (ALK^0). In this model no phosphate is included and the alkalinity is estimated as a function of salinity and thus not independent. That is the reason why no correction for the regions in which denitrification occurs was done in this study (which would only be the case for the model run excluding isopycnal mixing). But it should be possible to make another model experiment where denitrification is taken into account. That would be done in the way that as soon as oxygen concentrations fall below a threshold value during integration, nitrogen is used instead. The activity of zooplankton would be also set to zero in that case. This should improve the $\Delta C^\star$ method in regions with low oxygen concentrations. Nevertheless this problem occurs only in the model run without isopycnal mixing. This is the case, because if no isopycnal mixing is included in the model, badly ventilated regions (like the OMZs off the coast of Africa) are ventilated even worse than in the reference model run with isopycnal mixing. Especially in these regions the strong equatorial currents leading to the east are much weaker in the model run excluding isopycnal mixing. This leads to less ventilation in the eastern part of the tropical Atlantic, and thereby the zones of low oxygen concentrations

are larger and have lower oxygen concentrations in comparison to the model run including isopycnal mixing. This leads, in addition to no denitrification included in the model, to unnaturally high DIC concentrations. Estimating now anthropogenic CO_2 using the ΔC^* method leads to too high anthropogenic CO_2 concentrations there.
Considering the water layer directly underneath the previously described water masses, representing the core or North Atlantic Intermediate water (σ_θ = 27.3 - 27.6), the volume between these isopycnal surfaces is increasing by about 6% compared to the model run including isopycnal mixing. The relative difference of the amount of DDIC and ACO2TR between the model run without isopycnal mixing and including isopycnal mixing is with 7% to 9% more anthropogenic CO_2 approximately the same amount of increase as the volume. But in contrast to that using the TTD method with CFC12 the amount of anthropogenic CO_2 is about 4% smaller and using the ΔC^* method leads to about 27% less anthropogenic CO_2 inventory on these isopycnal surfaces in the experiment without isopycnal mixing (Tables 5.1 and 5.2).

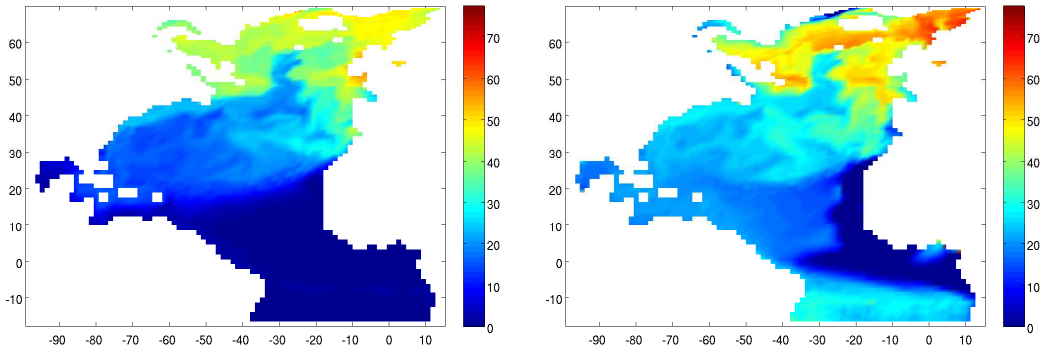

Figure 5.5: Anthropogenic CO_2 concentration [mmol m^{-3}] on σ_θ = 27.3 - 27.6; left: DDIC; right: ΔC^* method with ideal age; year 1996 of the model run without isopycnal mixing and starting in 1765.

This can also be seen in Figure 5.5 which shows the anthropogenic CO_2 concentration (in mmol m^{-3}) of DDIC and the ΔC^* method using ideal age for age information. It is striking to note that especially for anthropogenic CO_2 using the ΔC^* method the absolute concentrations are slightly higher north of about 40°N. In contrast to that, along the equator and off the coast of Africa between 10°S and 20°N concentrations of 0 mmol m^{-3} or even negative values occur. These negative values are an artefact of still highly undersaturated oxygen in this region. But in contrast of the isopycnic layer above, the DIC concentrations are higher in this region. Which is the case, because the oxygen concentrations are not so low, that denitrification would occur. In addition

to that the depth of this isopycnal is so deep that the light limits the growth rate of phytoplankton and zooplankton. This leads to the conclusion that adapting the ΔC^* method to a model which does not include isopycnal mixing, leads to large errors in the whole model domain. This is not that surprising, because the ΔC^* method includes the assumption that anthropogenic CO_2 penetrates into the ocean predominantly along isopycnal surfaces. But switching off isopycnal mixing in a model run, prevents the tracers to mix well along these isopycnals, which leads to lower horizontal advection and higher vertical mixing compared to the model run including isopycnal mixing.

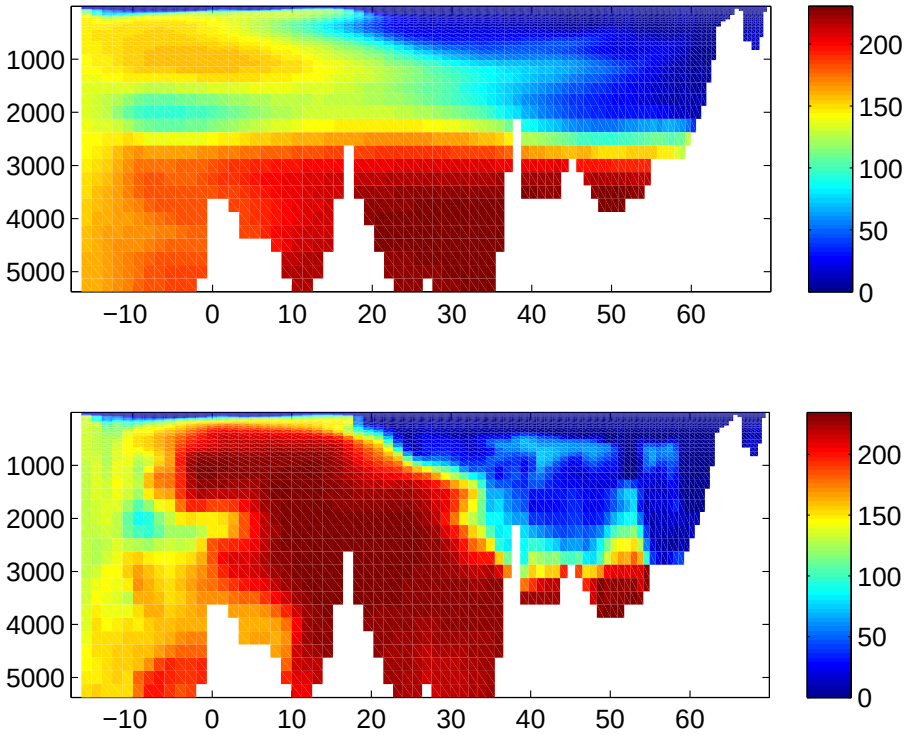

Figure 5.6: Ideal age [years] along a section at 25°W in the model year 1996 of the model runs starting in 1765. Upper: Model run including isopycnal mixing; lower: Model run without isopycnal mixing.

Figure 5.6 shows the section of ideal age along 25 °W for the model year 1996. It can be clearly seen that in contrast to the model run including isopycnal mixing, the water is more mixed in the vertical than along isopycnal surfaces in the model run without isopycnal mixing. This leads to "fingers" of older water surrounded by younger water. And very old water is mixed up to about 500 m around the equator (10°S and 10°N),

leading to the misleading anthropogenic CO_2 concentrations using the ΔC^* method described above.

Table 5.1: Total anthropogenic CO_2 inventory of the model year 1996 on different isopycnals; model run without isopycnal mixing.

σ_θ	<26.0	26.0-26.7	26.7-27.3	27.3-27.6	27.6-27.7	27.7-27.8	27.8-27.9	>27.9
volume [10^6 km^3]	4.23	5.92	19.16	20.61	9.75	27.66	103.95	1.63
total inv. of DDIC [Gt C]	1.93	1.92	4.28	2.87	1.29	4.06	5.11	0.73
total inv. of ACO2TR [Gt C]	2.01	1.89	4.13	2.83	1.30	4.14	5.24	0.74
total inv. of ACO2EQDIFF [Gt C]	2.50	2.14	4.72	3.13	1.38	4.38	6.22	0.64
total inv. of CANT (ideal age) [Gt C]	2.48	4.25	10.29	4.57	2.18	7.93	43.73	0.47
total inv. of CANT (CFC12 age) [Gt C]	2.42	4.17	10.28	4.54	2.09	7.32	40.46	0.40
total inv. of TTD (CFC12 age) [Gt C]	2.44	2.23	4.78	3.04	1.34	4.22	5.68	0.57
quantum of total volume [%]	2.2	3.1	9.9	10.7	5.1	14.3	53.9	0.8
quantum of total inv. (DDIC) [%]	8.7	8.6	19.3	12.9	5.8	18.3	23.0	3.3
quantum of total inv. (ACO2TR) [%]	9.0	8.4	18.5	12.7	5.8	18.6	23.5	3.3
quantum of total (ACO2EQDIFF) [%]	9.9	8.5	18.8	12.5	5.5	17.4	24.8	2.6
quantum of total inv (TTD CFC12) [%]	10.0	9.2	19.7	12.5	5.5	17.4	23.4	2.4

Table 5.2: Total anthropogenic CO_2 inventory of the model year 1996 on different isopycnals.

σ_θ	<26.0	26.0-26.7	26.7-27.3	27.3-27.6	27.6-27.7	27.7-27.8	27.8-27.9	>27.9
volume [10^6 km^3]	3.88	5.97	19.25	19.48	8.20	23.28	111.25	1.58
total inv. of DDIC [Gt C]	1.76	2.09	4.30	2.67	1.07	3.81	7.3	0.62
total inv. of ACO2TR [Gt C]	1.84	2.02	4.07	2.58	1.06	3.84	7.40	0.63
total inv. of ACO2EQDIFF [Gt C]	2.33	2.14	4.29	2.94	1.19	4.09	8.40	0.54
total inv. of CANT (ideal age) [Gt C]	2.31	2.65	7.23	6.27	2.41	6.83	45.81	0.50
total inv. of CANT (CFC12 age) [Gt C]	2.27	2.73	7.40	6.20	2.34	6.64	43.41	0.46
total inv. of TTD (CFC12 age) [Gt C]	2.27	2.41	5.07	3.16	1.20	4.14	7.86	0.49
quantum of total volume [%]	2.0	3.1	10.0	10.1	4.3	12.1	57.7	0.8
quantum of total inv. (DDIC) [%]	7.5	8.8	18.2	11.3	4.5	16.1	30.9	2.6
quantum of total inv. (ACO2TR) [%]	7.8	8.6	17.4	11.0	4.5	16.4	31.6	2.7
quantum of total inv (ACO2EQDIFF) [%]	9.0	8.3	16.5	11.3	4.6	15.8	32.4	2.1
quantum of total inv (TTD CFC12) [%]	8.5	9.0	19.1	11.9	4.5	15.6	29.5	1.9

5.1 Summary and conclusions

Switching off isopycnal mixing in the model aimed to point out that an estimation assuming mixing predominantly along isopycnals, as the $\Delta C^{\star}$ method, should fail in case of no isopycnal mixing. But as shown in the previous chapter, the magnitude of the difference of anthropogenic CO_2 concentrations using the $\Delta C^{\star}$ in comparison to modelled DDIC in the model run excluding isopycnal mixing is the same as in the model run including isopycnal mixing. Nevertheless extreme overestimation of anthropogenic CO_2 occurs in the shadow zones off the equatorial coast of Africa in depths of about 200 m to 700 m. That is where very old water is getting much closer to the surface in the model run without isopycnal mixing, due to lower horizontal mixing than in the experiment including isopycnal mixing. This leads to problems in the NPZD used here model, because in these regions extremely high DIC concentrations occur. Which are the result of coupling DIC to the sources and sinks of nutrients via Redfield ratios in the model, and the additional effect, that there is no denitrification in the biological model. If denitrification was part of the model, it could be supposed that the anthropogenic CO_2 concentrations using the $\Delta C^{\star}$ method were close to zero in this regions as for DDIC and the ACO2EQDIFF and the TTD method. In the total amount of anthropogenic CO_2 as well as for local concentrations there are no significant differences using the ACO2EQDIFF or TTD method in the model run without isopycnal mixing compared to the model run including isopycnal mixing.

Chapter 6

Sensitivity of the $\triangle C^{\star}$ method to inter-annual variability

In the previous sections different possibilities of estimating anthropogenic CO_2 in an ocean model were described and applied to an ocean circulation model of the North Atlantic forced by climatological mean winds. For getting information about the influence of inter-annual variability on the different estimation methods for anthropogenic CO_2, anomalies from the NCEP/NCAR climatology were added to the climatological forcing in the period from 1948 to 2001. For parts of this time period there was much data collected in the Bermuda Atlantic Time-Series Study (BATS), so that the model output could be compared to this observations.

For the years 1988 to 1998 Bates [2001] evaluated data collected at the Bermuda Atlantic Time-Series Study (BATS; 64°W 32°N) site in the Sargasso Sea, located in the North Atlantic subtropical gyre. There he found that the DIC had a characteristic seasonal cycle of 30 - 40 μmol kg^{-1} and a surface seawater pCO_2 variability of 80 ppm - 100 ppm. Such seasonal variability of DIC and pCO_2 can also be seen in the model for the ocean surface pCO_2 computed including the NPZD model in this region. In contrast to that the seasonal variability of surface pCO_2 used for the anthropogenic CO_2 tracer approach is much too small and additionally anti-correlated to the directly modelled surface pCO_2, which shows the same variation as the observed pCO_2 shown by Bates [2001] (Figures 6.1 and 6.2). In contrast to that the seasonal variability of the anthropogenic CO_2 tracer is larger than that of modelled DDIC (not shown in this figure). Additionally Bates [2001] tried to find correlations for the observed hydrographic and biogeochemical anomalies at BATS to modes of climate variability as the Southern Oscillation Index (SOI) or the North Atlantic Oscillation (NAO). For

a 6-month running mean of the anomaly of surface DIC he found a correlation to the NAO of about -0.46 and a similar correlation for surface temperature. He concluded that his analyses indicate that the observed inverse relationships between temperature and biogeochemical properties in the Sargasso Sea were linked to NAO variability.

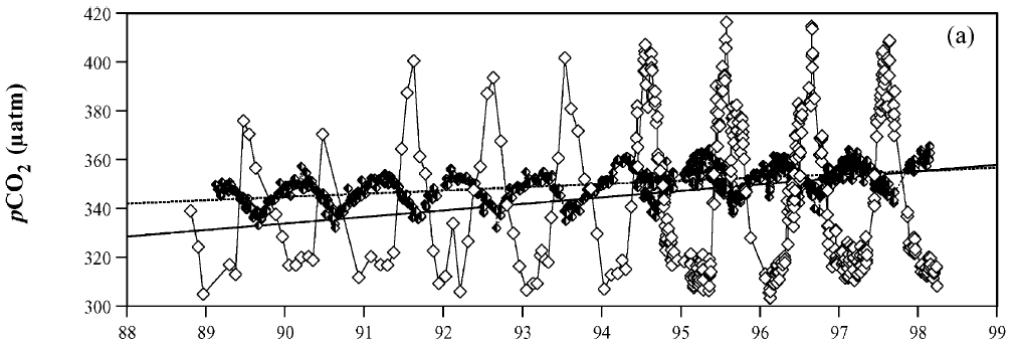

Figure 6.1: Figure 3a of Bates [2001]:Time series of water column, surface and atmospheric properties at the BATS site from 1988 to 1998. (a) Surface seawater pCO_2 ($\mu atm\, yr^{-1}$, open diamond) and atmospheric pCO_2 ($\mu atm\, yr^{-1}$, closed diamond). The slopes of the regression lines are 2.66 (seawater pCO_2) and 1.33 (atmospheric pCO_2) $\mu at\, yr^{-1}$, respectively.

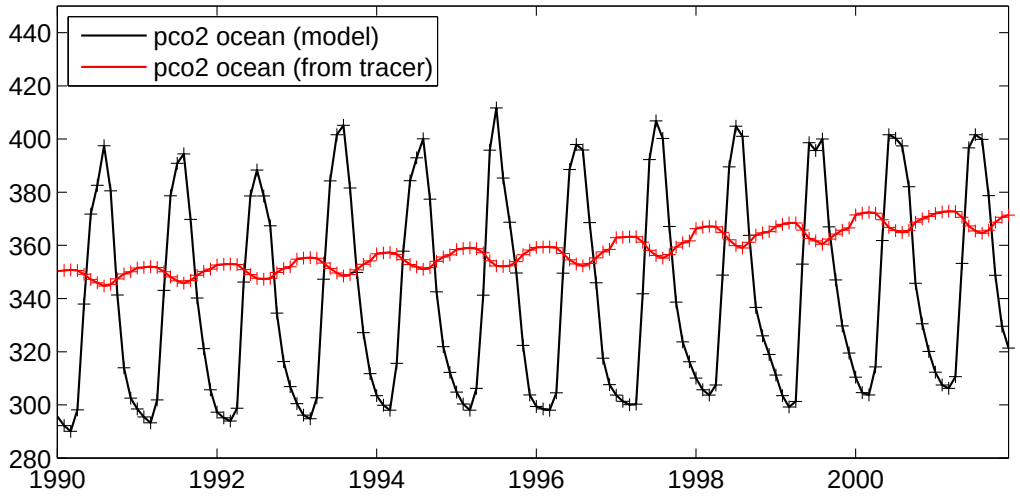

Figure 6.2: Time series of surface pCO_2 for the years 1990 until 2001 from monthly means of the model run including inter-annual variable surface forcing. Modelled surface pCO_2 is shown in black and surface pCO_2 from the anthropogenic CO_2 tracer approach is shown in red.

As shown by Dickson et al. [1996], NAO variability is related to formation of deep waters in the Labrador Sea. In high NAO phases there is supposed to be deeper convection

in the Labrador Sea and vice versa in low NAO phases. So there is the possibility that estimation methods for anthropogenic CO_2 which are very sensitive to deep convection or the amount of production of mode waters, show more sensitivity to inter-annual variability than methods which are not that sensitive to these processes. On a basin wide scale the inter-annual variability is not detectable. As shown in the basin wide inventory of anthropogenic CO_2, where no significant influence of inter-annual variability on DDIC and ACO2EQDIFF (Figure 6.3) can be detected. In Figure 6.3 the relative difference of total anthropogenic CO_2 (of the whole model domain) from the inter-annual variable model experiment to the climatological run is shown. For DDIC the difference between the two is less than 1% and for ACO2EQDIFF it is less than 0.6%. Considering the anthropogenic CO_2 accumulation on different isopycnals some influence of the inter-annual forcing is detectable. In Figure 6.4 the relative difference of the total inventory of anthropogenic CO_2 between the inter-annual and the climatological model run, estimated by three different methods ("true" anthropogenic CO_2 of the model (DDIC; black), difference of two equilibration concentrations using ideal age (ACO2EQDIFF; red) and using the $\Delta C^\star$ method also with ideal age (blue)) is shown on three isopycnic intervals representing mode-, central- and upper deep waters of the North Atlantic. On every isopycnic interval showed in Figure 6.4 the relative difference of the total inventory taking DDIC and ACO2EQDIFF gives very similar results. Estimating anthropogenic CO_2 using the TTD method leads on all isopycnal intervals to nearly the same results as the DDIC and ACO2EQDIFF concentrations (not shown in the figure). For these three methods the biggest signal can be seen on the uppermost isopycnal, which is representing mode water regions (σ_θ = 26.0 - 26.7). Until about 1975 of the model runs the variations are less than 3%, but from 1975 onwards the total inventory is about 5% to 10% higher in the model run using inter annual forcing than in the climatological run. Using the $\Delta C^\star$ method things look quite different. The variation of total anthropogenic CO_2 inventory is much higher for this method comparing to DDIC and ACO2EQDIFF inventories. Relative differences of +12% to -12% comparing to the climatological run occur on the deepest isopycnal (σ_θ = 27.3 - 27.7) representing the upper NADW.

Estimating the same component (anthropogenic CO_2 in this case), the correlation of the total inventory from all methods should be well correlated. But this is not the case. The results using DDIC and ACO2EQDIFF are well correlated (with a correlation $>$0.98) on all three isopycnal intervals. But using the $\Delta C^\star$ method is conform to DDIC total inventory only on the uppermost isopycnal interval (σ_θ = 26.0 - 26.7) with a correlation

0.88. On the other two intervals showed in Figure 6.4 the correlation is less than 0.5. This correlation increases to about 0.94 for the isopycnal interval σ_θ = 26.0 - 26.7, if only the time period after 1982 is taken into account. But nevertheless also for this time period the correlation between the results using the $\Delta C^{\star}$ method and DDIC are lower than 0.4 on the deepest isopycnal (σ_θ = 27.3 - 27.7). And the same correlation is about 0.67 for the isopycnal interval σ_θ = 26.7 - 27.3. A reason for this might be, that the inter-annual surface forcing starting in the year 1948 needs some time to let the information propagate into the deep ocean, so that differences in oxygen saturation or DIC saturation, which have a great influence on anthropogenic CO_2 concentrations using the $\Delta C^{\star}$ method, but not to the other methods, are leading to these discrepancies. In addition to this also the CFC saturation, which was assumed to be 100% has an influence on the anthropogenic CO_2 concentration. Especially in the formation regions of deep water this saturation can be far less than 100% (see for instance Tanhua et al. [2008]), leading lower anthropogenic CO_2 concentrations compared to the modelled DDIC. This might also explain the higher variability of anthropogenic CO_2 on the deepest isopycnal shown in Figure 6.4.

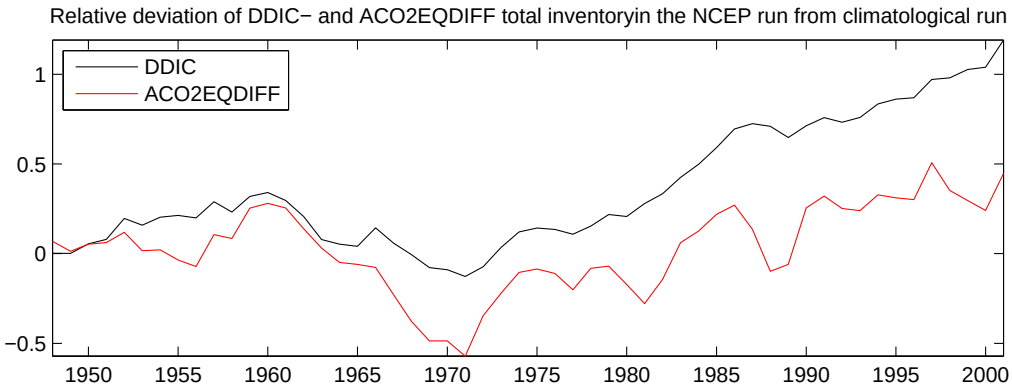

Figure 6.3: Relative difference of total anthropogenic CO_2 ((ncep - clim) / clim*100); black: DDIC; red: ACO2EQDIFF (with ideal age).

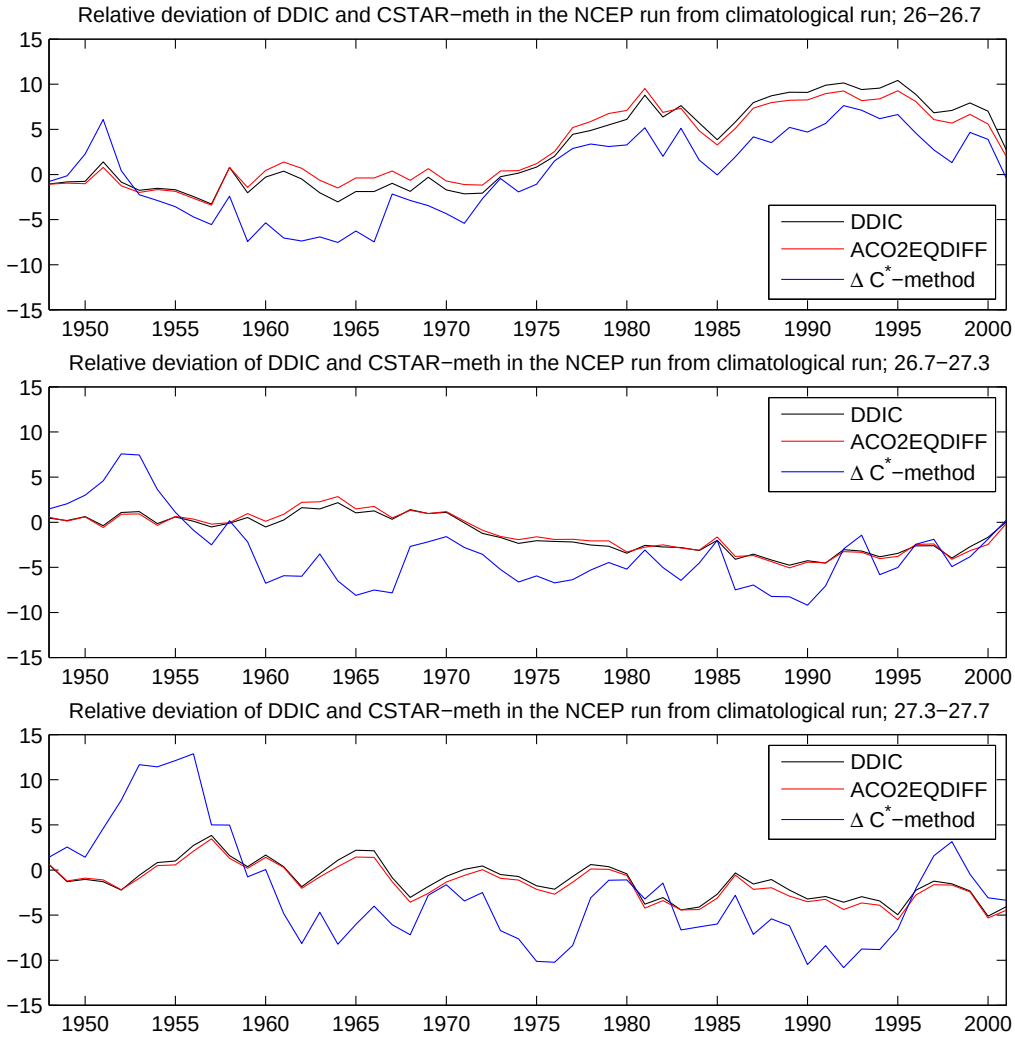

Figure 6.4: Relative difference of total anthropogenic CO_2 ((ncep - clim) / clim*100) on different isopycnals: upper: σ_θ = 26.0 - 26.7; middle: σ_θ = 26.7 - 27.3; lower: σ_θ = 27.3 - 27.7; black: DDIC; red: ACO2EQDIFF (with ideal age); blue: Δ C* method (with ideal age).

Chapter 7

Summary

The aim of this study was to contribute to the understanding of modelling anthropogenic CO_2 as well as confirming ways of estimating anthropogenic CO_2 out of observable parameters with the help of an ocean general circulation model of the North Atlantic. In this case three different methods for the estimation of anthropogenic CO_2, which are commonly used in observations, were adapted to a coarse resolution ($4/3^{\circ}$) ocean model of the North Atlantic. These are the $\Delta C\star$ method after Gruber et al. [1996], computing the difference of two DIC equilibrium concentrations (by using a single tracer derived water age or modelled ideal age), and the TTD method (as in Waugh et al. [2006]), which uses the differences of DIC equilibrium concentrations as well. The "true" anthropogenic CO_2 concentrations of the model are known and compared to the results of estimating anthropogenic CO_2 by using the different methods also used in observations.

For a model there are two different ways of computing anthropogenic CO_2, one coupling a biological model to the physical model and another including anthropogenic CO_2 as a passive tracer. Introducing anthropogenic CO_2 as a passive tracer to the regional North Atlantic model used here by using the original parametrisation of Sarmiento and Orr [1992] leads to lower anthropogenic CO_2 concentrations compared to the "true" modelled anthropogenic CO_2 concentrations including a biological model (DDIC) by about 15% to 20%. After improvement of this parametrisation, by using more realistic surface pCO_2 concentrations of a model run including biology, these two modelled anthropogenic CO_2 concentrations are nearly identical (with differences less than 7% and less than 2% for the total amount of anthropogenic CO_2 in the model). Comparing results of Sabine et al. [2004] showed that the distribution of the modelled anthropogenic CO_2 is well represented in the ocean model used for this study.

Adapting the $\Delta C^\star$ method to the model leads to anthropogenic CO_2 concentrations which are higher by 50% and more in the deep ocean compared to the "true" modelled anthropogenic CO_2 (DDIC). This is predominantly, because of the assumption that the quasi conservative tracer $\Delta C_t^\star$ is assumed to be constant along isopycnal surfaces, which is not the case in the model. But in regions where the water age is supposed to be younger than 25 years (for a "sample" year in the 1990s), the estimated anthropogenic CO_2 concentrations by using the $\Delta C^\star$ method is close to the modelled anthropogenic CO_2. Estimating anthropogenic CO_2 by the TTD method or by using the difference of two DIC equilibrium concentrations with ideal model age are leading to anthropogenic CO_2 concentrations differing less than about 10% from the "true" anthropogenic CO_2 concentrations. These better results are due to the fact that on the one hand, by computing the difference of two DIC equilibrium concentrations, the air-sea disequilibrium is computed for every grid point, instead of a mean value on an isopycnal surface (by using the $\Delta C^\star$ method). On the other hand not a single tracer derived water mass age is used in the TTD method, but a time range which takes mixing into account. As a conclusion can be said that in well ventilated regions all adapted methods are leading to anthropogenic CO_2 concentrations close to the modelled ones. But in older water the TTD method leads to the best results, because by considering an age spectrum instead of a single water age mixing is taken into account.

It was supposed that estimating anthropogenic CO_2 using the $\Delta C^\star$ method in a model run without isopycnal mixing would lead to problems, because anthropogenic CO_2 is assumed to penetrate predominantly along isopycnal surfaces into the ocean. But by switching off isopycnal mixing in the model, there is no significant difference in CO_2 concentrations detectable in comparison to the model run including isopycnal mixing. One exception is that without isopycnal mixing, problems with the biological model occur in the shadow zones in the eastern North Atlantic (off the equatorial African coast), which lead to unrealistically high anthropogenic CO_2 concentrations when using the $\Delta C^\star$ method there.

Furthermore inter-annual variability seems to have no significant influence on the different estimation methods adapted to the model. Nevertheless the $\Delta C^\star$ method shows the highest inter-annual variability in different regions. Especially in the regions influenced by deep water formation (as occurring in the Labrador Sea) this might be the result of saturation differences of DIC, oxygen or CFCs, which have a great influence on anthropogenic CO_2 concentrations estimated by using the $\Delta C^\star$ method.

To sum up the results Figure 7.1 shows the specific inventory of anthropogenic CO_2

on 10° latitude bands compared to GLODAP data for the year 1994. As pointed out previously the differences of anthropogenic CO_2 concentrations in the three different model experiments are smaller than the difference to the GLODAP data. Regional differences south of 20°N can be explained by the closed southern boundary condition of the model, with restoring to preindustrial conditions for DDIC. The lower anthropogenic CO_2 concentrations in the run excluding isopycnal mixing in this region are due to the fact that model problems occur in this region.

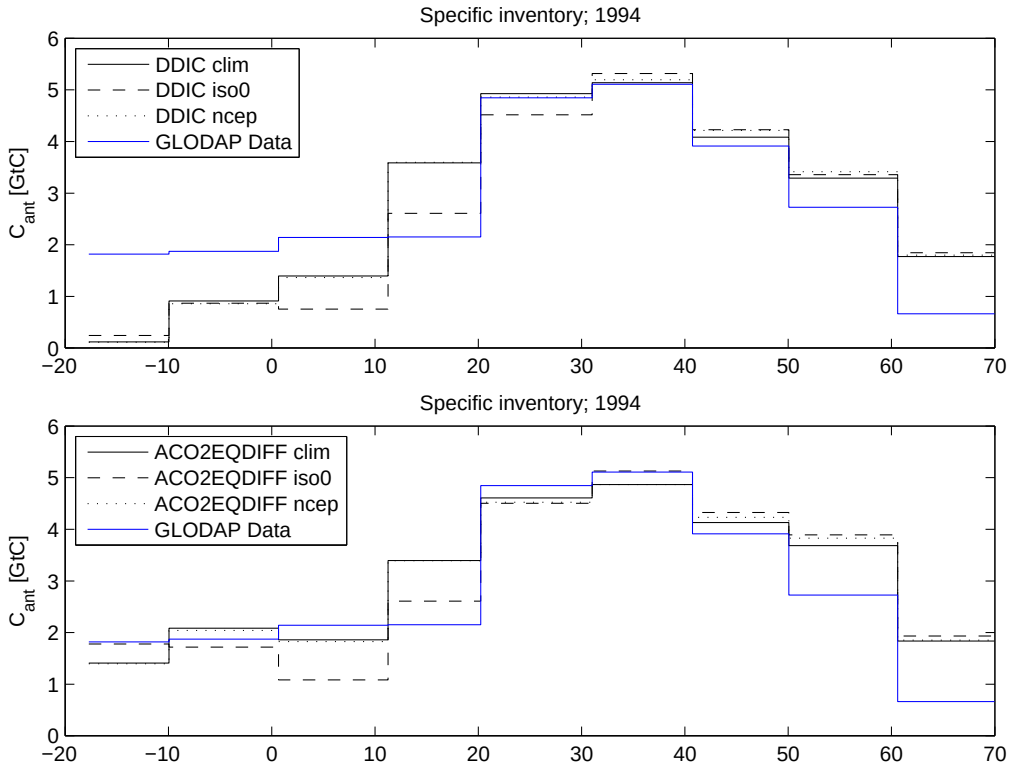

Figure 7.1: Total inventory of anthropogenic CO_2 on 10° latitude bands of model year 1994 (from the model runs starting in 1765) in comparison with GLODAP data. In the upper are the black lines DDIC and in the lower figure ACO2EQDIFF concentrations. Black solid: climatological model including isopycnal mixing run; black dashed: climatoligical model run without isopycnal mixing; black dotted: model run with inter-annual forcing; blue: GLODAP data.

For improvement and further experiments it would be interesting to test whether a biological model including denitrification, could give more information about the influence of isopycnal mixing, especially for the widely used ΔC^* method. By coupling a more complex biological model, where perhaps not only one tracer for nutrients and especially alkalinity is included, to a physical model, it would be possible to adapt the

TrOCA method for estimating anthropogenic CO_2 to the model as well. Additionally then the method proposed by Matsumoto and Gruber [2005] for taking denitrification into account could be compared to the results of a model run already including denitrification. Which, for the North Atlantic, would be interesting for the experiment, where isopycnal mixing is switched off, because only there denitrification could occur in the model, whereas no denitrification was observed in the North Atlantic ocean, but in some parts of the tropical Pacific and the Indian Ocean (Arabian Sea). As in the future more and more observations can be taken into account, and especially many hydrographic sections could be re-sampled, it will be possible to evaluate DIC changes directly out of these observations. A challenge for the future would be to develop new methods to separate observed DIC changes into changes driven by atmospherical CO_2 changes and changes of the natural carbon cycle. The changes of the natural carbon cycle can have their origin either by natural climate variability or anthropogenic climate change. Furthermore these new methods should be tested not only in observations but as well with the help of ocean models, including a complex enough biological model, where the anthropogenic CO_2 is known.

Appendix A

Estimation of DIC_{eq}

For fitting DIC_{eq} with a cubic fit the linear equation-system:

$$\begin{aligned} Mx &= b \quad \text{is solved for } x \text{ so that} \\ x &= (M'M)^{-1}M'b \end{aligned}$$

where x is a vector containing factors for the cubic polynom, b is a vector of the "true" DIC_{eq} from the model and M a matrix containing a temperature-, salt-, and pCO_{2air}-range. The temperature ($t_1 ... t_n$) ranges from -5 - 24 °C, salt ($s_1 ... s_m$) from 32 - 37 and pCO_{2air} ($p_1 ... p_l$) from 278 - 378 ppm. M is constructed as followed:

$$M = \begin{pmatrix} 1 & t_1 & s_1 & p_1 & t_1^2 & s_1^2 & p_1^2 & t_1p_1 & t_1s_1 & s_1p_1 & t_1^3 & \cdots & t_1s_1p_1 \\ 1 & t_2 & s_1 & p_1 & \cdots & & & & & & & & \\ \vdots & & & & & & & & & & & & \\ 1 & t_n & s_1 & p_1 & \cdots & & & & & & & & \\ 1 & t_1 & s_2 & p_1 & \cdots & & & & & & & & \\ \vdots & & & & & & & & & & & & \\ 1 & t_n & s_m & p_l & \cdots & & & & & & & & \end{pmatrix}$$

With this solution for x and given temperature (T), salinity (S) and pCO_{2air} (P) DIC_{eq}^{fit} can be calculated as a matrix multiplication of one line of M with the row vector x:

$$
\begin{aligned}
DIC_{eq}^{fit} &= \begin{pmatrix} 1 & T & S & P & T^2 & \cdots & T^3 & \cdots & TSP \end{pmatrix} \begin{pmatrix} x_1 \\ x_2 \\ x_3 \\ \vdots \\ x_{20} \end{pmatrix} \\
&= x_1 + x_2 T + x_3 S + x_4 P + x_5 T^2 + \cdots + x_{20} TSP
\end{aligned}
$$

Abbreviations

AABW	Antarctic Bottom Water
ACO2EQDIFF	anthropogenic CO_2 as the difference of two equilibrium concentrations
ACO2TR	anthropogenic CO_2 introduced as a passive tracer
CFC	ChloroFluorCarbon
DDIC	anthropogenic CO_2 as difference of DIC (model run with realistic atm. pCO_2 minus the one with preindustrial pCO_2)
DIC	dissolved inorganic carbon
Δ**C***	quasi conservative tracer: $DIC^{obs} - \Delta DIC_{bio} - DIC_{eq}^{pi}$
GLODAP	GLobal Ocean Data Analysis Project
LSW	Labrador Sea Water
NADW	North Atlantic Deep Water
NAO	North Atlantic Oscillation
SOI	Southern Oscillation Index
SST	Sea Surface Temperature
TrOCA	Tracer combining Oxygen, inorganic Carbon and total Alkalinity
TTD	Transient Tracer Distribution

List of Figures

Bibliography

B. Barnier, L. Siegfridt, and P. Marchesiello. Thermal forcing for a global ocean circulation model using a three year climatology of ECMWF analysis. *Journal of Marine Systems*, 6:363–380, 1995.

J. M. Barnola, M. Anklin, J. Porcheron, D. Raynaud, J. Schwander, and B. Stauffer. CO_2 evolution during the last millennium as recorded by Antarctic and Greenland Ice. *Tellus*, 1995.

N. R. Bates. Interannual variability of oceanic CO_2 and biogeochemical properties in the Western North Atlatic subtropical gyre. *Deep-Sea Research II*, (48):1507–1528, 2001.

J.-O. Beismann and R. Redler. Model simulations of CFC uptake in North Atlantic Deep Water: Effects of parameterizations and grid resolution. *Journal of Geophysical Research*, 108(C5):10.1029/2001JC001253, 3159, 2003.

A. Biastoch, C. Völker, and C. W. Böning. Uptake and spreading of anthropogenic trace gases in an eddy-permitting model of the Atlantic Ocean. *Journal of Geophysical Research*, 112(C09017):10.1029/2006JC003966, 2007.

C. W. Böning, W. R. Holland, O. Bryan, G. Danabasoglu, and J. C. Mc Williams. An Overlooked Problem in Model Simulations of the Thermohaline Circulation and Heat Transport in the North Atlantic. *Journal of Climate*, 8(3):515–523, 1995.

T. P. Boyer and S. Levitus. Objective analysis of temperature and salinity for the World Ocean on a $1/4^\circ$ grid. Technical Report 11, NOAA Atlas NESDIS, 1997.

P.G. Brewer. Direct observation of coeanic CO_2 increase. *Geophysical Research Letters*, 5(12):997–1000, 1978.

W. S. Broecker, T. Takahashi, and T.-H. Peng. Reconstrucion of past atmospheric CO_2 from the chemistry of the contemporary ocean: An evaluation. *Tech. Rep. TRO 20. U.S. Dep. of Energy, Washington D. C.*, 1985.

K. Caldeira and P.D. Duffy. The Role of the Southern Ocean in Uptake and Storage of Anthropogenic Carbon Dioxide. *Science*, 287, 2000.

C.-T. A. Chen. On the distribution of anthropogenic CO_2 penetration in the Atlantic and Pacific Oceans. *Deep-Sea Research*, 29:563–580, 1982.

C.-T. A. Chen and F. J. Millero. Gradual increas of oceanic CO_2. *nature*, 227:205–206, 1979.

M. Cox. Isopycnal diffusion in a z-coordinate model. *Ocean Modell*, 74:1–5, 1987.

P. F. Cummins, G. Holloway, and A. E. Gargett. Sensitivity of the GFDL ocean general circulation model to a parameterization of vertical diffusion. *Journal of Physical Oceanography*, 20:817–830, 1990.

R. Dickson, J. Lazier, J. Meincke, P. Rhines, and J.Swift. Long-term coordinated changes in the convective activity of the North Atlantic. *Progress in Oceanography*, 38:241–295, 1996.

R. Döscher and R. Redler. The relative influence of North Atlantic overflow and subpolar deep convection on the thermohaline circulation in an OGCM. *Journal of Physical Oceanography*, 27:1894–1902, 1997.

C. Eden. *Interannual to interdecadal variability in the North Atlantic Ocean*. PhD thesis, Christian-Albrechts-Universität zu Kiel, 1999.

M. H. England and G. Holloway. Simulations of CFC content and water mass age in the deep North Atlantic. *Journal of Geophysical Research*, 1998.

I.G. Enting, T. M. L. Wigley, and M. Heimann. Future emissions and concentrations of carbon dioxide. Technical Report 31, CSIRO Division of Atmospheric Research, 1994.

ETOPO5. Digital relief of the surface of the earth. Worldwide bathymetry/topography data announcement 88-MGG-02. Technical report, National Geophysical Data Center, 1988.

The FLAME group. FLAME a Family of Linked Atlantic Model Experiments. Technical report, AWI Bremerhaven, 1999.

T. Friedrich, A. Oschlies, and C. Eden. Role of wind stress and heat fluxes in generating interannual to decadal variability of air-sea CO_2 and O_2 fluxes in a North Atlantic model. *Geophysical Research Letters*, 33(L21S04):doi:10.1029/2006GL026538, 2006.

K. Friis. *Separation von anthropogenen CO_2 im Nordatlantik - Methodische Entwicklungen und Messungen*. PhD thesis, Institut fr Meereskunde, Kiel, 2001.

K. Friis, A. Körtzinger, J. Pätsch, and D. W. R. Wallace. On the temporal increase of anthropogenic CO_2 in the subpolar North Atlantic. *Deep-Sea Research*, pages 681–698, 2005.

A. E. Gargett. Vertical eddy diffusivity in the ocean interior. *Journal of Marine Research*, 42:359–393, 1984.

P. Gaspar, Y. Grégoris, and J. Lefevre. A simple eddy kinetic energy model for simulations of the oceanic vertical mixing: Tests at Station Papa and long-term upper ocean study site. *Journal of Geophysical Research*, 95:16179–16193, September 1990.

P. Gent and J.McWilliams. The wind-driven ocean circulation with an isopycnal-thickness mixing parameterization. *Journal of Physical Oceanography*, 24:46–65, 1994.

P. Gent and J. McWilliams. Isopycnal mixing in ocean circulation models. *Journal of Physical Oceanography*, 20:1023–1026, 1990.

C. Goyet and P. G. Brewer. *Biochemical Properties Of The Oceanic Carbon Cycle*, volume 11 of *Nato Asi Series, Ser. I*, chapter Modelling Oceanic Climate Interactions, pages 271–297. Springer Verlag, New York, 1993.

C. Goyet, R. Adams, and G. Eischeid. Observations Of The CO_2 System Properties In The Tropical Atlantic Ocean. *Marine Chemistry*, 60:49–61, 1998.

The DYNAMO group. Dynamics of the North Atlantic Circulation: Simulation and assimilation with high-resolution models. Technical report, Ber. Institut füer Meereskunde, Universität Kiel, 1997.

N. Gruber. Anthropogenic CO_2 in the Atlantic Ocean. *Global Biogeochemical Cycles*, 12:165–191, 1998.

N. Gruber and J. L. Sarmiento. Global patterns of marine nitrogen fixation and denitrification. *Global Biogeochemical Cycles*, 11(2):235–266, June 1997.

N. Gruber, J. L. Sarmiento, and T. F. Stocker. An improved method for detecting anthropogenic CO_2 in the oceans. *Global Biogeochemical Cycles*, 10(4):809–837, December 1996.

T. W. N. Haine and T. M. Hall. A generalized transport theory: water-mass composition and age. *Journal of Physical Oceanography*, (32):1932–1946, 2002.

T. M. Hall and R. A. Plumb. Age as a diagnostic of stratospheric transport. *Journal of Geophysical Research*, (99):1059–1070, 1994.

T. M. Hall, T. W. N. Haine, and D. W. Waugh. Inferring the concentration of anthropogenic carbon in the ocean from tracers. *Global Biogeochemical Cycles*, 16, 2002.

T. M. Hall, D. W. Waugh, T. W. N. Haine, P. E. Robbins, and S. Khatiwala. Estimates of anthropogenic carbon in the Indian Ocean with allowance for mixing and time-varying air-sea CO_2 disequilibrium. *Global Biogeochemical Cycles*, 18, 2004.

R. Haney. Surface thermal boundary conditions for ocean circulation models. *Journal of Physical Oceanography*, 1:241–248, 1971.

J. T. Houghton, Y. Ding, D. J. Griggs, M. Noguer, P. J. van der Linden, X. Dai, K. Maskell, and C. A. Johnson, editors. *Climate Change 2001: The Scientific Basis*. Cambridge University Press, 2001.

F. Joos, R. Meyer, M. Bruno, and M. Leuenberger. The Variability in the Carbon Sinks as Reconstructed for the Last 1000 Years. *Geophysical Research Letters*, 1999.

E. Kalnay, M. Kanamitsu, R. Kistler, W. Collins, D. Deaven, L. Gandin, M. Iredell, S. Saha, G. White, J. Woollen, Y. Zhu, M. Chelliah, W. Ebiszusaki, W. Higgins, J. Janowiak, K. Mo, C. Ropelewski, J. Wang, A. Leetmaa, R. Reynolds, R. Jenne, and D. Joseph. The NCEP/NCAR 40-years reanalysis project. *Bulletin of the American Meteorological Society*, 77:437–471, 1996.

R. M. Key, A. Kozyr, C. L. Sabine, K. Lee, R. Wanninkhof, J. L. Bullister, R. A. Feely, F. J. Millero, C. Mordy, and T.-H. Peng. A global ocean carbon climatology: Results from Global Data Analysis Projekt (GLODAP). *Global Biogeochemical Cycles*, 18, 2004.

S. Khatiwala, M. Visbeck, and P. Schlosser. Age Tracers in an Ocean GCM. *Deep-Sea Research I*, (48):1423–1441, 2001.

P. D. Killworth. Time interpolation of forcing fields in ocean models. *Journal of Physical Oceanography*, 26:136–143, 1996.

A. Körtzinger, L. Mintrop, and J. C. Duinker. On the penetration of anthropogenic CO_2 into the North Atlantic Ocean. *Journal of Geophysical Research*, 103(C9): 18681–18689, August 1998.

J. P. Lafore, J. Stein, N. Asenico, P. Bougeault, V. Ducrocq, J. Duron, C. Fischer, P. Hereil, P. Mascart, V. Masson, J. P. Pinty, J. L. Redelsperger, E. Richard, and J. Vila-Gureau de Arellano. The Meso-NH atmospheric simulation system . Part I: Adiabatic formulation and control simulations. *Annales Geophysicae*, 16:90–109, 1998.

K. Lee, S.-D. Choi, G.-H. Park, R. Wanninkhof, T.-H. Peng, R. M. Key, C. L. Sabine, R. A. Feely, J. L. Bullister, F. J. Millero, and A. Kozyr. An updated anthropogenic CO_2 inventory in the Atlantic Ocean. *Global Biogeochemical Cycles*, 2003.

B. P. Leonard. A stable and accurate convective modelling procedure based on quadratic upstream interpolation. *Computer Methods in applied Mechanics and Engineering*, 19:59–98, 1979.

S. Levitus and T. P. Boyer. Climatological atlas of the world ocean. Technical report, NOAA, 1994.

G. Marland, T. A. Boden, and R. J. Andres. Global, regional, and natural CO_2 emissions. In *Trends: A Compendium of Data on Global Change*. Carbon Dioxide Information Analysis Center, Oak Ridge National Laboratory, U. S. Department of Energy, Oak Ridge, Tenn. USA, 2007.

J. Marotzke. *Decadal Climate Variability*, chapter Analysis of Thermohaline Feedbacks, pages 334–378. Springer Verlag Berlin, 1996.

R. J. Matear, C. S. Wong, and L. Xie. Can CFCs be used to determine anthropogenic CO_2? *Global Biogeochemical Cycles*, 17(1), 2003.

K. Matsumoto and N. Gruber. How accurate is the estimation of anthrogpogenic carbon in the ocean? An evaluation of ΔC^* method. *Global Biogeochemical Cycles*, 19, 2005.

B. I. McNeil, R. J. Matear, R. M. Key, J. L. Bullister, and J. L. Sarmiento. Anthropogenic CO_2 Uptake by the Ocean Based on the Global Chloroflourcarbon Data Set. *Science*, 2003.

J. C. Orr, E. Maier-Reimer, U. Mikolajewicz, P. Monfray, J. L. Sarmiento, J. R. Toggweiler, N. K. Taylor, J. Palmer, N. Gruber, C. L. Sabine, C. Le Quéré, R. M. Key, and J. Boutin. Estimates of anthropogenic carbon uptake from four three-dimensional global ocean models. 2001.

A. Oschlies and V. Garçon. An eddy-permitting coupled physical-biological model of the North Atlantic 1. Sensitivity to advection numerics and mixed layer physics. *Global Biogeochemical Cycles*, 13:135–160, 1999.

R. C. Pacanowski. MOM2 Documentation, User's Guide and Reference Manual. *Technical report 3, GFDL Ocean Group*, 1995.

A. Papaud and A. Poisson. Distribution of dissolved CO_2 in the Red Sea and correlation with other geochemical tracers. *Journal of Marine Research*, 44:385–402, 1986.

F. F. Pérez, M. Àlvarez, and A. F. Ríos. Improvments on the back-calculation technique for estimating anthropogenic CO_2. *Deep-Sea Research I*, 2002.

A. Poisson and C.-T. A. Chen. Why is there little anthropogenic CO_2 in the Antarctic Bottom Water? *Deep-Sea Research*, 34:1255–1275, 1987.

S. Rahmstorf. Bifurcations of the Atlantic thermohaline circulation in response to changes in the hydrological cycle. *nature*, 378:145–149, 1995.

A. F. Rios, F. F. Peres, and F. Fraga. Long-term (1977-1997) measurements of carbon dioxide in the Eastern North Atlantic: evaluation of anthropogenic input. *Deep-Sea Research II*, 48:2227–2239, 2001.

C. L. Sabine, R. M. Key, K. M. Johnsons, F. J. Millero, A. Poisson, J. L. Sarmiento, D. W. R. Wallace, and C. D. Winn. Anthropogenic CO_2 inventory of the Indian Ocean. *Global Biogeochemical Cycles*, 13(1):179–198, march 1999.

C. L. Sabine, R. A. Feely, N. Gruber, R. M. Key, K. Lee, J. L. Bullister, R. Wanninkhof, C. S. Wong, D. W. R. Wallace, B. Tilbrook, F. J. Millero, T.-H. Peng, A. Kozyr, T. Ono, and A. F. Rios. The Oceanic Sink for Anthropogenic CO_2. *Science*, 305: 367–371, July 2004.

J. L. Sarmiento and J. C. Orr. A Prerturbation Simulation of CO_2 Uptake in an Ocean General Circulation Model. *Journal of Geophysical Research*, 97:3621–3645, 1992.

U. Schuster and J.Watson. A variable and decreasing sink for atmospheric CO_2 in the North Atlantic. *Journal of Geophysical Research*, 2007.

U. Schweckendiek. *The North Atlantic Ocean in the Greenhouse - Overturning Response and Sensitivities*. PhD thesis, Christian-Albrechts-Universität zu Kiel, 2003.

A. M. Shiller. Calcultating the oceanic CO_2 increase: A need for caution. *Journal of Geophysical Research*, 86:11083–11088, 1981.

U. Siegenthaler and J. L. Sarmiento. Atmospheric carbon dioxide and the ocean. *Nature*, (365):119–125, September 1993.

W. M. Smethie and R. A. Fine. Rates of North Atlantic Deep Water formation calculated from chloroflourcarbon inventories. *Deep-Sea Research I*, (48):189–215, January 2001.

S. Solomon, D. Qin, M. Maning, Z. Chen, M. Marouis, K. B. Averyt, M. Tignor, and H. L. Miller, editors. *Climate Change 2007: The Physical Basis. Contribution of Working Group I to the Fourth Assessment Report of the Intergovernmental Panel on Climate Change*. Cambridge University Press, Cambridge, United Kingdom and New York, NY, USA, 2007.

T. Takahashi, R. A. Feely, R. F. Weiss, R. H. Wanninkhof, D. W. Chipman, S. C. Sutherland, and T. T. Takahashi. Global air-sea flux of CO_2: An estimate based on measurements of sea-air pCO_2 difference. *PNAS*, 94:8292–8299, August 1997.

T. Tanhua, A. Biastosch, A. Körtzinger, H. Lüger, C. Böning, and D. W. R. Wallace. Changes of anthropogenic CO_2 and CFCs in the North Atlantic between 1981 and 2004. *Global Biogeochemical Cycles*, 20, 2006.

T. Tanhua, A. Körtzinger, K. Friis, D. W. Waugh, and D. W. R. Wallace. An estimate of anthropogenic CO_2 inventory from decadal changes in oceanic carbon content. *PNAS*, 104(9):3037–3042, 2007.

T. Tanhua, D. W. Waugh, and D. W. R. Wallace. Use of SF_6 to estimate anthropogenic CO_2 in the upper ocean. *Journal of Geophysical Research*, 113, 2008.

H. Thomas and V. Ittekkot. Determination of anthropogenic CO_2 in the North Atlantic Ocean using water mass ages and CO_2 equilibrium chemistry. *Journal of Marine Systems*, 2001.

H. Thomas, M. H. England, and V. Ittekkot. An off-line 3D model of anthropogenic CO_2 uptake by the oceans. *Geophysical Research Letters*, 2001.

F. Touratier and C. Goyet. Definition, properties, and Atlantic Ocean distribution of the new tracer TrOCA. *Journal of Marine Systems*, 2004a.

F. Touratier and C. Goyet. Applying the new TrOCA approach to assess the distribution of anthropogenic CO_2 in the Atlantic Ocean. *Journal of Marine Systems*, 2004b.

C. Völker, J. Willebrand, and J. Dengg. Anthropogenic carbon uptake in the Atlantic studied with a basin-sacle ocean general circulation model. submitted to J. Mar. Res., April 2001.

D. W. R. Wallace. Monitoring global ocean carbon inventories. *OOSDP Background Report No. 5, Texas A and M University, College Station, Texas, USA*, 1995.

R. Wanninkhof. Relationship Between Wind Speed and Gas Exchange Over the Ocean. *Journal of Geophysical Research*, 97:7373–7382, 1992.

M. J. Warner and R. F. Weiss. Solubilities of chlorofluorcarbons 11 and 12 in water and seawater. *Deep-Sea Research I*, 32(12):1484–1497, 1985.

D. W. Waugh, T. M. Hall, and T. W. N. Haine. Relationship among tracer ages. *Journal of Geophysical Research*, 108, 2003.

D. W. Waugh, T. W. N. Haine, and T. M. Hall. Transport times and anthropogenic carbon in the subpolar North Atlantic Ocean. *Deep-Sea Research I*, 2004.

D. W. Waugh, T. M. Hall, B. I. McNeil, R. Key, and R. J. Matear. Anthropogenic CO_2 in the oceans estimated using transit time distributions. *Tellus*, (58B):376–389, July 2006.

R. F. Weiss. Carbon dioxide in water and seawater: The solubility of a non-ideal gas. *Marine Chemistry*, 2:203–215, 1974.

Danksagung

Entscheidend für das Gelingen dieser Arbeit war die hervorragende Betreuung durch Prof. Dr. Andreas Oschlies. Vielen Dank für die vielen Anregungen und den steten motivierenden Zuspruch.

Desweiteren möchte ich Carsten Eden für die Bereitstellung des Modellcodes danken. Ohne seine Hilfe hätte ich die notwendigen Modellläufe nicht durchführen können.

Bei Toste Tanhua möchte ich mich für die Anregungen und Hilfe zum Verständnis, speziell der TTD-Methode, bedanken.

Für das Korrekturlesen möchte ich mich besonders bei Mirjam, Julia, Toste, Kirsten und Birte bedanken. Mirjam auch vielen Dank für die nette Zeit in der Alten Botanik.

Außerdem vielen Dank an alle die wissen, dass sie an dieser Stelle gemeint sind.

Erklärung

Hiermit erkläre ich, dass ich die vorliegende Dissertation - abgesehen von der Beratung durch meine akademischen Lehrer - selbständig verfasst habe und keine weiteren Quellen und Hilfsmittel als die hier angegebenen verwendet habe.
Diese Arbeit hat werder ganz, noch in Teilen, bereits an anderer Stelle einer Promotionskommission zur Erlangung des Doktorgrades vorgelegen.
Ich erkläre, dass die vorliegende Arbeit gemäß der Grundsätze zur Sicherung guter wissenschaftlicher Praxis der Deutschen Forschungsgemeinschaft erstellt wurde.

Kiel, den 12. September 2008